DISPERSAL AND DISEASE DYNAMICS IN POPULATIONS WITH AND WITHOUT DEMOGRAPHY

A Dissertation

Presented to the Faculty of the Graduate School

of Cornell University

in Partial Fulfillment of the Requirements for the Degree of

Doctor of Philosophy

by

Karen R. Ríos-Soto

August 2008

DISPERSAL AND DISEASE DYNAMICS IN POPULATIONS WITH AND WITHOUT DEMOGRAPHY

Karen R. Ríos-Soto, Ph.D.

Cornell University 2008

An integrodifference equation model is introduced to study the spatial spread of epidemics through populations with overlapping and non-overlapping epidemiological generations. Monotone and non-monotone epidemic growth functions are considered. The focus is on the application of a recent theory of existence of travelling wave solutions for integrodifference equations. Numerical studies with emphasis on the minimum asymptotic speed of propagation (c^*) are conducted. The results presented are contrasted with similar works carried out in the context of ecological invasions. The theoretical results are illustrated numerically in the context of SI (susceptible-infected) and SIS (susceptible-infected-susceptible) epidemic models. The simulations are carried out in one and two spatial dimensions using various dispersal kernels.

In order to explore future possibilities, an alternative framework for dispersal model is introduced via the use of a metapopulation approach. That is, a system of nonlinear ordinary differential equations is used to model the impact of transient populations on disease dynamics. A preliminary study of a simple two group model is conducted in the context of the interactions between migratory and local bird populations. The motivation comes from the recent avian influenza epidemic.

BIOGRAPHICAL SKETCH

Karen Rios-Soto was born in Santurce, Puerto Rico, the first of three children. At a young age Karen proved to be an outstanding student choosing always math as her favorite subject. In high school she took advance placement courses, Calculus being the one she loved the most. Karen exhibited great leadership skills from an early age. She was the president of the math club in her high school, tutor students for the college board examination and competed in math Olympics around the island receiving various awards. In her senior year she received a scholarship from the College of Engineering and Surveillance in Puerto Rico, an award given to just one person each year.

As a freshman, Karen entered the Industrial Engineering Department at the University of Puerto Rico at Mayagüez. After a year and a half exploring two engineering majors, she realized that she did not want to be an engineer and became a math major. During her sophomore year, she attended SIMU 1999 (Summer Institute of Mathematics for Undergraduates) at Humacao, Puerto Rico where she had her first encounter with research and of course, she loved it. After five years, a revised version of her research at SIMU was published, being her first co-authored publication. While in the 1999 SACNAS conference (Society for the Advancement of Chicanos and Native American in Sciences) she met her Ph.D. advisor Dr. Carlos Castillo-Chavez. At the time he was the director of MTBI (Mathematical and Theoretical Biology Institute) at Cornell University. He encouraged her to apply for his summer program. She remembered saying to herself: Oh please, that is Cornell University, what are you thinking?. To her surprise, but with lots of joy, she got accepted. She attended MTBI as an undergraduate student for three con-

secutive summers (2000, 2001 and 2002). It was after MTBI that Karen decided to pursue a Ph.D. in Mathematical Biology. She concluded that this is what she wants to do forever. Both of her 2000 and 2002 MTBI research projects won mathematics poster presentation awards, the first at the 2000 SACNAS conference and the latter at the 2003 Joint Mathematics Meeting. The research that she conducted in 2001 and 2002 resulted in co-authored manuscripts that were published.

In 2002 she earned her Bachelor in Mathematics from the University of Puerto Rico at Mayagüez. In the same year Karen enrolled in a Ph.D. program at Cornell University with a four year Sloan and SUNY fellowship awarded via the department of Biological Statistics and Computational Biology. Dr. Carlos Castillo-Chavez agreed to become her Ph.D. advisor. As Dr. Castillo-Chavez's student she has had a wonderful ride. She spent more than half a year (2003) as a graduate research assistant in the T-Division (LANL) at Los Alamos National Laboratory. She kept working for MTBI (2003, 2004, 2005, 2006, 2007) as an assistant conducting research and mentoring students in their undergraduate research projects. MTBI will be part of her forever. In January 2005, she joined Dr. Castillo-Chavez at Arizona State University (ASU) where she has had the opportunity to teach undergraduate calculus. At ASU her interests became focused on research in mathematical epidemiology and ecology. Her work lives at the interface of social dynamics, modeling, ecology, epidemiology and dynamical systems.

Karen never imagined that she would go to graduate school nor obtain a Ph.D. degree. Now she is facing new challenges. She will return to her beloved Puerto Rico and to her family. She will join the Department of Mathematics as an assistant professor of applied mathematics at her alma mater, the University of Puerto Rico at Mayagüez.

A mami, papi y el resto de mi familia... gracias.

ACKNOWLEDGEMENTS

My deepest gratitude goes to my Ph.D. adviser Dr. Carlos Castillo-Chavez for his incredible support, academic advice, and for his continuous role on my intellectual and personal growth. Special thanks to my committee members: Dr. Richard Rand and Dr. Martin Wells. Thanks to Dr. Carlos Bustamante for joining my Ph.D. committee as a proxy under very short notice. I would like to acknowledge some incredible research collaborators: Dr. Michael Neubert, Dr. Edriss Titi and Dr. Adbul Aziz-Yakubu. Thanks to MTBI visitors for sharing their knowledge and time with me. The list is endless and includes: Dr. Baojun Song, Dr. Christopher Kribs, Dr. Bingtuan Li, Dr. Kailash C. Patidar, Dr. Faina Berezovsky and Dr. Maia Martcheva among others. Thanks to my fellow graduate students David Murillo, for his help in the simulations of the two dimensional space model, Anuj Mubayi for many mathematical discussions and now Dr. Jan Medlock for sharing his partial differential equations code.

Thanks to my high school teacher Merisbel Roman and my college professor Dr. Rafael Martinez-Planell for putting me through meaningful intellectual challenges and helping me to discover my love for math. Warmest thanks to my alma mater University of Puerto Rico at Mayag*üez*, the Department of Mathematics, their faculty and my accomplices: Nywrka Rivera, Keyla Engadys, Edoardo Carta, Christian Roldan, Reyes Ortiz, Eva Rivera, Waleska Castro and others. Thanks to Dr. Ivelisse Rubio, Dr.John Little, Dr. Rebecca Pablo and the Summer Institute of Mathematics for Undergraduates (SIMU 1999) for my first exposure to the real deal. To my beloved Mathematical and Theoretical Biology Institute (MTBI 2000-2008) thanks for all the knowledge acquired through the years and many life

lessons. Thanks to the staff members of the Biological Statistics and Computational Biology department at Cornell University for their incredible help. I would like to express my gratitude in particular to Pam Archin and Beatrix Johnson. Thanks to the Center of Non-Linear Studies at Los Alamos National Laboratory and the Department of Mathematics at Arizona State University especially Lee Cruz. Thanks to my research group members and friends at Cornell University and Arizona State University, you were the best and made my journey enjoyable.

Finally, my greatest debt of gratitude goes to my family for all their support and patience. My parents Ramon Ríos-Jimenez and Norma Soto-Serrano, my brother Ramon Ríos-Soto, my sister Norimar Ríos-Soto, my fiance Gabriel Querales and my precious Dulche Chanel have all been instrumental on my climb to this new mountain.

This research was partially supported by the Sloan Foundation, Cornell University, the Mathematical and Theoretical Biology Institute, Los Alamos National Laboratory, the University of Puerto Rico at Mayag*üe*z, Arizona State University, the National Science Foundation and the National Security Agency.

TABLE OF CONTENTS

LIST OF TABLES

LIST OF FIGURES

CHAPTER 1

INTRODUCTION

A disease that successfully invades a population typically spreads until it reaches an endemic level of infection. Most theoretical work on disease dynamics has been carried out for epidemics where space is not explicitly formulated (albeit there is significant exceptions, see below). Here, we deal primarily with models that focus on the spatial spread of disease, that is, we study the dynamics of disease distributions in space and time. The emphasis is on travelling wave solutions and their speed of spatial propagation. In other words, we focus on increasing our understanding on the nature of epidemic fronts.

Models on the spread of epidemics in space and time have been developed since 1960's (Hadeler 2003). Two kinds of models are typically identified: contact distribution models (Kendall 1965, Mollison 1977) and models that average the movements of individuals in space, diffusion models. In an important article, Mollison (1977) describes well-behaved contact distributions models. The focus of his modeling approach is on how the locations of the individuals and their movement are spatially related to the infectious process. Naturally, the position of an individual relative to that of those who infected him/her is important. Hadeler (2003) provides a clear description of both approaches. He identifies connections between both approaches through the scaling of migration and infection rates. He emphasized the validity of each approach as a function of the question and scenario. He observed, for example, that contact models may better model disease spread tied in to the frequent travels of relatively few infectious individuals. On the other hand, diffusion approximations may better capture disease spread attributed to

slow transport mechanisms. A common feature of both modeling approaches is their support of traveling waves solutions where the speed of propagation depends on the parameters of the model including those associated with the spatial process.

The classical set of examples of models that describe the movements of individuals in space includes reaction-diffusion models. Perhaps the best known such model in biology is given by Fisher's equation (1937). Fisher uses it to describe the simultaneous growth and diffusion of a population. Fisher's equation was originally introduced to study the spread of an advantageous allele, that is, in populations genetics. The model is given by the following nonlinear partial differential equation

$$\frac{\partial u}{\partial t} = f(u) + D\frac{\partial^2 u}{\partial x^2} \tag{1.1}$$

where $u(x,t)$ represents the population density (at position x and time t), $f(u)$ its density dependent growth function and D the diffusion coefficient. Skellam (1951) applied this equation in the study of ecological invasions (for muskrats populations), including two dimensions. For variants and expansions, see the books by Okubo (1980) and Okubo and Levin (2001).

The focus of most of this dissertation is on the study of a general model that incorporates population growth, disease dynamics and dispersal. A key feature, is the assumption that individuals reproduce in discrete generations. In fact, the growth and dispersal of such populations is modeled using nonlinear integrodifference equation of the form

$$N_{t+1}(x) = \int_{-\infty}^{\infty} g(N_t(y))\, k(x,y)\, dy, \tag{1.2}$$

where $N_t(x)$ denotes the total population at time t and position x, $g(N_t(y))$ denotes its nonlinear growth function, and $k(x,y)$ the dispersal redistribution kernel. Integrodifference equations of this type, are known as discrete spatial contact models.

They can be viewed as the discrete analogues of reaction-diffusion models. These integrodifference equations are given by functional maps that simultaneously describe local growth for populations with discrete, nonoverlapping and overlapping generations. The role of dispersal will be explored using various redistribution kernels. Numerical and partial analysis of integrodifference equations of this type has been carried out in ecological contexts (Kot 1989, Kot et al. 1996). Integrodifference equation analyses paid limited attention to the computation of the shapes of traveling waves until Kot (1992) focused on them.

A highly sophisticated mathematical theory on the existence and uniqueness of travelling wave solutions was developed by Weinberger (1978, 1982). In these dense and important papers, he identifies necessary and sufficient conditions on the contact distribution, growth function and initial conditions that guarantee the existence and uniqueness of travelling wave solutions. Weinberger's study focuses (or was motivated) in the spatial spread of an advantageous gene, that is, by Fisher's work. He reformulated Model (1.2) in the operator form, $u_{n+1} = Q[u_n]$, a form that links the state u_n of the nth generation to the state u_{n+1} of the $(n+1)st$ generation. Typically, Q is an operator acting on a set of functions with values in the interval $[0, 1]$. Weinberger's results are extensive. He identifies a minimal speed of propagation c^* (the asymptotic speed of propagation for solutions of the recursion formula under the integrodifference equation), establishes the existence of traveling waves solutions for each speed c where $|c| \leqslant c^*$, and characterizes the asymptotic behavior of the waves for restricted growth functions g and redistribution kernels $k(x, y)$.

The focus of this dissertation is on the application of Weinberger's framework and recent extensions by Li et al. (2008) to study the spread of an infectious disease

through a susceptible population that reproduces in discrete generations. Naturally, we focus on travelling wave solutions and the computation of the minimum asymptotic speed of propagation c^* in the context of epidemics.

Chapter 2 provides a brief review on diffusion models in biology, with emphasis on Fisher's and Skellam's (1951) work. Chapter 3 discusses existing work on discrete time epidemic models and integrodifference equations. It incorporates dispersal into these epidemic models using an appropriate system of integrodifference equations. Chapter 4, focuses on the study of integrodifference equation with non-monotone epidemic growth functions in one and two spatial dimensions. Chapter 5 provides a glimpse at an alternate approach approximating dispersal using metapopulations. A model of nonlinear ordinary differential equations is introduced to model the impact of transient populations on disease dynamics. The work is motivated by the impact that migratory birds have on local bird populations. The case of avian flu is used as a motivating example and a two group model is briefly analyzed. Chapter 6, collects our result, presents some conclusions and outlines future work.

CHAPTER 2

DIFFUSION MODELS IN BIOLOGY

The role of dispersal in evolution is a central topic in population biology. Classical works in biological dispersion includes the work of Fisher (1937) and Kolmogorov et al. (1937) on the spread of advantageous allele, Kendall's (1948) on the spread of epidemics, and Skellam's (1951) in ecology. Pioneering mathematical contributions include, in addition to those mentioned above, the work by Mollison's (1977) on epidemic spread, Okubo's (1980) monumental ecological work, Levin's (1986) seminal contributions in ecology and evolutionary biology, and Aronson and Weinberger (1975) and Weinberger's (1978, 1982) deep mathematical results. Moreover, Okubo and Levin (2001) provide a glimpse of some current directions of active research.

2.1 One-Dimensional Diffusion: A Simple Random Walk

Diffusion is described as the "net" movement of particles as a whole until an equilibrium is reached. The concept of particle is broad as it refers not only to microscopic objects but also groups and populations. Different schemes to understand the fundamentals of diffusion and corresponding descriptive equations have been developed in the past. Levin (1986) wrote a wonderful overview article where he provides a derivation of the diffusion equation from a random walk and an extensive perspective on applications. In order to provide a context for the work of this dissertation, we review this derivation briefly.

Consider the random one-dimensional motion (the simplest random walk process) of individuals (or particles) located at position 0 at time 0 as illustrated in

Figure 2.1. Each individual moves either to its left or to its right λ units with equal probability $\frac{1}{2}$ at discrete times $k\tau$ where $k \in \{0, \pm 1, \pm 2, ...\}$. The movement is assumed to be random. What will it be the form of the spatial distribution of the population after time $n\tau$ units of time have elapsed? In other words, what is the probability $p(m, n)$ that an individual reaches a point m in space after n time-steps?

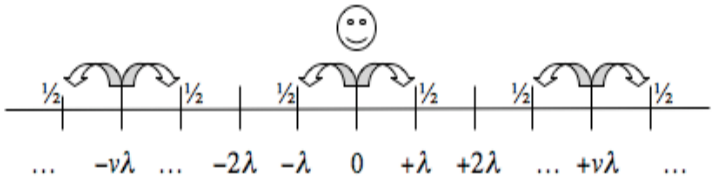

Figure 2.1: One-dimensional random walk model.

Clearly, the spatial distribution is not uniform. The release of individuals or particles at $x = 0$ implies that the probability that a particle (starting at $x = 0$) reaches the point $v\lambda$ (v large) after k steps is very small when compared to the probability of remaining near $x = 0$. An individual reaches the point $m\lambda$ steps to the right of the origin after $n\tau$ time units have elapsed if such individual has moved a steps to the right and b steps to the left where $a - b \equiv m$ and $a + b \equiv n$ (the total time-steps took to reach the point m). In other words, we have

$$a = \frac{n+m}{2} \qquad \text{and} \qquad b = \frac{n-m}{2}. \tag{2.1}$$

The number of possible paths that a particle can take to reach at the point $m\lambda$ in b steps to the left is

$$\binom{n}{b} = \frac{n!}{b!(n-b)!} = \frac{n!}{a!b!} = \frac{n!}{\left(\frac{n+m}{2}\right)!\left(\frac{n-m}{2}\right)!}. \tag{2.2}$$

The total number of possible n-steps paths is 2^n. Hence, the probability that an individual or a particle arrives at the point m after n ($n > m$) steps is given by

the Bernoulli (binomial) distribution

$$\binom{n}{b}\left(\frac{1}{2}\right)^{n}\left(\frac{1}{2}\right)^{n-b}=\left(\frac{1}{2}\right)^{n}\frac{n!}{\left(\frac{n+m}{2}\right)!\left(\frac{n-m}{2}\right)!}=u(m,n). \tag{2.3}$$

From the central limit theorem we know that as n goes to infinity, the binomial distribution $u(m,n)$ converges in distribution to the normal distribution

$$\chi(h)=\frac{1}{\sigma_n\sqrt{2\pi}}e^{-h^2/2}, \tag{2.4}$$

where $\mu_n = np$, $\sigma_n = \sqrt{np(1-p)}$ and $h = (m-\mu_n)/\sigma_n$. In this case $\mu_n = n/2$, $\sigma_n = \sqrt{n}/2$ and $h = (2m-n)/\sqrt{n}$. Formally,

$$\lim_{n\to\infty} u(m,n)=\sqrt{\frac{2}{\pi n}}\;exp(-m^2/2n), \qquad m >> 1, \qquad n >> 1. \tag{2.5}$$

If we let $m\lambda = x$ and $t = n\tau$, Eq. (2.5) becomes

$$\frac{u(\frac{x}{\lambda},\frac{t}{\tau})}{2\lambda}=\sqrt{\frac{\tau}{2\pi t\lambda^2}}\;exp\left\{\frac{-x^2}{2t}\frac{\tau}{\lambda^2}\right\}, \tag{2.6}$$

and if we assume that

$$\lim_{\lambda,\tau\to 0}(\lambda^2/2\tau) = D \neq 0 \tag{2.7}$$

then

$$u(x,t)=\frac{1}{2\sqrt{\pi Dt}}\;exp(-x^2/4Dt), \tag{2.8}$$

that is, $u(x,t)$ has a Gaussian distribution with mean 0 and standard deviation $\sqrt{2Dt}$. Here D is called the *diffusion coefficient* (constant of diffusivity). If we differentiate Eq. (2.8) once with respect to t and twice with respect to x, we find that the temporal rate of change of u (the population density) is directly proportional to the second derivative of the population density with respect to x. That is, Eq. (2.8) satisfies the diffusion or heat equation

$$\frac{\partial u}{\partial t}=D\frac{\partial^2 u}{\partial x^2}. \tag{2.9}$$

Eq. (2.9) describes the spread of a diffusing population. In a physical context (heat equation), the use of initial x conditions

$$u(x,0) = \phi(x) = \begin{cases} U_1 & \text{for } x < 0 \\ U_2 & \text{for } x > 0, \end{cases} \tag{2.10}$$

with $U_1 \neq U_2$, at $t = 0$ show that at any point $x \in (-\infty, \infty)$ the temperature becomes positive as soon as t becomes positive. That is, heat is conducted at an infinite speed of propagation. This is a property of the mathematical equation (an approximation) rather than the heat conduction itself (Zachmanoglou and Thoe 1986). Despite this non-physical or non-biological behavior, the heat equation gives good approximations on the process of heat conduction or population dispersal. Alternative derivations of the diffusion equation can be seen in Okubo and Levin (2001) and Murray (2002).

2.2 Reaction-Diffusion Equations

The coupling of reaction kinetics and diffusion in biochemical models produces alternative solutions than those arising from the straight diffusional processes governed by equations, like Eq. (2.9). Such coupling gives rise to what is known as reaction-diffusion equations. A one dimensional example of a reaction-diffusion equation is given by

$$\frac{\partial u}{\partial t} = f(u) + D\frac{\partial^2 u}{\partial x^2} \tag{2.11}$$

where u represents the concentration of a chemical (or population density), $f(u)$ represents kinetics (local population growth) and D is the diffusion coefficient (in this example a case constant). In the ecological literature Eq. (2.11) is a

modification of the diffusion equation, Eq. (2.9), when the growth and spread of the population occur simultaneously, that is, $f(u)$ models the growth rate of the population under study at position x.

Eq. (2.11), known as the Fisher-Kolmogorov (FK) equation, was discovered simultaneously by Fisher (1937) and Kolmogorov et al. (1937). Fisher modeled the spatial spread of an advantageous allele using a particular form of $f(u)$ while Kolmogorov et al. studied the propagation problem for a general class of functions $f(u)$. Solutions of Eq. (2.11) include travelling wave solutions. Extensive discussions can be found in the books by Britton (1986) and Murray (2002).

2.2.1 Travelling Waves

There are different kinds of travelling waves associated with the phase portraits of dynamical systems. A travelling front corresponds to a heteroclinic orbit, that is, a trajectory in space that joins two different fixed points (see Appendix A), for example (as we will see in the case of Fisher's equation) a saddle and a node. A travelling pulse corresponds to an homoclinic orbit, that is, a trajectory in space that joins a fixed point to itself, it connects a saddle fixed point to itself.

A travelling wave is a bounded solution that travels *without changing its shape*, that is, at a fixed speed. If $u(x,t)$ represents a traveling wave solution then the *shape* must be the same for all time. Hence, the speed of propagation must remain constant, say c. Typically, we describe travelling wave solutions as solutions (if they exist) of the form

$$u(x,t) \equiv u(x-ct) \equiv U(z), \tag{2.12}$$

where $z = x - ct$. Here, $U(z)$ is a traveling wave that moves in the positive

x-direction, if $c > 0$ and negative x-direction, if $c < 0$.

2.2.2 Fisher-Kolmogorov Equation

The most famous nonlinear reaction-diffusion equation is the Fisher-Kolmogoroff (FK) equation (using the f selected by Fisher) given by

$$\frac{\partial u}{\partial t} = D\frac{\partial^2 u}{\partial x^2} + ku(1-u), \tag{2.13}$$

where k is a growth parameter of the local population and D is the diffusion coefficient, both positive parameters. A rescaling of Eq. (2.13) with $t^* = kt$ and $x^* = x\sqrt{\frac{k}{D}}$ gives (omitting the asterisk to keep simple notation)

$$\frac{\partial u}{\partial t} = k\frac{\partial u}{\partial t} \tag{2.14}$$

and

$$\frac{\partial^2 u}{\partial x^2} = \frac{k}{D}\frac{\partial^2 u}{\partial x^2} \tag{2.15}$$

leading to

$$\frac{\partial u}{\partial t} = \frac{\partial^2 u}{\partial x^2} + u(1-u). \tag{2.16}$$

For the spatially homogeneous situation, we have that $\tilde{u} = \tilde{u}(x)$ satisfies

$$\frac{d^2\tilde{u}}{dx^2} + \tilde{u}(1-\tilde{u}) = 0. \tag{2.17}$$

The steady states are $\tilde{u} = 0$ (unstable) and $\tilde{u} = 1$ (stable). Thus travelling waves solutions are considered when $0 \leq u \leq 1$. Since Eq. (2.16) is invariant in the spatial direction, that is, we see the same dynamics when x_0 is replaced by $-x_0$, then it does not matter if the constant c is negative or positive. Hence, we assume without loss of generality that $c \geq 0$. Substitution of the traveling waveform

$u(x,t) = u(x-ct) = U(z)$ into Eq. (2.16) results in the following second order ordinary differential equation for $U(z)$

$$U'' + cU' + U(1-U) = 0, \tag{2.18}$$

where $'$ denotes differentiation with respect to z.

The task is to find the value of c such that a solution of the wavefront U will exist that satisfies

$$\lim_{z\to\infty} U(z) = 0, \qquad \lim_{z\to-\infty} U(z) = 1, \tag{2.19}$$

that is, solutions that connect the equilibrium points $U = 0$ and $U = 1$. The study of Eq. (2.18) is equivalent to the study of the two-dimensional system

$$U' = V, \qquad V' = -cV - U(1-U). \tag{2.20}$$

Phase plane trajectories of System (2.20) in the (U,V) plane are solutions of the nonlinear equation

$$\frac{dV}{dU} = \frac{-cV - U(1-U)}{V}. \tag{2.21}$$

The equilibrium points for System (2.20) in the (U,V) plane are $(0,0)$ and $(1,0)$. The linear stability analysis of System (2.20) shows that the eigenvalues λ for these equilibria are given by $\lambda_{1,2} = \tau \pm (\tau^2 - 4\Delta)^{1/2}$ where τ and Δ are the trace and determinant, respectively, of the corresponding Jacobian matrix evaluated at each equilibrium point. In fact, we have that for

$$(0,0) \quad : \qquad \lambda_{1,2} = \frac{1}{2}\left[-c \pm (c^2-4)^{\frac{1}{2}}\right] \implies \begin{cases} (0,0) \text{ is a stable node} & \text{if } c^2 > 4 \\ (0,0) \text{ is a stable spiral} & \text{if } c^2 < 4 \end{cases}$$

$$(1,0) \quad : \qquad \lambda_{1,2} = \frac{1}{2}\left[-c \pm (c^2+4)^{\frac{1}{2}}\right] \implies (1,0) \text{ is a saddle point.}$$

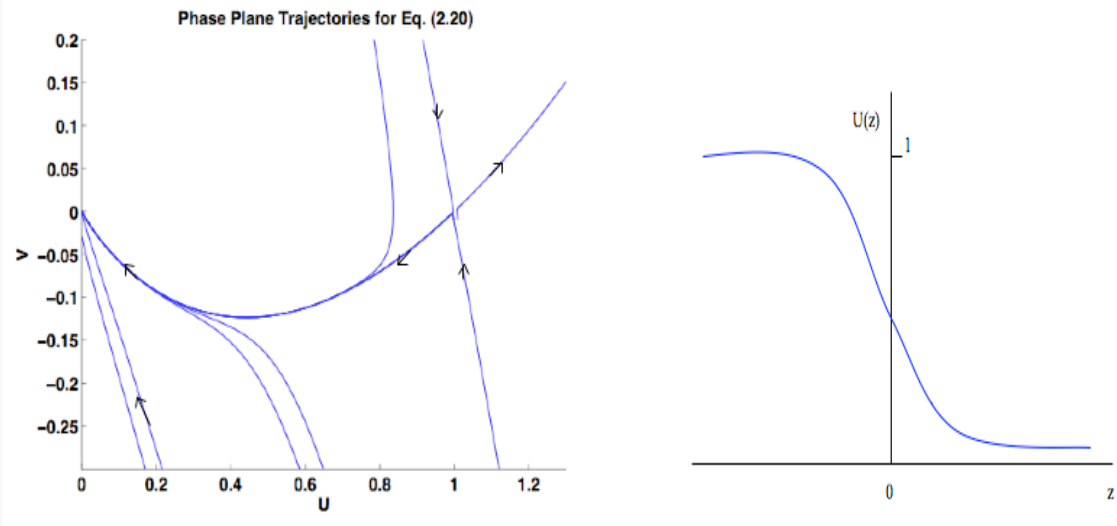

Figure 2.2: The figure on the left shows the phase plane trajectories for Eq. (2.20) for the travelling wave front solution where $c^2 > 4$. The figure on the right shows the travelling wave front solution of the Fisher's equation for $c \geq 2$.

Hence, a travelling wave front supporting a hereroclinic orbit that connects the equilibrium points $U = 1$ to $U = 0$ is expected, see Figure 2.2. Note that if $c \geq c_{\min} = 2$ then the origin is a stable node. In terms of the original parameters in the model (Model (2.13)), we have that

$$c \geq c_{\min} = 2\sqrt{kD}, \tag{2.22}$$

where the minimum speed corresponds to a stable solution. Certainly, there are travelling waves solutions for $c < 2$ but because in this case $U < 0$ they are biologically irrelevant, U spirals around $(0, 0)$. For the reaction-diffusion equation

$$\frac{\partial u}{\partial t} = \frac{\partial^2 u}{\partial x^2} + u(1 - u), \tag{2.23}$$

Kolmogoroff et al. (1937) proved (for a class of functions) that if initial conditions

have compact support or specifically if

$$u(x,0) = u_0(x) \geq 0, \qquad u_0(x) = \begin{cases} 1 & \text{if } x \leq x_1, \\ 0 & \text{if } x \geq x_2 \end{cases} \tag{2.24}$$

where $x_1 < x_2$ and $u_0(x)$ is continuous in $x_1 < x < x_2$ then the solution $u(x,t)$ evolves into a travelling wavefront solution. Therefore, a travelling wavefront solution $U(z)$ with $z = x - 2t$ exist for speeds greater than or equal to the *minimum* speed $c_{\min} = 2$, see Figure 2.3.

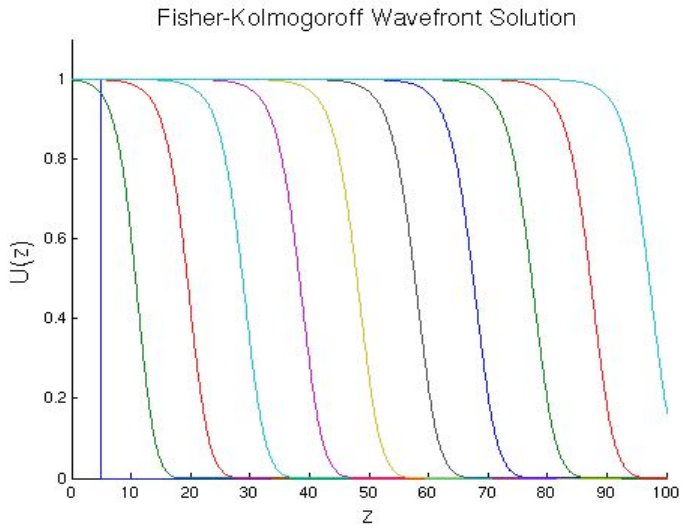

Figure 2.3: Travelling wavefront solution for the Fisher-Kolmogoroff equation with $f(u) = u(1-u)$ where the wave velocity $c \geq 2$.

2.3 Ecological Invasion

The classical work on the use of diffusion models in ecology is that of Skellam (1951). He was among the first to model the movement of individuals as a diffusion process, that is, the random dispersal of continuously reproducing individuals

over two spatial dimensions. Skellam deduced and applied the law of diffusion in order to quantify the spatial distribution of the population density in linear and two dimensional habitats. The equilibrium states and stability of various analytical models were studied in relation to the size of the habitat and analytical formulations were extended to various biological situations in his work. By combining the diffusion equation with different types of population growth functions Skellam found the travelling wave of an invasive population advancing at a constant velocity.

2.3.1 An Ecological Problem

Skellam's work was motivated by the study of the spread of muskrats populations in central Europe after their introduction in 1905. Muskrats were introduced for fur breeding but some escaped, spread, reproduced and took over the European continent in less than 50 years (Shigesada and Kawasaki 2001). Skellam calculated the enclosed area occupied by the muskrat population based on the map of Ulbrich (1930). Taking the square root of the area estimated by concentric circles of radius r led him to the identification of a linear relationship between the time and the square root of the area $\sqrt{\pi}r$. Figure 2.4 shows the boundaries of the muskrats for certain years based on geographic data by Ulbrich (1930) and the linear relationship found by Skellam. The range of the muskrats advance turn out to be well-approximated by a constant speed (provided by the slope of the line).

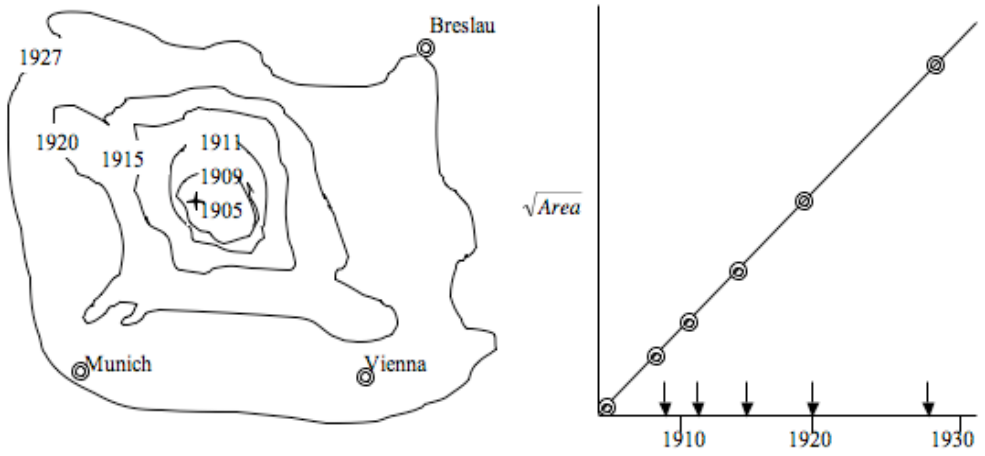

Figure A Figure B

Figure 2.4: Re-created from Skellam (1951): Figure A on the left shows the boundaries of the muskrat population in central Europe based on Ulbrich (1930) while Figure B on the right shows the linear relantionship between the time and $\sqrt{Area}$ occupied by the muskrat populations.

2.3.2 Population Growth

Typically, it is assumed that growth and dispersal occur at different stages. In these situations, the size of the population will determine which equation models the population growth. If the population is small a Malthusian model

$$\frac{du}{dt} = lu \tag{2.25}$$

will suffice. However, for larger populations the logistic model

$$\frac{du}{dt} = u(l - ku), \tag{2.26}$$

$$= lu\left(1 - \frac{u}{l/k}\right) \tag{2.27}$$

is more realistic. Here l represents the per-capita population growth rate and l/k the carrying capacity of the population under study. A stable population level will exist at $u^* = l/k$.

2.3.3 A Diffusion Problem

Mathematically, it is simple to consider linear habitats such as those modeled via Fisher's equation (1937). One dimensional models have been used to study diffusion in coastal zones or bank of rivers (see for example, Lubina and Levin 1988). Therefore, if u denotes the population density as a function of time and space then a one dimensional form expressing random dispersal coupled with Malthusian population growth produces the equation

$$\frac{\partial u}{\partial t} = D\frac{\partial^2 u}{\partial x^2} + lu \tag{2.28}$$

where D represents the displacement of individuals in any direction at particular fixed time intervals. The condition for the existence of a steady state will depend on the ability of the population in favorable regions to make up for the decline in unfavorable ones. Therefore, assuming that such compensation mechanism exist, the condition for steady state will be given by solutions $\tilde{u} = \tilde{u}(x)$ of

$$\frac{d^2\tilde{u}}{dx^2} + \frac{l}{D}\tilde{u} = 0. \tag{2.29}$$

We see that the only steady state is $\tilde{u} = 0$ (see discussion below). The case of diffusion coupled with logistic growth is modeled precisely by Fisher's equation which was discussed before.

Skellam (1951) was the first one to model dispersal of individuals in two spatial dimension using Fisher's equation. He studied the corresponding two dimensional versions using malthusian and logistic growth. Two dimensional problems, that support radially symmetric solutions, turned out to be useful and easy to analyze. The fact that two dimensional regions can be approximated by circles gave his work empirical value as well. In fact, it has been applied to study dispersal in islands,

hill tops and patches of woodland. The two dimensional form of reaction-diffusion equation combining the effects of diffusion with geometric growth is given by

$$\frac{\partial u}{\partial t} = D\left(\frac{\partial^2 u}{\partial x^2} + \frac{\partial^2 u}{\partial y^2}\right) + lu. \tag{2.30}$$

For radially symmetrical cases the above equation reduces to

$$\frac{\partial u}{\partial t} = D\left(\frac{\partial^2 u}{\partial r^2} + \frac{1}{r}\frac{\partial u}{\partial r}\right) + lu, \tag{2.31}$$

where $r^2 = x^2 + y^2$. The solution of Eq. (2.31) with inital condition $u(x, 0) = u_0$ is given by

$$u(r, t) = \frac{u_0}{4\pi Dt} exp\left(lt - \frac{r^2}{4Dt}\right) \tag{2.32}$$

(Shigesada and Kawasaki 2001). Other two-dimensional solutions for various biological situations can be found in Skellam (1951).

The combined effect of diffusion and logistic growth in two dimensional habitats is expressed by

$$\frac{\partial u}{\partial t} = D\left(\frac{\partial^2 u}{\partial x^2} + \frac{\partial^2 u}{\partial y^2}\right) + u(l - ku). \tag{2.33}$$

In the radially symmetrical cases, it reduces to

$$\frac{\partial u}{\partial t} = D\left(\frac{\partial^2 u}{\partial r^2} + \frac{1}{r}\frac{\partial u}{\partial r}\right) + u(l - ku), \tag{2.34}$$

where $r^2 = x^2 + y^2$. Skellam numerically simulated Eq. (2.34). He plotted the trajectories for general solutions of population density (spatial distributions) for different cases in order to capture a region of extinction, circular and annular survival regions. He concluded that habitats below a "critical" size (a result that depends on initial conditions) are insufficient to maintain a species undergoing unrestricted random dispersal. On the other hand, habitats that are slightly larger than the estimate size can maintain dome-shaped population densities. Larger habitats supported plateau population densities.

2.4 Integrodifference Equations

Integrodifference equations naturally arise as models for the study of the spatial spread of populations for organisms with non-overlapping generations for biological situations with distinct growth and dispersal stages (Kot and Schaeffer 1986). Their use in the study of dispersal has gain acceptance over the last three decades, in part, because integrodifference equations allow for the study of populations with dispersal distances other than normal (Kot et al. 1996). Reaction difussion equations often assume that individuals disperse in each direction with equal probability.

Integrodifference equations, in their simplest form, are easy to describe. Let $N_t(x)$ denote the population density at location $x \in \mathbb{R}$ and time $t \in \mathbb{Z}^+ = 0, 1, 2, ...$ The population density at time $t + 1$ is the result of population growth and a dispersal process. First, the number of offspring produced at location y is given by the function $g(N_t(y))$. These offspring disperse from location y to location x as prescribed by the *dispersal kernel* $k(x, y)$. The dispersal kernel typically takes the form of a probability density function, that is, the probability that an individual will disperse from location y to the interval $(x-\frac{1}{2}dx, x+\frac{1}{2}dx)$ is modeled by $k(x, y)dx$, where $k(x, y) \geq 0$. In the case of non-overlapping generation (the parents are all assumed to perish after reproducing), we have that

$$N_{t+1}(x) = \int_{-\infty}^{\infty} g(N_t(y))\, k(x, y)\, dy. \tag{2.35}$$

Often, for simplicity it is assumed that the environment is homogeneous and isotropic. This implies that the dispersal kernel depends only on the relative distance between x and y. Thus $k(x, y)$ can be written as $k(x - y)$, that is, it

is symmetric with respect to this single argument. In this case Eq. (2.35) becomes

$$N_{t+1}(x) = \int_{-\infty}^{\infty} g(N_t(y))\, k(x-y)\, dy. \tag{2.36}$$

It is further assumed that $k(x-y)$ is continuous, that there is no mortality during the dispersal phase (i. e. $\int_{-\infty}^{\infty} k(y)\, dy = 1$), and that initial conditions have compact support, that is,

$$N_0(x) > 0,\ x \in [-\delta, \delta] \text{ and } N_0(x) = 0,\ x \notin [-\delta, \delta]$$

for some δ small.

The dynamics of integrodifference equation models that incorporate realistic dispersal kernels (Neubert et al. 1995) and classical discrete-time population dynamic models have been used in ecological studies of spatial pattern formation (Kot 1989, Neubert et al. 1995), transient dynamics (Hastings and Higgins 1994, Neubert et al. 2002), the determination of minimum feasible habitat sizes (Kot and Schaeffer 1986, Van Kirk and Lewis 1997, Latore et al. 1998), and competition (Allen et al. 1996) to name a few.

Mathematical and ecological research on invasion makes use of integrodifference-equation models (see, for example, the paper by Neubert and Parker (2004) and references therein). Interest in biological invasions has been stimulated in part by the work of Kot et al. (1996), who showed that the rate of spread of an invading species (through space) is particularly sensitive to the shape of the tail of the dispersal redistribution kernel. Kot et al. (1996) showed numerically that fat-tailed redistribution kernels can lead to accelerating rather than constant speed traveling waves. These researches observed that normal redistribution kernels can grossly underestimate rates of spread of invading populations when compared with those

of models that incorporate more realistic leptokurtic distributions. In other words, the shape of the redistribution kernel has a big impact on the speed of invasion.

2.4.1 Travelling Wave Solutions for Integrodifference Equations

Kot et al. (1992) identified the rate of spread of the invasion with that of the speed of a travelling wave solution of the form

$$N_{t+1}(x) = N_t(x - c), \tag{2.37}$$

where c, the speed of the travelling wave, is a constant. Direct substitution of Eq. (2.37) into Eq. (2.36) gives rise to the following condition

$$N(x - c) = \int_{-\infty}^{\infty} g(N(y))\ k(x - y)\ dy \tag{2.38}$$

for the existence of travelling wave solutions.

Weinberger (1978) showed that travelling wave solutions of Eq. (2.36) exist for all speeds c greater than a minimum wave speed c^* (Eq. (2.40) provided below), if

(i) $g(N)$ is continuously differentiable on the interval $[0, N^*]$;

(ii) $g(0) = 0$ and $g(N^*) = N^*$;

(iii) $g'(N) \geq 0$, $N < g(N) \leq g'(0)N$ in $(0, N^*)$;

(iv) $k(x)$ is exponentially bounded (i.e., $k(x) \leq Ae^{-\mu|x|}$ for some $A, \mu > 0$).

Condition (ii) implies the existence of two spatially homogeneous equilibria: $N_t(x) \equiv 0$ and $N_t(x) \equiv N^*$. Condition (iii) requires that these are the only equilibria in the interval $[0, N^*]$, that 0 is unstable and N^* is stable. Each travelling wave solution

represents a temporal transition from 0 to N^* at every location, i.e., a heteroclinic connection. Condition (iv) implies the existence (finiteness) of the moment generating function

$$m(\rho) = \int_{-\infty}^{\infty} e^{\rho x}\ k(x)\, dx. \tag{2.39}$$

Weinberger (1978) showed that, for such exponentially bounded kernels, initial conditions with *compact support* converge to travelling waves with minimum speed

$$c^* = \min_{\rho>0} \left\{ \frac{1}{\rho}\ \ln\left[g'(0)\ m(\rho)\right] \right\}. \tag{2.40}$$

The monotonicity of g plays a key role in the proof of this result. Dispersal kernels that are not exponentially bounded (so called "fat-tailed" kernels) may produce accelerating invasions (Kot et al. 1996, Allen and Ernest 2002). These kernels will not be studied here. Weinberger et al. (2002), building on the work of Lui (1989), extended these results to cooperative systems of integrodifference equations. Neubert and Caswell (2000) explored the sensitivity of the invasion speed to both demographic and dispersal parameters in demographically structured systems.

In the next two chapters integrodifference equations will be used to study the spatial spread of infectious diseases through susceptible populations.

CHAPTER 3

EPIDEMIC SPREAD IN POPULATIONS AT DEMOGRAPHIC EQUILIBRIUM

Integrodifference equations are frequently used to understand the spread of invasive species. As discussed in the introduction, previous studies have focussed on invading species spreading into previously unoccupied habitats. In contrast, the focus here is on the spread of an infectious disease through a susceptible population, that is, within a habitat full of susceptibles. Specifically, this study is on the role of dispersal on disease dynamics in SI (susceptible-infected) and SIS (susceptible-infected-susceptible) epidemic models with non-overlapping and overlapping epidemiological generations. That is, this study focuses on the dynamics of diseases where infected individuals may or may not return to the susceptible class. The epidemiological processes are modeled from first principles but the models are necessarily simple so that, at this stage of our investigation they can be fitted into existing complex mathematical theory.

Simple epidemic models for populations with discrete generations that can be reduced, under some assumptions, to one dimensional maps of the form $I_{t+1} = g(I_t)$ where I_t denotes the density of infectives in generation t and g is the local disease reproductive function, are formulated. As long as infection does not modify the dispersal process, the problem of finding the rate of spread of infection reduces to the study of the following integrodifference equation

$$I_{t+1}(x) = \int_{-\infty}^{\infty} g(I_t(y))\, k(x-y)\, dy. \tag{3.1}$$

The infectious reproductive function $g(I_t)$ is used to model populations with *overlapping and non-overlapping* epidemiological generations of infectious individuals.

The form of g is derived from first principles. Non-monotonic increasing reproductive disease functions g arise naturally in models derived from first principles. Hence, in general g will not satisfy Condition (iii) (page 20) in Weinberger's result. Thus, the need to account for the role of non-monotone g's on the spatial spread of disease is of critical importance. This will be pursued in Chapter 4. In general, we proceed to identify g-invariant subsets $[0, I^*]$ (0 and $I^* > 0$ fixed points of g) because on these sets g tends to be monotone. When g is monotone in $[0, I^*]$ Weinberger's (1978) results apply provided that the rest of the required assumptions are met.

3.1 Epidemic Models

We build spatial epidemic models using integrodifference equations using discrete-time models for the local disease dynamics. A process for constructing well-defined epidemic processes on populations with well understood demography has been recently introduced (Castillo-Chavez and Yakubu 2001). These researches let P_t denote the population size at time t and $f(P_t)$ denotes the number of newborn individuals produced at time t that survive to time $t+1$. If $\gamma \in [0, 1)$ denotes the constant fraction of individuals of age 1 or older who survive from time t to $t+1$ then the local population dynamics are governed by

$$P_{t+1} = f(P_t) + \gamma P_t. \tag{3.2}$$

Depending on the choice of f, Eq. (3.2) can support from simple to chaotic dynamics. It is on the dynamics governed by Eq. (3.2) that we build epidemic processes. To do this, we let the population be further subdivided into two epidemiological classes: susceptible (S_t) and infected (I_t) under the restriction that all individuals

belong to one of these two classes, that is, we must have that

$$P_t = S_t + I_t, \tag{3.3}$$

where the dynamics of P_t are governed by Eq. (3.2).

It is assumed that mortality for general causes are included in γ and f. It is also assumed that the mortality associated with the disease dynamics or the dispersal process is negligible compared to the mortality for general causes (γ) or from mortality associated with reproduction (f). Hence, changes in population size are driven primarily by (potentially density-dependent) effects on the birth/recruitment process described by f and on the ability of individuals to survive from generation to generation (γ) in the absence of disease.

Assuming that the process of reproduction, infection, and mortality occur sequentially (and in this particular order), one can write the following SIS epidemic model

$$\begin{aligned} S_{t+1} &= \varphi(S_t, I_t) = Q(z_t)f(P_t) + \gamma Q(z_t)S_t + \gamma(1-\sigma)I_t, & \text{(3.4a)} \\ I_{t+1} &= \psi(S_t, I_t) = (1-Q(z_t))f(P_t) + \gamma(1-Q(z_t))S_t + \gamma\sigma I_t & \text{(3.4b)} \end{aligned}$$

with incidence,

$$z_t = \frac{I_t}{P_t + f(P_t)}. \tag{3.5}$$

In Model (3.4), the function $Q(z_t)$ denotes the proportion of susceptible individuals that do not become infected at time t given that the disease prevalence is z_t. In general, $Q : [0, \infty) \to [0, 1)$ is a monotone, concave function with $Q(0) = 1$; $Q'(u) < 0$; $Q''(u) \geq 0$ for all $u \in [0, \infty)$. As it is common (Castillo-Chavez and Yakubu 2001, 2002 and Perez Velazquez 1999), the "probability" of not becoming

infected (for specific examples) is modeled as

$$Q(z_t) = e^{-\alpha z_t}. \tag{3.6}$$

That is, encounters that lead to infection are modeled via a Poisson process. Thus, the probability of n successful encounters is modeled as a Poisson distribution $p(n) = \frac{e^{-\lambda}\lambda^n}{n!}$, where λ is the parameter of the Poisson distribution and $p(0) = e^{-\lambda}$ represents the probability that a given event does not occur (zero encounters), hence Eq. (3.6). The positive parameter α is identified as the transmission coefficient, $1-\gamma$ is the fraction of individuals that are removed (death) after birth, and σ denotes the fraction of infected individuals that remain infected from one time to the next. The remaining fraction $(1-\sigma)$ recover and return to the susceptible class. Reductions on births are only the result of density dependent effects and hence included in f. Note that by summing the equations in System (3.4) the population dynamics reduced to those modeled by Eq. (3.2).

In contrast to the model of Castillo-Chavez and Yakubu (2001), this model allows for the infection of newborn individuals (as captured by the first terms on the right-hand side of Eqs. (3.4)). Since generations must overlap at least long enough for this to happen, the denominator of z_t in Eq. (3.6) must include both P_t and $f(P_t)$. Model (3.4) has (under some conditions that will be discussed later) two equilibria $I_1 = 0$ and $I_2 = I^* > 0$.

Assuming that dispersal occurs after mortality, and that the disease does not affect the dispersal process we can add dispersal to the epidemic model that takes

us to the following system of integrodifference equations:

$$S_{t+1}(x) = \int_{-\infty}^{\infty} \varphi(S_t(y), I_t(y))\, k(x-y)\, dy, \tag{3.7a}$$

$$I_{t+1}(x) = \int_{-\infty}^{\infty} \psi(S_t(y), I_t(y))\, k(x-y)\, dy. \tag{3.7b}$$

Note that the sum of these two equations leads to the recovery of the "standard" dispersal model

$$P_{t+1}(x) = \int_{-\infty}^{\infty} [f(P_t(y)) + \gamma P_t(y)]\, k(x-y)\, dy. \tag{3.8}$$

3.2 Constant Recruitment

The dynamics of populations governed by Eq. (3.2) as well as those that model the spread of epidemics on such populations, can be quite complicated (Castillo-Chavez and Yakubu 2001). To simplify matters and illustrate some possibilities, we assume that $f(P_t) = \Lambda$, where Λ a positive constant. This assumption is relevant in at least two biological scenarios. In the first, the carrying capacity of the environment is small relative to the reproductive capacity of the species; in essence, one individual could produce enough offspring to take up all the available space locally. In the second scenario, the population is considered "open", that is, recruitment is independent of local population density. Populations of coastal invertebrate species are often described in this way (Caley et al. 1996).

With $f(P_t) = \Lambda$, in the absence of dispersal, we have from Eq. (3.2) that

$$P_t = \frac{\Lambda}{1-\gamma} + \gamma^t \left(P_0 - \frac{\Lambda}{1-\gamma} \right). \tag{3.9}$$

Thus

$$\Lambda^* \equiv \lim_{t\to\infty} P_t = \frac{\Lambda}{1-\gamma} \tag{3.10}$$

is the demographic steady state of the total population.

3.2.1 Basic Reproductive Number with Constant Recruitment

An important threshold condition in epidemiology is given by the basic reproductive number, R_0. This dimensionless quantity is derived from the linearization of the model described by Eqs. (3.4b) and (3.6) around its disease free equilibrium $(S_0, I_0) = (\Lambda^*, 0)$. The linearization leads to $I_{t+1} \approx g'(0)I_t$ with $g'(0) = \alpha[p + \gamma(1-p)] + \gamma\sigma$ where $p = \frac{\Lambda}{\Lambda+\Lambda^*}$ denotes the proportion of newborns in generation $t+1$ and $\gamma(1-p)$ the proportion of residents that survived to generation $t+1$. Hence, an epidemic will ensue if $g'(0) > 1$ or equivalently if

$$R_0 = \frac{\alpha}{1-\gamma\sigma}[p + \gamma(1-p)] \tag{3.11}$$

is greater than one. The basic reproductive number, R_0, is interpreted as the average number of secondary infections generated by the introduction of a "typical" infectious individual in a population of mostly susceptibles at a demographic steady state (that is, $P_t = \Lambda^*$). In order to make the meaning of R_0 clear, we make the following observations:

(a) $\gamma\sigma$ denotes the proportion of infected that survive from generation t to generation $t+1$. Hence $\frac{1}{1-\gamma\sigma}$ denotes the average number of generations and individual lives as infected before death or recovery.

(b) α denotes the average effective transmission rate and $p\alpha$ the contribution to secondary cases of infections by new infections in newborns with $(1-p)\alpha$ the contribution from susceptible adults that become infected.

The effect of α on p or $(1-p)$ takes place during the "average" window of opportunities $\frac{\alpha}{1-\gamma\sigma}$. In the example generated by Model (3.4) and Eq. (3.6) (Poisson process) in populations at demographic equilibrium R_0 reduces to

$$R_0 = \frac{\alpha}{1-\gamma\sigma}\frac{1}{(2-\gamma)}. \tag{3.12}$$

Locally, $R_0 > 1$ correspond to epidemic growth while $0 \leq R_0 \leq 1$ corresponds to the local extinction of the disease. In fact, as long as $R_0 > 1$ the disease will become locally endemic. That is, $I_{t+1} = g(I_t)$ has two equilibria $I_1 = 0$ and $I_2 = I^* > 0$, with I^* globally stable whenever $R_0 > 1$.

Theoretical results on the qualitative dynamics equivalence of autonomous and non-autonomous systems have been established by Thieme (1992) in the context of continuous time dynamical systems and by Zhao (1996) for discrete time dynamical systems. Their results identify conditions under which autonomous and non-autonomous systems have the same qualitative dynamics. Here, we use these results (or special initial conditions) to reduce two-dimensional systems to a one-dimensional equation as it was done in Castillo-Chavez and Yakubu (2001).

Theorem 3.2.1. *Let α be a positive constant.*

(a) If $R_0 < 1$, then the solutions (S_t, I_t) of System (3.4) approach the disease-free equilibrium, $(\Lambda^*, 0)$, as $t \to \infty$.

(b) If $R_0 > 1$, then the solutions (S_t, I_t) of System (3.4) approach a unique positive endemic equilibrium, $(1-I^*, I^*) \in (0,\infty)\times(0,\infty)$, as $t \to \infty$.

Proof. The function for the proportion of infected individuals is given by

$$h(I) = \left(1 - e^{\left(\frac{-\alpha I}{\Lambda+\Lambda^*}\right)}\right)\Lambda + \gamma\left(1 - e^{\left(\frac{-\alpha I}{\Lambda+\Lambda^*}\right)}\right)(\Lambda^* - I) + \gamma\sigma I, \tag{3.13}$$

where $h(0) = 0$ and $0 \leq I \leq \Lambda^*$. The set of iterates of h is equivalent to the set of density sequence generated by Eq. (3.4b). Differentiation with respect to I gives

$$h'(I) = \left(\frac{\alpha\Lambda}{\Lambda+\Lambda^*}\right) e^{\left(\frac{-\alpha I}{\Lambda+\Lambda^*}\right)} - \gamma(1 - e^{\left(\frac{-\alpha I}{\Lambda+\Lambda^*}\right)}) + \left(\frac{\alpha\gamma}{\Lambda+\Lambda^*}\right) e^{\left(\frac{-\alpha I}{\Lambda+\Lambda^*}\right)}(\Lambda^* - I) + \gamma\sigma$$

and

$$h''(I) = -\left(\frac{\alpha}{\Lambda+\Lambda^*}\right)^2 \Lambda e^{\left(\frac{-\alpha I}{\Lambda+\Lambda^*}\right)} - 2\left(\frac{\alpha\gamma}{\Lambda+\Lambda^*}\right) e^{\left(\frac{-\alpha I}{\Lambda+\Lambda^*}\right)} - \gamma\left(\frac{\alpha}{\Lambda+\Lambda^*}\right)^2 e^{\left(\frac{-\alpha y}{\Lambda+\Lambda^*}\right)}(\Lambda^* - I).$$

To establish the results of the theorem, we will show that $R_0 < 1$ implies $0 < h'(0) < 1$, $R_0 > 1$ implies $h'(0) > 1$ and, $h''(I) < 0$ for $I \in (0, \Lambda^*]$.

Note that $0 < R_0 < 1$ implies $0 < h'(0) = \alpha[p + \gamma(1-p)] + \gamma\sigma < 1$. Therefore, the fixed point $\{0\}$ is locally stable under h-iteration. Since $h''(I) < 0$ for $I \in [0, \Lambda^*]$ therefore, the monotonicity condition on h' and the fact that $h'(0) < 1$ imply that $h'(I) < 1$ or $h(I) < I$ for $I \in [0, \Lambda^*]$. Hence the sequence, $\{I_t\}_{t\geq 0}$, a strictly decreasing sequence bounded below by zero, converges to the only fixed point of h in the interval $[0, \Lambda^*]$, zero. This proves condition (a).

The case of $R_0 > 1$ implies that $h'(0) = \alpha[p+\gamma(1-p)]+\gamma\sigma > 1$ and, therefore, the fixed point $\{0\}$ is locally unstable under h-iteration. Let I^* denote the smallest positive fixed point of h in $[0, \Lambda^*]$, and note that since $\Lambda = (1-\gamma)\Lambda^*$ then

$$\begin{aligned} h(\Lambda^*) &= (1 - e^{\left(\frac{-\alpha\Lambda^*}{\Lambda+\Lambda^*}\right)})\Lambda + \gamma\sigma\Lambda^* && (3.14) \\ &= \Lambda^*(1 - \gamma(1-\sigma) - (1-\gamma)e^{\left(\frac{-\alpha}{2-\gamma}\right)}), && (3.15) \\ &< \Lambda^*. && (3.16) \end{aligned}$$

The intermediate value theorem guarantees the existence of a positive fixed point $I^* \in (0, \Lambda^*)$ satisfying $h(I^*) = I^*$ and $h(I) > I$ for $I \in (0, I^*)$ and, consequently, $h'(I^*) \leq 1$. Since $h''(I) < 0$ implies that $h'(I) < h'(I^*) \leq 1$ for $I \in (I^*, \Lambda^*)$,

then $\int_{I^*}^{I} h'(x)dx < \int_{I^*}^{I} dx$ and, we have $h(I) < I$ for $I \in (I^*, \Lambda^*)$. Hence, h has a unique positive fixed point $I^* \in (0, \Lambda^*)$. Furthermore, $h(I) > I$ for $I \in (0, I^*)$ and $h(I) < I$ for $I \in (I^*, \Lambda^*)$.

To establish the global stability of I^*, we first prove the non-existence of non-trivial two-cycles for h. First, we show that $1 + h'(I) > 0$. Note that

$$\begin{aligned} 1 + h'(I) &= 1 + \left(\frac{\alpha\Lambda}{\Lambda + \Lambda^*}\right) e^{\left(\frac{-\alpha I}{\Lambda+\Lambda^*}\right)} - \gamma\left(1 - e^{\left(\frac{-\alpha I}{\Lambda+\Lambda^*}\right)}\right) + \left(\frac{\alpha\gamma}{\Lambda + \Lambda^*}\right) e^{\left(\frac{-\alpha I}{\Lambda+\Lambda^*}\right)}(\Lambda^* - y) \\ &\quad +\gamma\sigma \\ &= (1-\gamma) + \left(\frac{\alpha\Lambda}{\Lambda + \Lambda^*}\right) e^{\left(\frac{-\alpha I}{\Lambda+\Lambda^*}\right)} + \gamma e^{\left(\frac{-\alpha I}{\Lambda+\Lambda^*}\right)} + \left(\frac{\alpha\gamma}{\Lambda + \Lambda^*}\right) e^{\left(\frac{-\alpha I}{\Lambda+\Lambda^*}\right)}(\Lambda^* - y) \\ &\quad +\gamma\sigma, \\ &> 0. \end{aligned}$$

Hence, $1 + h'(I) \neq 0$ for $I \in (0, \Lambda^*]$. Suppose h has a non-trivial 2-cycle $\{p, q\}$, where $p, q \in [0, \Lambda^*]$, then $h(p) = q$ and $h(q) = p$ where $p \neq q$. The mean value theorem guarantees the existence of a point k between p and q such that $h'(k) = h(p) - h(q)/p - q = -1$, and $1 + h'(k) = 0$, a contradiction. Hence, h has no non-trivial 2 cycles in $[0, \Lambda^*]$. From results in Cull (1986) and McCluskey and Muldowney (1998); the non-existence of non-trivial 2-cycles for h implies global stability of the positive fixed point I^*.

□

3.3 Integrodifference Epidemic Models with Constant Recruitment

Here, we focus in the case where $P_0(x) = \Lambda^*$ for all x and t which implies that $P_t(x) = \Lambda^*$ for all x and t. That is, we focus on the study of a disease spreading

through populations at demographic equilibrium. In this case, it is possible to eliminate $S_t(x)$ from System (3.7), that is, the problem reduces to the study of the single integrodifference equation

$$I_{t+1}(x) = \int_{-\infty}^{\infty} g(I_t(y))\, k(x-y)\, dy, \tag{3.17}$$

where

$$g(I_t(y)) = [1 - Q(z_t(y))][\Lambda^* - \gamma I_t(y)] + \gamma\sigma I_t(y), \tag{3.18}$$

and

$$z_t(y) = \frac{I_t(y)}{\Lambda^* + \Lambda}. \tag{3.19}$$

The function g is nonnegative since $I_t \leq \Lambda^*$ and $g'(0) = \alpha[p + \gamma(1-p)] + \gamma\sigma$ corresponds to the linearization that leads to the computation of R_0. That is, the R_0 associated with local epidemic growth at any location is the same as the one in Eq. (3.11), see calculations in Appendix B.

The task now is to determine the conditions under which the function g satisfies Weinberger's conditions, specifically Conditions (ii) and (iii) (page 20) when $f(P_t) = \Lambda$ and $Q(z_t) = e^{-\alpha z_t}$.

3.3.1 Example with Overlapping Generations ($SIS, \gamma > 0$)

Consider the case where the probability of survival is positive (i.e., $\gamma > 0$), then the model under consideration is

$$S_{t+1} = \varphi(S_t, I_t) = Q(z_t)f(P_t) + \gamma Q(z_t)S_t + \gamma(1-\sigma)I_t, \tag{3.20a}$$

$$I_{t+1} = \psi(S_t, I_t) = (1 - Q(z_t))f(P_t) + \gamma(1 - Q(z_t))S_t + \gamma\sigma I_t. \tag{3.20b}$$

Here,

$$g(I_t(y)) = \left(1 - \exp\left[\frac{-\alpha I_t(y)}{\Lambda + \Lambda^*}\right]\right)(\Lambda^* - \gamma I_t(y)) + \gamma\sigma I_t(y), \tag{3.21}$$

and $g'(0) = \frac{\alpha}{2-\gamma} + \gamma\sigma$. The function g defined by Eq. (3.21) satisfies all Weinberger's conditions (pages 20-20) except Condition (iii) since g is not monotonic increasing unless

$$(\Lambda^* - \gamma I_t(y)) \left(\frac{\alpha}{\Lambda + \Lambda^*}\right) \exp\left[\frac{-\alpha I_t(y)}{\Lambda + \Lambda^*}\right] > \gamma \left((1-\sigma) - \exp\left[\frac{-\alpha I_t(y)}{\Lambda + \Lambda^*}\right]\right) \quad (3.22)$$

or

$$\left(\frac{\alpha}{2-\gamma} + \gamma\right) \exp\left[\frac{-\alpha I_t(y)}{\Lambda + \Lambda^*}\right] > \gamma \left((1-\sigma) + \frac{\alpha I_t(y)}{\Lambda + \Lambda^*} \exp\left[\frac{-\alpha I_t(y)}{\Lambda + \Lambda^*}\right]\right). \quad (3.23)$$

Hence, there are simple SIS models with travelling wave solutions when the function g is monotonic increasing in invariant sets such as $[0, I^*]$, that is, when Eq. (3.22) is satisfied. The disease will spread as long as $R_0 = \frac{\alpha}{1-\gamma\sigma} \frac{1}{(2-\gamma)} > 1$.

3.3.2 Example with Non-Overlapping Generations (SI, $\gamma \equiv 0$)

The case $\gamma = 0$ corresponds to a semelparous organism with non-overlapping generations. In this case, Model (3.20) becomes

$$S_{t+1} = \varphi(S_t, I_t) = Q(z_t) f(P_t), \quad (3.24a)$$

$$I_{t+1} = \psi(S_t, I_t) = (1 - Q(z_t)) f(P_t), \quad (3.24b)$$

that is, a SI (susceptible-infected) model. Setting $\Lambda = \Lambda^*$ gives

$$g(I_t(y)) = \Lambda \left(1 - \exp\left[\frac{-\alpha I_t(y)}{2\Lambda}\right]\right) \quad (3.25)$$

and $g'(0) = \alpha/2$. The basic reproductive number is given by $R_0 = g'(0) = \alpha/2$. Weinberger's conditions holds in this case thus, $g(0) = 0$, there exist I^* such that

$g(I^*) = I^*$, $g'(I) \geq 0$ and $I < g(I) \leq g'(0)I$ for $I \in (0, I^*)$. Hence, the disease will grow whenever $\alpha > 2$ and initial conditions have compact support. The disease invasion condition is independent of Λ because of the choice of disease prevalence z_t. If $z_t = I_t$ then the basic reproductive number would be $R_0 = \alpha\Lambda > 1$.

3.3.3 Example with Overlapping Generations ($SI, \gamma > 0$ and $\sigma = 1$)

The case where $\gamma > 0$ and $\sigma = 1$ (no recovery) leads to the SI model given by the following system

$$S_{t+1} = \varphi(S_t, I_t) = Q(z_t)f(P_t) + \gamma Q(z_t)S_t, \tag{3.26a}$$

$$I_{t+1} = \psi(S_t, I_t) = (1 - Q(z_t))f(P_t) + \gamma(1 - Q(z_t))S_t + \gamma I_t. \tag{3.26b}$$

The model's basic reproductive number is

$$R_0 = \frac{\alpha}{1-\gamma}\frac{1}{(2-\gamma)}, \tag{3.27}$$

and the corresponding

$$g(I_t(y)) \equiv [1 - Q(z_t(y))][\Lambda^* - \gamma I_t(y)] + \gamma I_t(y), \tag{3.28}$$

with

$$z_t(y) = \frac{I_t(y)}{\Lambda^* + \Lambda}, \tag{3.29}$$

or

$$g(I_t(y)) = \left(1 - \exp\left[\frac{-\alpha I_t(y)}{\Lambda + \Lambda^*}\right]\right)(\Lambda^* - \gamma I_t(y)) + \gamma I_t(y), \tag{3.30}$$

with $g'(0) = \frac{\alpha}{2-\gamma} + \gamma$. The disease will become established as long as $R_0 = \frac{\alpha}{1-\gamma}\frac{1}{(2-\gamma)} > 1$. Since Eq. (3.30) satisfies Conditions (i)-(iii) (pages 20-20), the

work of Weinberger (1978) applies. Consequently, when dispersal is added to Model (3.26) travelling wave solutions with a minimal speed of propagation exists. The minimal speed c^* of disease propagation can be "identified" and computed for specific kernels.

For all three examples, the addition of dispersal to the epidemic models ((3.20), (3.24), (3.26)) lead to travelling wave solutions with a minimal speed of propagation if $R_0 > 1$, that is, if the disease has the ability to spread locally through populations at demographic equilibrium. Initial conditions with compact support are required, and Weinberger's conditions on g need to be met.

3.4 Geometric Growth

If new recruits arrive at the rate $\mu > 0$ per generation, that is, if $f(P_t) = \mu P_t$ then Eq. (3.2) becomes

$$P_{t+1} = \mu P_t + \gamma P_t = (\mu + \gamma) P_t \tag{3.31}$$

implies

$$P_t = (\mu + \gamma)^t P_0. \tag{3.32}$$

Hence P_t converges to zero when $|\mu + \gamma| < 1$. If we define the demographic basic reproductive number R_d as the average number of offsprings produced by a typically small pioneer population (P_0) over its lifetime then

$$R_d = \frac{\mu}{1 - \gamma}. \tag{3.33}$$

If $R_d < 1$, the population becomes extinct while if $R_d > 1$, the population grows at a geometric rate.

The epidemic Model (3.4), with geometric growth becomes

$$S_{t+1} = \varphi(S_t, I_t) = Q(z_t)\mu P_t + \gamma Q(z_t)S_t + \gamma(1-\sigma)I_t, \tag{3.34a}$$

$$I_{t+1} = \psi(S_t, I_t) = (1-Q(z_t))\mu P_t + \gamma(1-Q(z_t))S_t + \gamma\sigma I_t, \tag{3.34b}$$

with incidence,

$$z_t = \frac{I_t}{(\mu+1)P_t}. \tag{3.35}$$

System (3.34) can be reduced to a single equation via the use of proportions. In fact, letting $s_t = \frac{S_t}{P_t}$ and $i_t = \frac{I_t}{P_t}$ $(s_t + i_t = 1)$ we see that

$$s_{t+1} = \varphi(s_t, i_t) = \frac{\mu}{\mu+\gamma}Q(z_t) + \frac{\gamma}{\mu+\gamma}Q(z_t)s_t + \frac{\gamma}{\mu+\gamma}(1-\sigma)i_t, \tag{3.36a}$$

$$i_{t+1} = \psi(s_t, i_t) = \frac{\mu}{\mu+\gamma}(1-Q(z_t)) + \frac{\gamma}{\mu+\gamma}(1-Q(z_t))s_t + \frac{\gamma}{\mu+\gamma}\sigma i_t \tag{3.36b}$$

with incidence

$$z_t = \frac{i_t}{(\mu+1)}. \tag{3.37}$$

The substitution $s_t = 1 - i_t$ reduces System (3.36) to the following one-dimensional autonomous system for i_t

$$i_{t+1} = \frac{\mu}{\mu+\gamma}(1-Q(z_t)) + \frac{\gamma}{\mu+\gamma}(1-Q(z_t))(1-i_t) + \frac{\gamma}{\mu+\gamma}\sigma i_t. \tag{3.38}$$

3.4.1 Basic Reproductive Number with Geometric Growth

The basic reproductive number, R_0, can be easily computed from the linearization of the one dimensional equation Eq. (3.38), near the disease free equilibrium $(s_0, i_0) = (1, 0)$ with incidence provided by Eq. (3.37). In fact, since $g'(0) = \frac{\alpha}{\mu+1} + \frac{\gamma\sigma}{\mu+\gamma}$ therefore

$$R_0 = \frac{\alpha(1-\gamma)R_d + \alpha\gamma}{[(1-\gamma)R_d + 1][(1-\gamma)R_d + \gamma(1-\sigma)]}\ , \tag{3.39}$$

where

(a) $\frac{1}{[(1-\gamma)R_d+1][1-\gamma+\gamma(1-\sigma)]}$ denotes the average number of generations an individual spends as infected before death or recovery, weighted by demographic effects.

(b) α denotes the average effective transmission rate and $\alpha(1-\gamma)R_d = \alpha\mu$ the contribution to secondary cases by infected offsprings, weighted by demographic effects.

In the absence of demography, $R_d = 1$, Eq. (3.39) reduces to $R_0 = \frac{\alpha}{(2-\gamma)(1-\gamma\sigma)}$, that is, we recover the formula for the basic reproductive number of the epidemic model with constant recruitment. If $R_d \neq 1$, demography impacts disease dynamics, that is, it plays a role in R_0. When $R_0 > 1$, the epidemic grows but when $0 \leq R_0 \leq 1$, the disease dies out. The following theorem collect these results (Castillo-Chavez and Yakubu 2001).

Theorem 3.4.1. *Let α be a positive constant.*

(a) If $R_d < 1$, the total population, $P_t = S_t + I_t$, decreases to zero at a geometric rate; if $R_d > 1$, the total population increases at a geometric rate; and if $R_d = 1$ the total population remains fixed at its initial value.

(b) When $R_d < 1$ and $R_0 < 1$ the proportion $\frac{I_t}{P_t}$ of infectives in the total population tends to zero as $t \to \infty$, while the proportion $\frac{S_t}{P_t}$ of susceptibles tends to one as $t \to \infty$. That is, they tend to the disease free equilibrium $(1, 0)$, where S_t decreases at the same (geometric) rate as P_t.

(c) When $R_d < 1$ and $R_0 > 1$ the proportion $\frac{I_t}{P_t}$ of infectives and $\frac{S_t}{P_t}$ of susceptibles tends to the positive numbers, $\frac{I^*}{P^*}$ as $t \to \infty$ and $1 - \frac{I^*}{P^*}$ as $t \to \infty$, respectively. That is, they tend to the endemic equilibrium $\left(1 - \frac{I^*}{P^*}, \frac{I^*}{P^*}\right)$, where S_t, I_t and P_t all decrease at the same (geometric) rate.

(d) When $R_d > 1$ and $R_0 < 1$ the proportion $\frac{I_t}{P_t}$ of infectives in the total population tends to zero as $t \to \infty$, while the proportion $\frac{S_t}{P_t}$ of susceptibles tends to one as $t \to \infty$. Therefore, the population tends to the disease free equilibrium $(1, 0)$ with S_t increasing at the same (geometric) rate as P_t.

(e) When $R_d > 1$ and $R_0 > 1$ the proportion $\frac{I_t}{P_t}$ of infectives and $\frac{S_t}{P_t}$ of susceptibles in the total population tend to the positive numbers, $\frac{I^*}{P^*}$ as $t \to \infty$ and $1 - \frac{I^*}{P^*}$ as $t \to \infty$, respectively. Therefore, these proportions tend to the endemic equilibrium $\left(1 - \frac{I^*}{P^*}, \frac{I^*}{P^*}\right)$. Here S_t, I_t and P_t increase at the same (geometric) rate.

Proof. The total population obeys, $P_{t+1} = (\mu + \gamma)P_t$ which implies that the demographic reproductive number is $R_d = \frac{\mu}{1-\gamma}$. That is, $R_d < 1$ implies that P_t decreases geometrically to zero while $R_d > 1$ implies that P_t increases geometrically to infinity.

Now we let $s_t = \frac{S_t}{P_t}$ and $i_t = \frac{I_t}{P_t}$ and prove that if $R_0 < 1$ then solutions (s_t, i_t) of System (3.36) approach the equilibrium $(1, 0)$ as $t \to \infty$ while if $R_0 > 1$, the solutions (s_t, i_t) of System (3.36) tends to an unique endemic equilibrium, $(s^*, i^*) \in (0, 1) \times (0, 1)$ as $t \to \infty$ $(s_t + i_t = 1)$.

The proof of the theorem is exactly as the proof of Theorem 3.2.1 with the rescaled (by $(\mu+\gamma)P_t$) reproduction function for the infected individuals of System (3.36) given by $(s_t = 1 - i_t)$

$$h(i) = \frac{\mu}{\mu + \gamma}(1 - e^{\frac{-\alpha i}{\mu+1}}) + \frac{\gamma}{\mu + \gamma}(1 - e^{\frac{-\alpha i}{\mu+1}})(1 - i) + \frac{\gamma}{\mu + \gamma}\sigma i.$$

where $h : [0, 1] \to [0, 1]$. □

In 2007 Yakubu extended the framework of the model presented here and in Rios-Soto et al. (2006) to include both compensatory and overcompensatory pop-

ulation dynamics with and without Allee effect. He showed that the demographic dynamics drive both the susceptible and infective dynamics.

3.5 Integrodifference Epidemic Models with Geometric Growth

If we assume (as above) that dispersal follows mortality and that the disease does not affect the dispersal process, then we can formulate the following systems of integrodifference equations:

$$S_{t+1}(x) = \int_{-\infty}^{\infty} \varphi(S_t(y), I_t(y))\, k(x-y)\, dy, \tag{3.40a}$$

$$I_{t+1}(x) = \int_{-\infty}^{\infty} \psi(S_t(y), I_t(y))\, k(x-y)\, dy \tag{3.40b}$$

with S_{t+1} and I_{t+1} given by Model (3.34). Note that by summing these two equations, under geometric growth, we obtain

$$P_{t+1}(x) = \int_{-\infty}^{\infty} [f(P_t(y)) + \gamma P_t(y)]\, k(x-y)\, dy \tag{3.41}$$

where $f(P_t) = \mu P_t$. Using proportions, the system reduces to

$$s_{t+1}(x) = \int_{-\infty}^{\infty} \varphi(s_t(y), i_t(y))\, k(x-y)\, dy, \tag{3.42a}$$

$$i_{t+1}(x) = \int_{-\infty}^{\infty} \psi(s_t(y), i_t(y))\, k(x-y)\, dy \tag{3.42b}$$

with $s_t + i_t = 1$.

System (3.42) is equivalent, using $s_t + i_t = 1$, to the single integrodifference equation

$$i_{t+1}(x) = \int_{-\infty}^{\infty} g(i_t(y))\, k(x-y)\, dy \tag{3.43}$$

with

$$g(i_t(y)) = \frac{\mu}{\mu+\gamma}(1 - Q(z_t(y))) + \frac{\gamma}{\mu+\gamma}(1 - Q(z_t(y)))(1 - i_t(y)) + \frac{\gamma}{\mu+\gamma}\sigma i_t(y), \tag{3.44}$$

where

$$z_t(y) = \frac{i_t(y)}{\mu+1} \qquad \text{and} \qquad R_d = \frac{\mu}{1-\gamma}. \tag{3.45}$$

The function g is nonnegative and $g'(0) = \frac{\alpha}{\mu+1} + \frac{\gamma\sigma}{\mu+\gamma}$ gives the linearization that generates R_0. The task once again is to determine the conditions under which the function g satisfies Weinberger's conditions, specifically Conditions (ii) and (iii) (page 20) when $f(P_t) = \mu P_t$ and $Q(z_t) = e^{-\alpha z_t}$.

3.5.1 Example with Overlapping Generations (SIS)

The case where $\gamma > 0$ leads to

$$S_{t+1} = \varphi(S_t, I_t) = Q(z_t)\mu P_t + \gamma Q(z_t)S_t + \gamma(1-\sigma)I_t, \tag{3.46a}$$

$$I_{t+1} = \psi(S_t, I_t) = (1 - Q(z_t))\mu P_t + \gamma(1 - Q(z_t))S_t + \gamma\sigma I_t \tag{3.46b}$$

or in re-scaled variables to

$$g(i_t(y)) = \frac{\mu}{\mu+\gamma}(1 - e^{\frac{-\alpha i_t(y)}{\mu+1}}) + \frac{\gamma}{\mu+\gamma}(1 - e^{\frac{-\alpha i_t(y)}{\mu+1}})(1 - i_t(y)) + \frac{\gamma}{\mu+\gamma}\sigma i_t(y) \tag{3.47}$$

with $g'(0) = \frac{\alpha}{\mu+1} + \frac{\gamma\sigma}{\mu+\gamma}$, and $s_t + i_t = 1$. The function defined by Eq. (3.47) satisfies all Weinberger's conditions in its natural form except Condition (iii). In particular g is not monotonic increasing unless

$$\frac{\alpha}{\mu+1}[\mu + \gamma(1 - i_t(y))e^{\frac{-\alpha i_t(y)}{\mu+1}}] + \gamma\sigma > \gamma(1 - e^{\frac{-\alpha i_t(y)}{\mu+1}}). \tag{3.48}$$

Hence, there are SIS epidemic models, with geometric growth that support travelling wave solutions (when the function g is monotonic increasing in invariant sets such as $[0, i^*]$, that is, Eq. (3.48) holds). The disease will spread as long as

$$R_0 = \frac{\alpha(1-\gamma)R_d + \alpha\gamma}{[(1-\gamma)R_d + 1][(1-\gamma)R_d + \gamma(1-\sigma)]} > 1 \tag{3.49}$$

and the disease spread does not depend on whether the population is geometrically increasing ($R_d > 1$) or decreasing ($R_d < 1$). As long as $R_0 > 1$, there will be disease spread and a travelling wave solution will exist (in the re-scaled variables provided Eq. (3.48) holds).

3.5.2 Example with Non-Overlapping Generations ($SI, \gamma \equiv 0$)

When $\gamma = 0$, Model (3.46) reduces to the SI (susceptible-infected) model

$$S_{t+1} = \varphi(S_t, I_t) = Q(z_t)\mu P_t, \tag{3.50a}$$

$$I_{t+1} = \psi(S_t, I_t) = (1 - Q(z_t))\mu P_t. \tag{3.50b}$$

The disease reproduction function in the rescaled variables become

$$g(i_t(y)) = \left(1 - \exp\left[\frac{-\alpha i_t(y)}{\mu + 1}\right]\right), \tag{3.51}$$

with $g'(0) = \frac{\alpha}{\mu+1}$ and $R_0 = \frac{\alpha}{\mu+1}$. Straightforward calculations show that Weinberger's conditions hold. Thus a spreading epidemic will ensue (travelling wave solutions will exist), as long as $\alpha > \mu + 1$.

3.5.3 Example with Overlapping Generations ($SI, \gamma > 0$ and $\sigma = 1$)

Consider the case where $\gamma > 0$ and $\sigma = 1$ (no recovery), then Model (3.34) for the SI case reduces to

$$S_{t+1} = \varphi(S_t, I_t) = Q(z_t)\mu P_t + \gamma Q(z_t)S_t, \tag{3.52a}$$

$$I_{t+1} = \psi(S_t, I_t) = (1 - Q(z_t))\mu P_t + \gamma(1 - Q(z_t))S_t + \gamma I_t, \tag{3.52b}$$

with basic reproductive number

$$R_0 = \frac{\alpha(1-\gamma)R_d + \alpha\gamma}{(1-\gamma)R_d[(1-\gamma)R_d + 1]}. \tag{3.53}$$

In this case (in re-scaled variables)

$$\begin{aligned} g(i_t(y)) &= \frac{\mu}{\mu+\gamma}\left(1 - \exp\left[\frac{-\alpha i_t(y)}{\mu+1}\right]\right) \\ &\quad + \frac{\gamma}{\mu+\gamma}\left(1 - \exp\left[\frac{-\alpha i_t(y)}{\mu+1}\right]\right)(1 - i_t(y)) + \frac{\gamma}{\mu+\gamma} i_t(y), \end{aligned} \tag{3.54}$$

with

$$z_t(y) = \frac{i_t(y)}{\mu+1} \tag{3.55}$$

and $g'(0) = \frac{\alpha}{\mu+1} + \frac{\gamma}{\mu+\gamma}$. Since Eq. (3.54) satisfies all Weinberger (1978) applies a spreading epidemic will occur as long as

$$R_0 = \frac{\alpha(1-\gamma)R_d + \alpha\gamma}{[(1-\gamma)R_d + 1][(1-\gamma)R_d]} > 1. \tag{3.56}$$

The epidemic will spread when $R_0 > 1$ even if the population is geometrically increasing ($R_d > 1$) or decreasing ($R_d < 1$). Therefore, epidemic spread will occur if $R_0 > 1$ and if initial conditions have compact support (even though the populations may be dying), that is, when dispersal is added to Model (3.52) a travelling wave solutions with minimal speed of propagation exist.

3.6 Travelling Wave Solutions and Minimal Speed of Propagation c^*

We search for travelling wave solutions of

$$I_{t+1}(x) = \int_{-\infty}^{\infty} g(I_t(y))\, k(x-y)\, dy, \tag{3.57}$$

that is, solutions of the form $I_t(x) = w(\phi)$ where $\phi = x - ct$. Direct substitution of this solution into (3.57) yields

$$w(\phi - c) = \int_{-\infty}^{\infty} g(w(\eta))\, k(\phi - \eta)\, d\eta \tag{3.58}$$

where $\eta = y - ct$.

The two fixed points $I_1 = 0$ and $I_2 = I^*$ are constant solutions of Eq. (3.58). Typically the focus is on non-negative heteroclinic curves that connect these two fixed points, that is, solutions that tend to $I_2 = I^*$ as $x \to -\infty$ and to $I_1 = 0$ as $x \to \infty$ yielding right moving waves.

The minimum wave speed can be obtained from the local behavior of Eq. (3.58) in the neighborhood of $I_0 = 0$. The minimum wave speed c^*, obtained in Weinberger (1978, 1982), is given by

$$c^* = \min_{\rho>0} \left\{ \frac{1}{\rho}\ \ln\left[g'(0)m(\rho)\right] \right\} \tag{3.59}$$

where $m(\rho) = \langle e^{\rho x} \rangle = \int_{-\infty}^{\infty} e^{\rho x} k(x) dx$ is the moment generating function of the kernel $k(x)$ and $\rho > 0$. Weinberger showed that models of integrodifference equations (under Conditions (i)-(iv) (page 20-20) satisfied by the examples, sometimes under some parameter restrictions) support travelling wave solutions with constant wave speeds c, $c \geq c^*$. Hence, c^*, the moment wave speed will be the speed at which the disease spreads.

Our spatial simulations on the spread of infectives use normal redistribution kernels $\mathcal{N}(0, \sigma_n)$:

$$k(x) = \frac{1}{\sigma_n\sqrt{2\pi}} \exp\left(-\frac{x^2}{2\sigma_n^2}\right), \tag{3.60}$$

that is, kernels with exponentially bounded tails, and initial conditions with compact support. For the normal redistribution kernel, with mean zero and standard deviation σ_n, the moment generating function is $m(\rho) = e^{\frac{\sigma_n^2\rho^2}{2}}$ and the corresponding minimum wave speed is

$$c^* = \min_{\rho>0}\left\{\frac{1}{\rho}\ \ln\left[g'(0)e^{\frac{\sigma_n^2\rho^2}{2}}\right]\right\} = \sigma_n\sqrt{2\ln[g'(0)]}. \tag{3.61}$$

The minimum speed for the dispersion of the infective population that uses the epidemic model given by Model (3.20) and normal redistribution kernel in Eq. (3.57) is

$$c^* \ = \ \sigma_n\sqrt{2\ \ln\left[\frac{\alpha}{(2-\gamma)} + \gamma\sigma\right]} \tag{3.62}$$

since $g'(0) = \frac{\alpha}{(2-\gamma)} + \gamma\sigma$. For the case of non-overlapping generations, that is, the case with $\gamma = 0$, the minimum speed c^* will be given by (3.61) but with $g'(0) = \frac{\alpha}{2}$; and for the case of overlapping generations SI, with $\gamma > 0, \sigma = 1$ the minimum speed of propagation will be given by (3.61) but with $g'(0) = \frac{\alpha}{(2-\gamma)} + \gamma$. Similarly formulas for the examples with geometric growth can be generated, i.e., for the case of the SIS with non-overlapping generations and normal redistribution kernel

$$c^* \ = \ \sigma_n\sqrt{2\ \ln\left[\frac{\alpha}{\mu+1} + \frac{\gamma\sigma}{\mu+\gamma}\right]}. \tag{3.63}$$

In general, extracting the shape of travelling waves is difficult. Kot (1992) computed the shape for the exponential and bilateral exponential kernels through his adaptation of the methods used in Murray (1989, 2002).

3.7 Illustrative Simulations

Figure 3.1 shows how the minimum speed of propagation c^* is affected by changes in parameters. We plot c^* versus the parameters γ, α, σ, and the standard deviation of the normal distribution σ_n using Eq. (3.62). The graphs show that c^* increases as these parameters increase. The graphs and the formula show that the standard deviation σ_n is directly proportional to c^* while σ and α, the fraction of individuals that remain infected and the transmission coefficient are the parameters from the epidemic model which affects the speed of propagation the most. That is, the higher the transmission rate ($\alpha > 0$) and the longer individuals remain infected the faster the speed of propagation. Hence, local and global measures of control, to prevent the advancement of an epidemic include decreasing the movement of infected individuals or reducing transmission coefficient and the average-infectious period (treatment or isolation), that is, increasing the recovery rate $1 - \sigma$.

Illustrative simulations for models with constant recruitment ((3.20), (3.24), (3.26)) and with geometric recruitment ((3.46), (3.50), (3.52)) with normal ($\mathcal{N}(0, \sigma_n)$) redistribution kernels are included using the parameter range where I^* is stable and g is monotone, thus the wave profile is monotone. The parameter range where g is non-monotone will be considered in the next chapter. The "probability" of not becoming infected is modeled by $Q(z_t) = e^{-\alpha z_t}$ where $z_t = \frac{I_t}{\Lambda + \Lambda^*}$ for the case of constant recruitment and $\Lambda \equiv 500$. For the case of geometric growth $z_t \equiv \frac{i_t}{\mu+1}$ with total population $s_t + i_t = 1$. In all figures we choose values of the parameters that guarantee $R_0 > 1$ and initial conditions with compact support, that is, for the case of constant recruitment,

$$I_0(x) > 0,\ x \in [-\delta, \delta] \text{ and } I_0(x) \equiv 0,\ x \notin [-\delta, \delta] \tag{3.64}$$

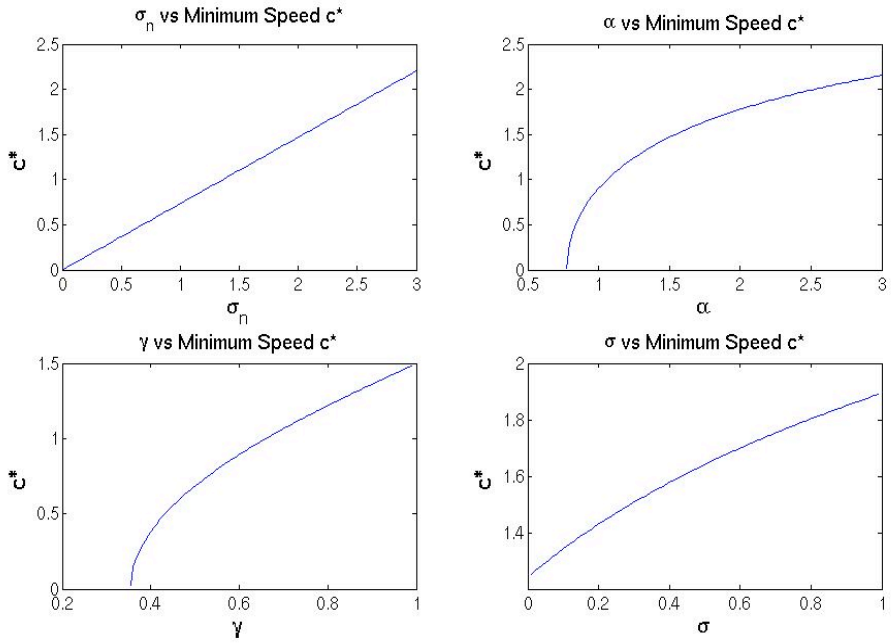

Figure 3.1: Minimum wave speed (Eq. (3.62)) of the integrodifference equation for SIS Model (3.20) with constant recruitment. The minimum wave speed is an increasing function of the four parameters γ, α, σ and the standard deviation of the normal distribution σ_n.

for some δ small. While initial conditions for the susceptibles are $S_0(x) \equiv \Lambda^* - I_0(x)$ for $x \in [-m, m]$ for some m large.

3.7.1 Simulations with Constant Recruitment

Figure 3.2 provides traveling waves for the SIS model with overlapping generations and constant recruitment where the probability of survival for each generation γ and the probability of not recovering σ, have been fixed at the values 0.98 and 0.25 respectively. Here, the transmission constant α is 1.5. Since $\Lambda \equiv 500$ the total population is $P_t = \Lambda^* \equiv 25000$. The integrodifference equation was iterated for times t=0 to t=22 on the domain $-15 \leq x \leq 15$ with initial data $I_0(x) = 750$ on

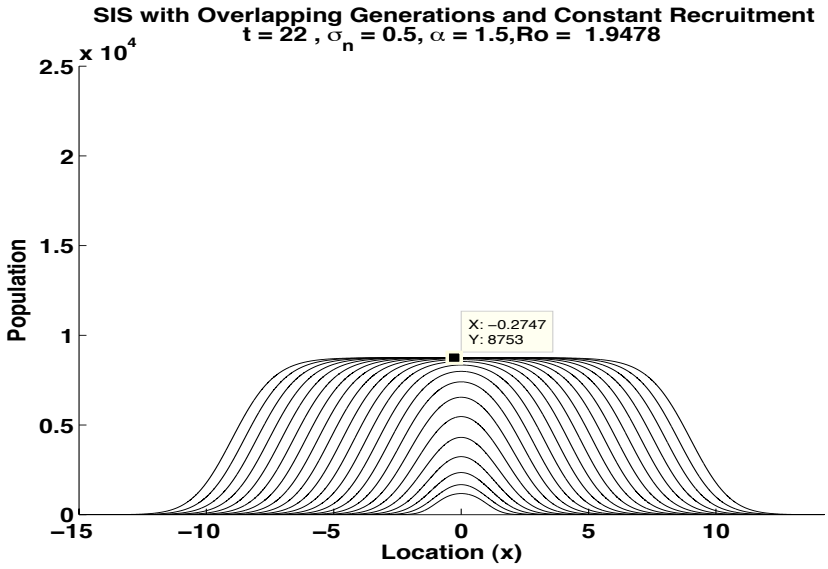

Figure 3.2: Travelling wave solutions for the SIS model with overlapping generations and constant recruitment using the normal redistribution kernel with $\sigma_n = 0.5$ and where $R_0 = 1.9478 > 1$. Here $I^* = 8753$ and $c^* = 0.5195$. The graph above represents a growing wave of infectious which is replacing the susceptible population.

$-1 \leq x \leq 1$ and $I_0(x) = 0$ elsewhere.

Figure 3.3 shows the case for the SI epidemic model with overlapping generations and constant recruitment, when the probability of survival is $\gamma = 0.55$ and the transmission constant α is 1.5. Thus with $\Lambda \equiv 500$ the total population is $P_t = \Lambda^* \approx 1111$. In this case the iteration was made for times t=0 to t=28 on the domain $-45 \leq x \leq 45$ with initial data $I_0(x) = 45$ on $-2 \leq x \leq 2$ and $I_0(x) = 0$ elsewhere.

The traveling waves for the SI model with non-overlapping generations and constant recruitment is shown in Figure 3.4 with $\alpha = 2.8$ and where the total population is $P_t = 500$, since in this case $\Lambda = \Lambda^*$. Here, the integrodifference equation was iterated for times t=0 to t=30 on the domain $-55 \leq x \leq 55$ with

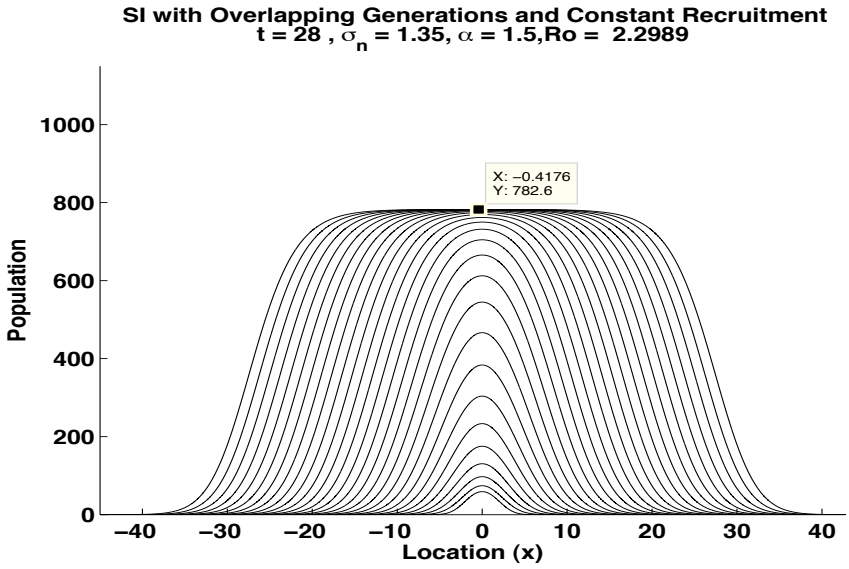

Figure 3.3: Travelling wave solutions for SI model with overlapping generations and constant recruitment, $\sigma_n = 1.35$, $I^* = 782$, $c^* = 1.295$ and $R_0 = 2.2989 > 1$.

initial data $I_0(x) = 9$ on $-3 \leq x \leq 3$ and $I_0(x) = 0$ elsewhere.

It has been shown numerically that distribution kernels with fat tails (leptokurtic distributions) lead to faster spread (dispersal) (Kot et al. 1996). These results are well known in the ecological literature for known growth functions that are monotonically increasing (Kot et al. 1996). Here, the comparable results in Allen and Ernest (2002) are confirmed using a kernel with exponentially bounded tail and monotone growth functions. The difference between Allen and Ernest's work and ours is that our discrete-time epidemic model is derived from first principles where as their discrete-time epidemic model can admit negative solutions. For population models with differential equations Medlock and Kot (2003) used integrodifferential equations to compare an SI epidemic model, with distributed contacts (Mollison 1972a, 1977) to a newer model (integrodifferential equations) with dispersing infectives. Similar to our work, Medlock and Kot found that symmetric kernels with

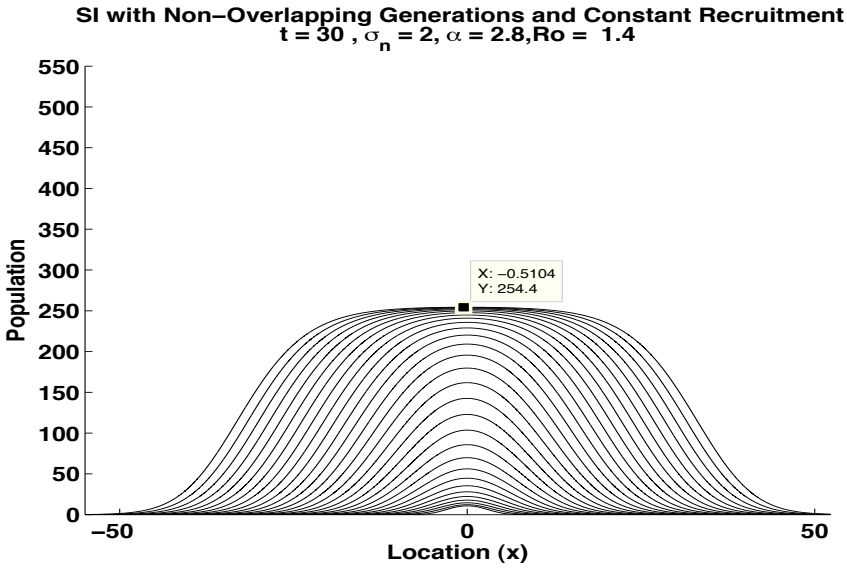

Figure 3.4: Travelling wave solutions for SI model with non-overlapping generations, $\sigma_n = 2$, $I^* = 254$, $c^* = 1.64$ and $R_0 = 1.4 > 1$.

moment generating functions (like the normal redistribution kernel) produce constant speed travelling waves. Medlock and Kot also approximated the shape of travelling waves for these two models.

3.7.2 Simulations with Geometric Growth

Illustrative simulations for the integrodifference equation system with geometric growth, System (3.42), and the SIS rescaled epidemic model with overlapping generations, Model (3.46), are given below. Values of the parameters that guarantee $R_0 > 1$ are chosen as well as initial conditions with compact support, where $s_0(x) = 1 - i_0(x)$.

Figure 3.5 provides traveling waves for the SIS model with overlapping generations and geometric recruitment when $R_d < 1$ and $R_0 > 1$. Here, $\gamma = 0.98$ and $\sigma = 0.25$. The transmission constant α is 1.2. The integrodifference equation

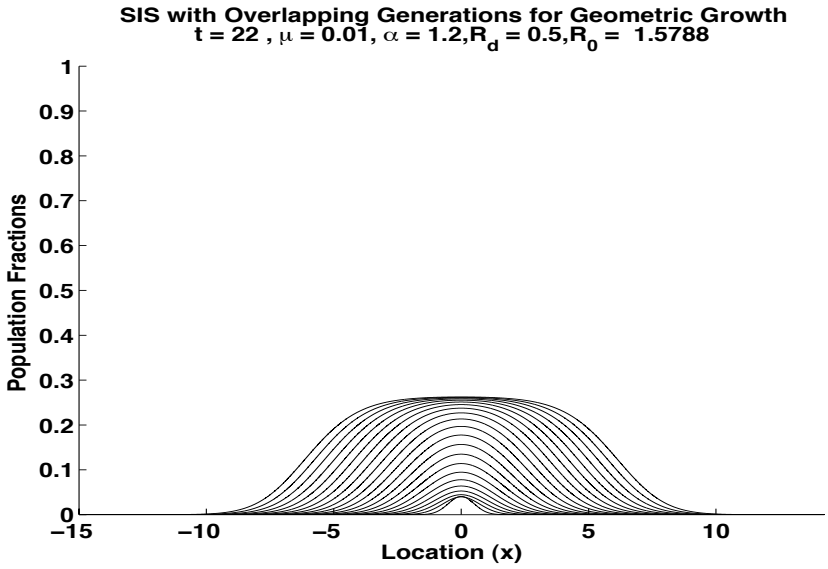

Figure 3.5: Travelling wave solutions for the SIS model with overlapping generations and geometric recruitment using the normal redistribution kernel with $\sigma_n = 0.5$, where $R_d = 0.5 < 1$, $R_0 = 1.5788 > 1$ and $c^* = 0.4252$.

was iterated for times t=0 to t=22 on the domain $-15 \leq x \leq 15$ with initial data $i_0(x) = 0.1$ on $-1 \leq x \leq 1$ and $i_0(x) = 0$ elsewhere.

In Figure 3.6, traveling waves for the SIS model with overlapping generations and geometric recruitment are shown when R_d and R_0 are both greater than one. The transmission constant is $\alpha = 1.2$. The integrodifference equation was iterated from t=0 to t=28 on the domain $-15 \leq x \leq 15$ with initial data $i_0(x) = 0.1$ on $-1 \leq x \leq 1$ and $i_0(x) = 0$ elsewhere. The graphs show travelling waves as long as $R_0 > 1$ regardless of the value of R_d (for an analogous situation, epidemic in dying populations, in the non-spatially explicit case see Faina et al. 2005).

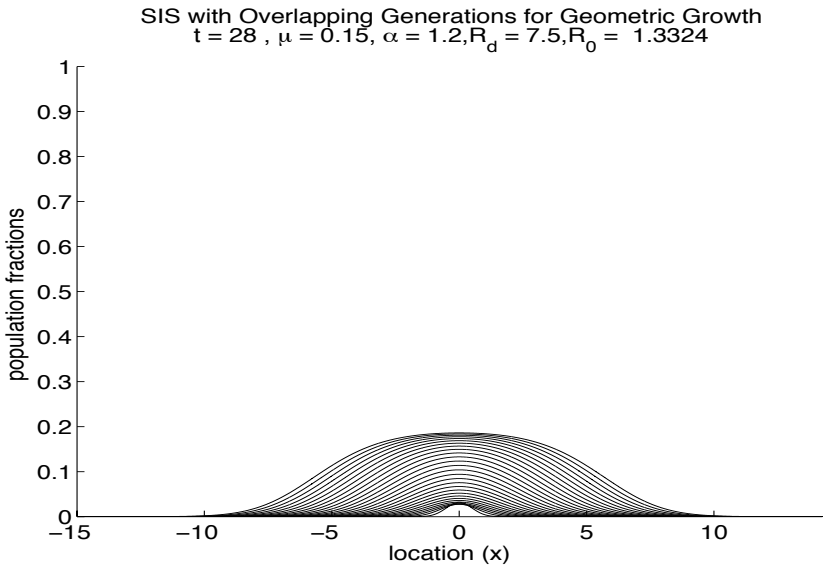

Figure 3.6: Travelling wave solutions for the SIS model with overlapping generations and geometric recruitment using the normal redistribution kernel with $\sigma_n = 0.5$, where $R_d = 7.5 > 1$, $R_0 = 1.3324 > 1$ and $c^* = 0.6983$.

3.8 Discussion

Traditionally one dimensional integrodifference equations models have been used to study the ecological invasion of populations with non-overlapping generations. In this chapter one dimensional integrodifference equations models are introduced to study epidemic invasions for populations with non-overlapping and overlapping demographic *epidemiological* generations. In oder to apply Weinberger's results, monotone growth functions are constructed from first principles for populations with overlapping and non-overlapping generations. The general discrete epidemic model used here is derived from first principles, that is, it is not a discretization of known continuous models. It is shown that when dispersal is added to the epidemic model, travelling wave solutions exist and the minimum speed of propagation can be "computed" as long as the epidemic growth function is monotonic increasing

and the initial conditions have compact support. This analysis applies when we restrict non-monotone g-maps to g-invariant subsets that is, subsets that are invariant under the map g, subsets where g is monotonic increasing. Simulations that relate the parameters of the model with the minimum speed of propagation c^* are included. Numerically, it is seen that c^* seem to be positively correlated to changes in γ, α, σ and σ_n (Fig. 3.1). In this case, we found that to control the advancement of an epidemic the attention should be on decreasing the movement of infected individuals as well as reducing the transmission coefficient (α) as well as the infectious period, that is, increasing $1 - \sigma$. Numerical simulations that corroborate the observations are also included using the normal redistribution kernel for $R_0 > 1$.

CHAPTER 4

EPIDEMIC SPREAD WITH NON-MONOTONE EPIDEMIC FUCTIONS

In the previous chapter an SIS (susceptible-infected-susceptible) epidemic model that allow for the infection of newborn individuals was introduced but the case where the epidemic growth function is non-monotone was not explored. Here, such a case is considered. In addition, numerical studies of epidemics spreading in two spatial dimensions are conducted.

The focused is on the SIS epidemic model (with overlapping generations)

$$S_{t+1} = \varphi(S_t, I_t) = Q(z_t)f(P_t) + \gamma Q(z_t)S_t + \gamma(1-\sigma)I_t, \tag{4.1a}$$

$$I_{t+1} = \psi(S_t, I_t) = (1-Q(z_t))f(P_t) + \gamma(1-Q(z_t))S_t + \gamma\sigma I_t \tag{4.1b}$$

where

$$z_t = \frac{I_t}{P_t + f(P_t)}, \tag{4.2}$$

and $Q(z_t) = e^{-\alpha z_t}$. The natural function g does not satisfy in general Condition (iii) (page 20), in Weinberger's result as it is decreasing somewhere over its range. In the previous case (Chapter 3), g-invariant subsets $[0, I^*]$ ($I^* > 0$ a fixed point of g) are identified where g is monotonic increasing. Over these invariant subsets, Weinberger's results naturally apply.

Non-monotone increasing reproductive infectious functions g arise frequently. Thus, the need to understand their role on the spatial spread of diseases is essential. First, we explore numerically the population dynamics using a known non-monotone growth function, the discrete logistic growth function. We proceed to outline recent mathematical advances to the case of non-monotone functions.

We use the most recent theoretical results (Li et al. 2008) to justify our numerical results.

4.1 Non-Monotone Growth Functions: The Logistic Equation

In Chapter 3, it was shown that when dispersal is added to epidemic models, travelling wave solutions exist and a minimum speed of propagation (c^*) can be identified under assumptions that include, a monotone increasing epidemic growth function and initial conditions with compact support. We use the fixed points $g(0) = 0$ and $g(I^*) = I^*$ to identify g-invariant subsets where g is monotone. Numerical simulations are carried out to gain insights in situations where g is non-monotone, that is, the case of overcompensation on disease dynamics ($[0, I^*]$ is no longer g-invariant). Typically, we will see that Condition (iii) (page 20) does not hold but that there is a stable fixed point I^*, an attracting spiral ($-1 < g'(I^*) < 0$), where attracting spiral translate into oscillations in the tail of the wave.

Kot (1992) was among the first to study integrodifference equations for models with complex g's, for example, g's that may include the rescaled logistic difference equation

$$N_{t+1} = (1 + r)N_t - rN_t^2, \tag{4.3}$$

where r correspond to the population per-capita geometric growth rate, $0 < r < 3$. Kot numerically studied Eq. (2.36), that is,

$$N_{t+1}(x) = \int_{-\infty}^{\infty} g(N_t(y))\, k(x - y)\, dy \tag{4.4}$$

with $g(N_t)(y) = (1 + r)N_t - rN_t^2$. He used a bilateral exponential redistribution kernel in his analysis to obtain the shape of the travelling wave as well as on the

simulations. The approach to equilibrium for the logistic growth function is non-monotone for some values of r. The logistic difference equation exhibits complex dynamics that are carried over to the integrodifference equation as r varies.

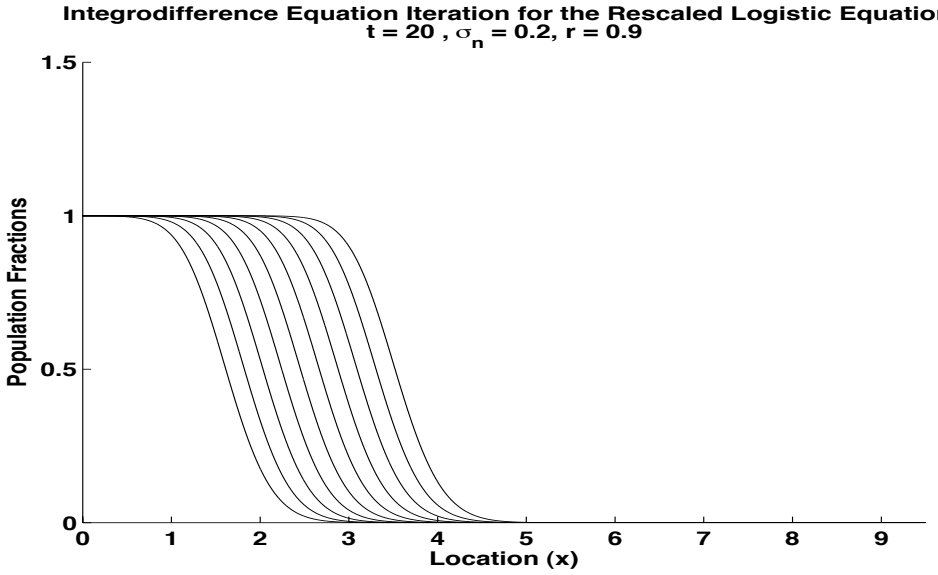

Figure 4.1: Travelling wave solutions for the integrodifference with logistic growth function using the normal redistribution kernel with $\sigma_n = 0.2$, $r = 0.9$ and where $c^* = 0.227$. The graph show the last 10 solutions of 20 iterations.

Eq. 4.3 has two fixed points $N_1^* = 0$ and $N_2^* = 1$, where $N_1^* = 0$ is stable for the parameter range $-2 < r < 0$ while $N_2^* = 1$ stable for $0 < r < 2$. Since the interest here is to connect the two fixed points to obtain the travelling wave front solution in

$$N_{t+1}(x) = \int_{-\infty}^{\infty} \left[(1+r)N_t(y) - rN_t^2(y)\right] k(x-y)\, dy, \tag{4.5}$$

the case where $N_2^* = 1$ is stable and $N_1^* = 0$ unstable is considered. First, the parameter range is restricted to values of $r \in (0, 2)$. For small values of r, that is, when $0 < r < 1$ the logistic equation is monotone. Hence, all four Weinberger conditions (page 20-20) are satisfied and a speed of propagation exists that can

be computed. Figure 4.1 shows the travelling wave solution for the rescaled logistic equation model with $r = 0.9 < 1$ using the normal redistribution kernel. Numerically it is obseved that for $r \in (0, 1)$ simple monotone travelling waves are obtained. Since the equilibrium $N_2^* = 1$ defines an invariant region ($[0, 1]$) where the logistic function is monotone the wave profile is monotone. It is a rightward moving wave with its positive speed provided by Eq. (3.61) with $g'(0)$ replaced by $N'(0) = 1 + r$.

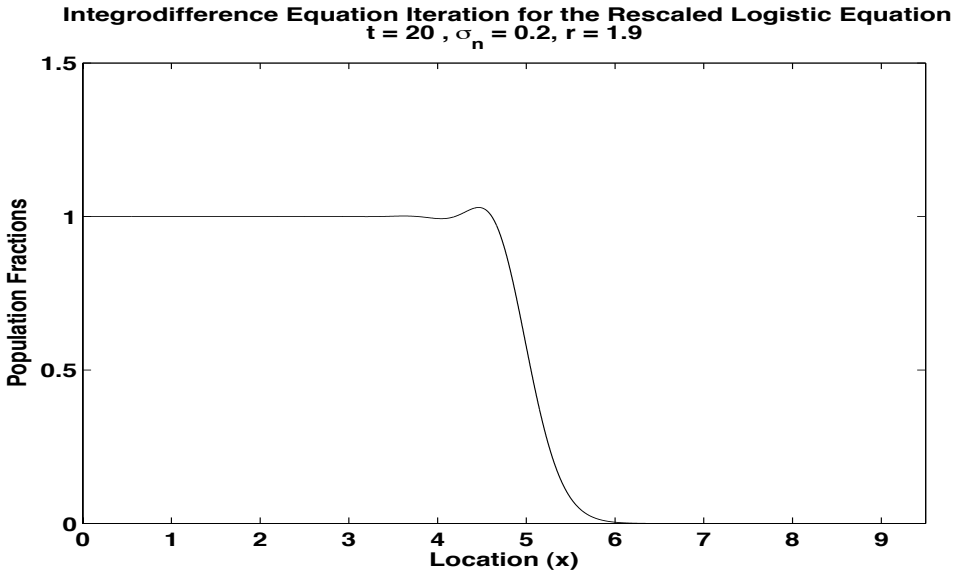

Figure 4.2: Travelling wave solutions with damped oscillations around the fixed point 1 for the rescaled integrodifference logistic equation using the normal redistribution kernel, here $\sigma_n = 0.2$, $r = 1.9$ and $c^* = 0.292$. The graph shows the last of 20 iterations.

At $r = 1$, $N_2^* = 1$ is stable but as r crosses 1 the logistic equation looses its monotonicity. Thus in the parameter range $1 \leq r < 2$ solutions tends to the fixed point $N_2^* = 1$, but via damped oscillations, that is, overshooting the fixed point in a neighborhood of $N_2^* = 1$. In this parameter range the logistic growth function will not satisfy Weinberger's Condition (iii). Numerically it is observed that travelling

wave solutions will exist but with a wave profile that exhibits damped oscillation. Figure 4.2 shows that this is indeed the case for $r = 1.9$ when we use the normal redistribution kernel.

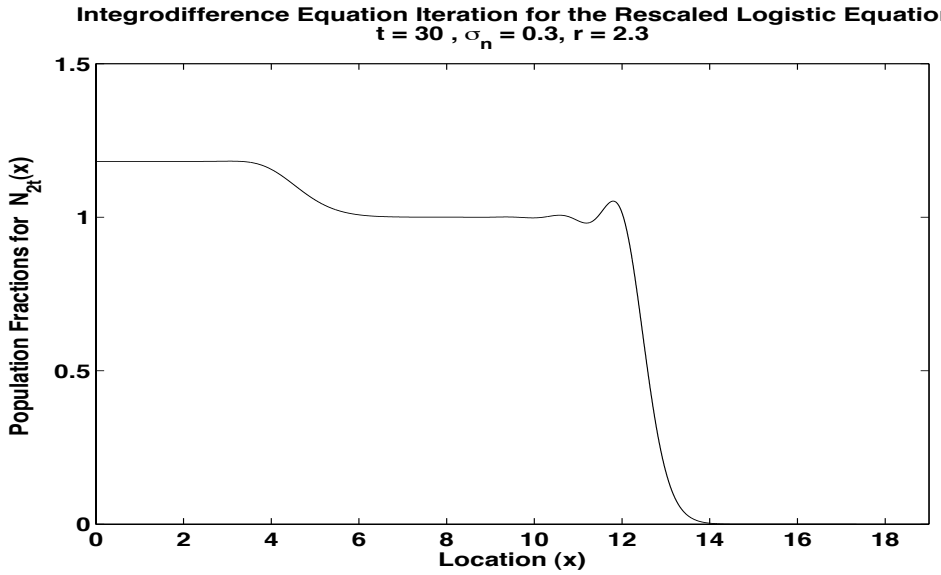

Figure 4.3: "Travelling two-cycle" from every second iterate $2t$ connecting one of the two new fixed points $N_3^* \approx 1.18$, from the second iteration of the logistic map, with zero. Here $\sigma_n = 0.3$ and $r = 2.3$.

For larger r e.g., $r > 2$, $N_2^* = 1$ becomes unstable, a period-2 cycle is born which is stable if $2 < r < \sqrt{6}$. That is, for values of $r \in (2, \sqrt{6})$ two stable fixed points (different than N_1^* or N_2^*) of the second iteration of the rescaled logistic map

$$N_{t+1}^2 = (r+1)^2 N_t - r(r+1)(r+2)N_t^2 + 2r^2(r+1)N_t^3 - r^3 N_t^4, \tag{4.6}$$

appear. The two new fixed points are

$$N_{3,4}^* = \frac{(2+r) \pm \sqrt{r^2 - 4}}{2r}. \tag{4.7}$$

In this case trajectories tend to oscillate around the two fixed points (of the second iterate) depending on initial conditions. Hence, not only Condition (iii) is not met

but also Condition (ii) is not met. There is no longer a travelling wave profile but the existence of a "travelling two-cycle" (Kot 1992), that arises from the two new stable fixed points supported by the second iterate is observed numerically. Simulations show that the wave alternates between two profiles, each linked to a new fixed point N_3^*, N_4^*. Figures 4.3 and 4.4 show the "travelling two-cycle" produce by the integrodifference equation for every second iterate when $r = 2.3$. In Figure 4.3, the "travelling two cycle" connects N_3^* with zero while in Figure 4.4 the "travelling two cycle" connects N_4^* with zero.

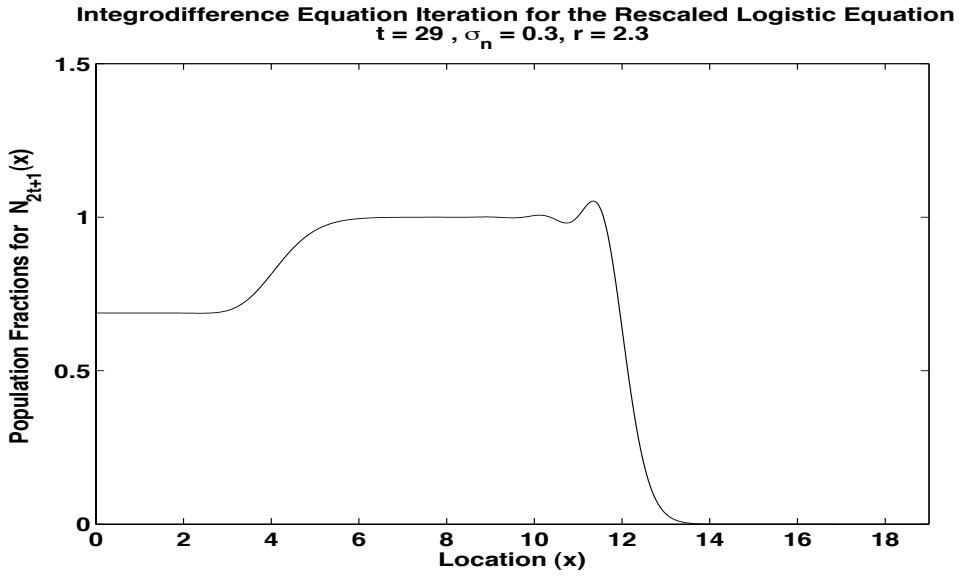

Figure 4.4: "Travelling wave two-cycle" from every second iterate $2t+1$ connecting $N_4^* \approx 0.69$ to zero. Here $\sigma_n = 0.3$ and $r = 2.3$.

The use of the discrete logistic equation in biology carries well understood limitations. The fact that it can take on negative values and that it is not derived from first principles are two of them. Next, we generate non-monotone reproduction functions g in the context of epidemics. The use of these functions does not generate "travelling two cycles" but on the other hand, the growth functions are

derived from first principles and naturally generate oscillatory waves. In other words, there is some hope that there models can be tied into epidemics in natural populations.

4.2 Non-Monotone Growth Functions: Some Theoretical Perspective

Recently, Li et al. (2008) expanded Weinberger's theory of integrodifference equations to include non-monotone growth functions. They show that a spreading speed can still be characterized as the slowest speed of a non-constant travelling wave. They not only proved some impressive theorems but also numerically generated travelling waves using the rescaled Ricker difference equation

$$N_{t+1} = N_t e^{r-N_t}, \tag{4.8}$$

where r is the per-capita growth rate of the population. Their simulations show that the tails of the waves may approach the fixed point either monotonically, in an oscillatory manner, or may continually oscillate around it. The behavior observed by Li et al. for the rescaled Ricker's equation is comparable to the behavior captured by our simulations of the logistic equation in the previous section. They show that travelling waves solutions for Eq. (2.36) with non-monotone growth functions exists for all speed c greater than a minimum rightward spreading speed c^* for, Eq. (2.40), if

(i) There is a positive constant κ_0 such that

a. $g(N)$ is continous for $0 \leq N \leq \kappa_0$;

b. $0 < g(N) \leq \kappa_0$ for $0 < N \leq \kappa_0$; and

c. $g(0) = 0$.

(ii) There is a positive $d \leq \kappa_0$ such that

a. $g(N)$ is nondecreasing for $0 \leq N \leq d$;

b. the specific net growth rate $g(N)/N$ is bounded and nonincreasing for $0 \leq N \leq d$;

c. $g(N)/N > 1$ for $0 \leq N \leq d$; and

d. $g(N)/N \leq g(d)/d$ for $d \leq N \leq \kappa_0$.

(iii) $k(x)$ is a continuous and nonnegative function such that

a. $\int_{-\infty}^{\infty} k(x)\,dx = 1$;

b. the integral

$$m(\epsilon) = \int_{-\infty}^{\infty} k(x)e^{\epsilon x}\,dx \tag{4.9}$$

is finite for at least one positive and one negative value of ϵ.

Condition (ib) requires the existence of an invariant set $0 \leq N \leq \kappa_0$ for g (related to the argument about invariant sets mentioned in Chapter 3). Conditions (iib) and (iic) require at least one fixed point for equation $g^+(N) = N$ on the interval $d \leq N \leq \kappa_0$ where

$$g^+(N) := \max_{0 \leq v \leq N} g(v) \tag{4.10}$$

for $0 \leq N \leq \kappa_0$ (thus κ is define as the smallest fixed point of $g^+(N) = N$ that is, $g^+(\kappa) = \kappa$). Condition (iib), (iic) and (iid) require that the function g is right differentiable at 0, that is, $g'(0) > 1$. The requirement $g(N) \leq g'(0)N$ for

$d \leq N \leq \kappa_0$ guarantees that the fixed point 0 is unstable while the fixed point N^* is stable. N^* is defined to be the smallest non-trivial fixed point of $g(N) = N$. Condition (iic) requires the existence of the smallest positive solution θ of the equation $g^-(N) = N$, where

$$g^-(N) := \min\{g(N), g^-(d)\} \tag{4.11}$$

when $0 \leq N \leq d$. The constant θ has the properties

$$0 < \theta \leq N^* \leq \kappa, g^-(\theta) = \theta, \text{ and } g^-(N) > N \text{ for } 0 < N < \theta. \tag{4.12}$$

Condition (iiib) implies the existence of a finite moment generating function, that is, a redistribution kernel with exponentially bounded tails.

The simulations in Kot (1992) suggest that solutions may approach an n-cycle which may converge in shape to a travelling wave with speed nc^*. There is no proof of Kot's conjecture.

For values of $r \in (0, 1)$ the logistic equation is monotone for $0 \leq N \leq 1$, hence Weinberger's result apply. However, when $r \in [1, 2)$, they do not. The logistic equation looses its monotonicity, at $r = 1$. For $r \in [1, 2)$ $N_1^* = 0$ is still unstable while $N_2^* = 1$ is stable, but g is non-monotone in $[0, 1]$. On the other hand, the existence (not uniqueness) of travelling wave solutions is guaranteed by Li et al.'s results as we show below.

The logistic equation (4.3) is increasing for $0 \leq N \leq x_{max}$ and decreasing for $N \geq x_{max}$ where

$$x_{max} = \frac{1 + r}{2r}. \tag{4.13}$$

The fixed point of the Eq. (4.3) are $N_1^* = 0$ and $N_2^* = 1$, for $1 \leq r < 2$, with N_1^* unstable and N_2^* stable. In order to apply Li et al.'s results, we observe that here

$\kappa_0 = g(x_{max}) = (1+r)^2/4r$ and d can be defined precisely as x_{max} or a number smaller than x_{max}. In fact, we take

$$g^+(u) = \begin{cases} g(u) & \text{if } u \leq 1 \\ g(x_{max}) = \frac{(1+r)^2}{4r} & \text{if } u \geq 1 \end{cases} \tag{4.14}$$

where, $\kappa \equiv \theta = g(x_{max})$ and $g^-(N) \equiv \min\{g(N), g(g(x_{max})) = \frac{(1+r)^3(3-r)}{4r}\}$. With these observations we see that Li et al.'s conditions are satisfied. The simulations in the previous section confirm Li et al.'s results. Therefore, we conclude that travelling wave solutions and a minimum speed of propagation c^* exist even when the growth function is non-monotone. It should be noted that, Li et al.'s results guarantee existence but no uniqueness.

4.3 Dynamics of the Epidemic Growth Function

In 2002 Yakubu and Castillo-Chavez define a function g_i as a *β-monotone concave map* if $g_i'(x_i) > 0$ and $g_i''(x_i) < 0$ for each $x_i \in [0, \beta]$. Population dynamics are compensatory at population sizes in $[0, \beta]$ whenever g_i is a *β-monotone concave map* with a unique positive fixed point in the open interval $(0, \beta)$. When the function is a *β-monotone concave map* and populations in the interval (β, ∞) overshoot the positive fixed point in the closed interval $[0, \beta]$, then g_i describe situations where there is compensatory dynamics at lower densities and overcompensatory dynamics at higher ones. For example, the logistic map for $0 < r < 1$ is an $\frac{1+r}{2r}$-*monotone concave map* since all positive initial populations with densities in the interval $[0, \frac{1+r}{2r}]$ approach the unique positive fixed point monotonically, but initial populations in $(\frac{1+r}{2r}, \infty)$ overshoot the positive fixed point. For values of $r > 1$ the

function fails to be a $\frac{1+r}{2r}$-*monotone concave map* because the unique positive fixed point is outside the interval $(0, \frac{1+r}{2r})$. In this case damped oscillation around the fixed point are observed.

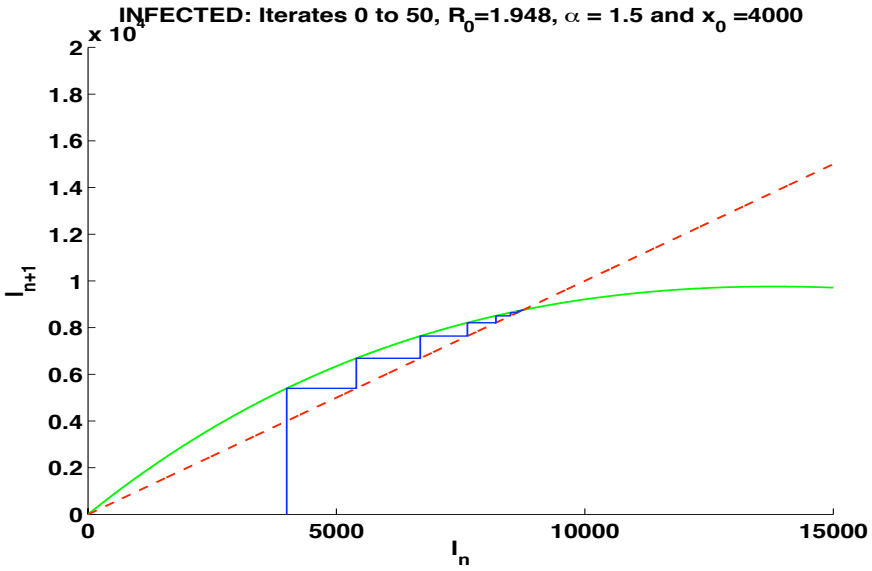

Figure 4.5: Cobweb diagram with 50 iterations for the epidemic growth function with constant recruitment where $\alpha = 1.5$, that is, for a parameter where the epidemic function in Model (3.20) is an I_{max}-*monotone concave map*. Solutions monotonically tend to the unique positive stable fixed point $I^* = 8753$.

The epidemic growth function of the SIS model with overlapping epidemiological generations behaves similar to the logistic equation in the range $r \in (0, 2]$, that is, as a single hump map with two fixed points ($N_1^* = 0$ unstable and $N_2^* = 1$ stable). However, the algebraic complexity of the epidemic equations means that the formulae for x_{max} or d in Li et al. (2008) theorem is difficult to compute explicitly. It is clear (numerically) that the epidemic growth function will be a β-*monotone concave map* for the parameter range up to the value where the function looses its monotonicity. In the case of the constant recruitment model, Model (3.20), if the transmission constant α varies, with the probability of survival and the probability

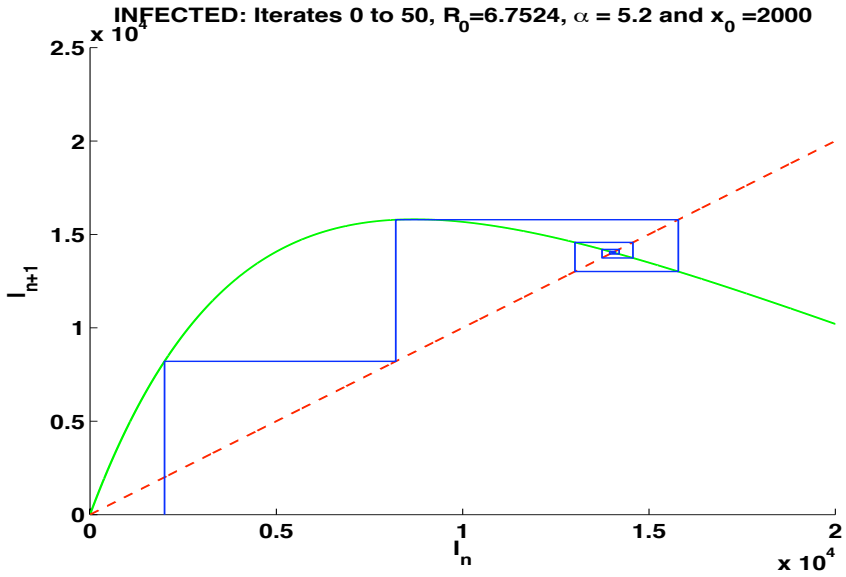

Figure 4.6: Cobweb diagram with 50 iterations for the epidemic growth function with constant recruitment where $\alpha = 5.2$. In this case iterations approach the unique positive fixed point through damped oscillations.

of recover fixed to $\gamma = 0.98$ and $\sigma = 0.25$, respectively, then the epidemic growth function will be an I_{max}-*monotone concave map* for $0 < \alpha < 2.75$, where I_{max} is the maximum point of the epidemic growth function.

Figure 4.5 shows a cobweb diagram for values of $\gamma = 0.98, \sigma = 0.25$ and $\alpha = 1.5$ where the epidemic growth function is an I_{max}-*monotone concave map*. The diagram shows that solutions will monotonically approach the unique positive stable fixed point, $I^* = 8753$. On the other hand, Figure 4.6 shows a cobweb diagram for a value of $\alpha > 2.75$, that is for a value of α where the epidemic growth function is no longer an I_{max}-*monotone concave map*. Here γ and σ are again set to 0.98 and 0.25, respectively, while $\alpha = 5.2$. The spiraling motion implies that iterations converge to the unique positive fixed point $I^* = 8753$ through damped oscillations. Corresponding cobweb diagram for the SIS epidemic model with geometric

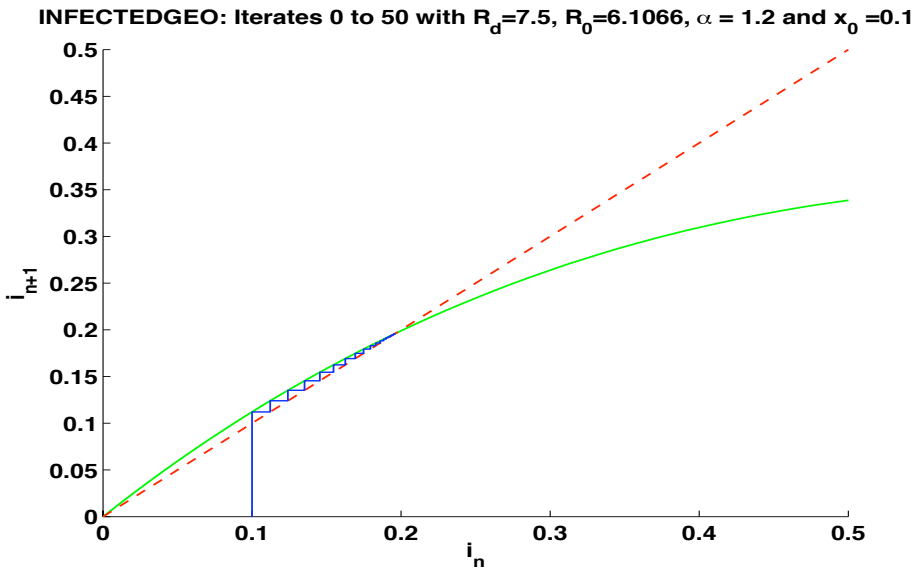

Figure 4.7: Cobweb diagram with 50 iterations for the epidemic growth function with geometric recruitment where $\alpha = 1.2$, that is, for a parameter where the epidemic function in Model (3.36) is an i_{max}-*monotone concave map*. Solutions tend to the unique positive stable fixed point $i^* = 0.18$. Here R_d and R_0 are both greater than one.

growth (in rescaled variables) and $R_d, R_0 > 1$ are shown in Figure 4.7 and Figure 4.8 for values of $\mu = 0.15$. Figure 4.7 shows the case of the i_{max}-*monotone concave map* with $\alpha = 1.2$ while Figure 4.8 shows the cobweb with $\alpha = 5.5$ for the case of damped oscillations around the fixed point i^*, in both figures $R_d, R_0 > 1$.

4.4 Non-monotone Epidemic Growth Function

Numerical simulations of the integrodifference equation for the SIS epidemic model with overlapping generations and either constant or geometric growth, using the normal redistribution kernel, are shown. Emphasis is on the case where the epidemic growth function is non-monotone. In the simulations the probability of survival and of recovery are set for convenience at 0.98 and 0.25, respectively.

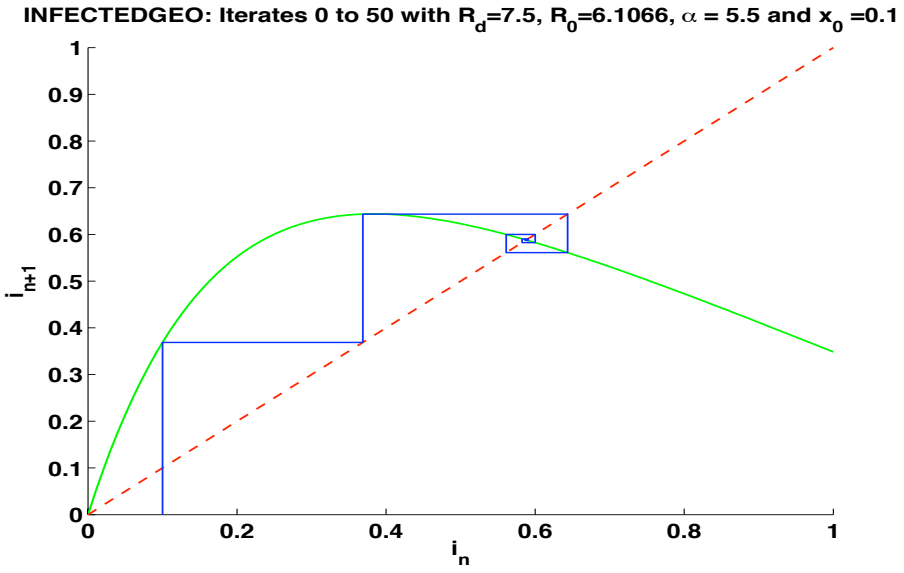

Figure 4.8: Cobweb diagram with 50 iterations for the epidemic growth function with geometric recruitment with R_d and R_0 both greater than one, where $\alpha = 5.5$.

We recall that the epidemic model with constant recruitment given by

$$S_{t+1} = \varphi(S_t, I_t) = f(P_t)Q(z_t) + \gamma Q(z_t)S_t + \gamma(1-\sigma)I_t, \tag{4.15a}$$

$$I_{t+1} = \psi(S_t, I_t) = f(P_t)(1-Q(z_t)) + \gamma(1-Q(z_t))S_t + \gamma\sigma I_t. \tag{4.15b}$$

where $z_t = \frac{I_t}{f(P_t)+P_t}$ and $Q(Z_t) = e^{-\alpha z_t}$ has two fixed points $I_1^* = 0$ and $I_2^* > 0$, with the fixed point 0 stable when $R_0 < 1$ and unstable when $R_0 > 1$ but I_2^* is stable when $R_0 > 1$. When dispersal is added to the SIS epidemic model and $R_0 < 1$ there are no travelling waves solutions for System (3.7). For the case of constant recruitment, $f(P_t) = \Lambda$, it is observed numerically that for values of the transmission constant between $0 < \alpha < 2.75$ the epidemic growth function is monotone, as seen in Figure 4.5 with $\alpha = 1.5$. Therefore, as in the case of the logistic equation for $0 < r < 1$, since g is monotone, the wave profile will be monotone. Figure 4.9 shows the travelling wave profile for the SIS epidemic model with constant recruitment and $\alpha = 1.5$, a rightward moving wave with positive speed

$c^* = 0.519$ provided by Eq.(3.61). Figure 4.10 shows the corresponding travelling wave solutions for the SIS integrodifference epidemic model with geometric growth.

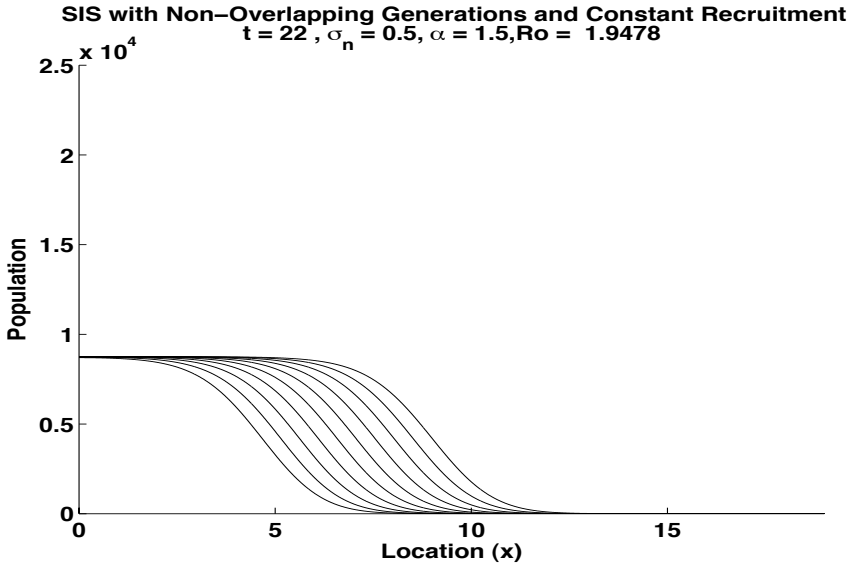

Figure 4.9: Travelling wave solutions for the SIS epidemic model with dispersal and constant recruitment using the normal redistribution kernel with $\sigma_n = 0.5$ and $\alpha = 1.5$. In this case the wave profile is monotone corresponding to the dynamics of the epidemic model. Here, the fixed point is $I^* = 8753$ and $c^* = 0.519$. The graph show the last 10 solutions of 22 iterations.

At $\alpha \approx 2.75$ (for $\gamma = 0.98$ and $\sigma = 0.25$) the epidemic growth function with constant recruitment,

$$g(I) = \left[1 - \exp\left(\frac{-\alpha I}{\Lambda^* + \Lambda}\right)\right][\Lambda^* - \gamma I] + \gamma\sigma I, \tag{4.16}$$

looses monotonicity. Thus, as seen in Figure 4.6, for $\alpha > 2.75$ iterations of the epidemic growth function tend to the unique fixed point $I_2^* > 0$, via damped oscillations. Therefore, solutions of the integrodifference equation will exhibit a travelling wave profile but with damped oscillations around the positive fixed point I_2^*. Figure 4.11 shows indeed that this is the case, where $c^* = 0.877$. Travelling

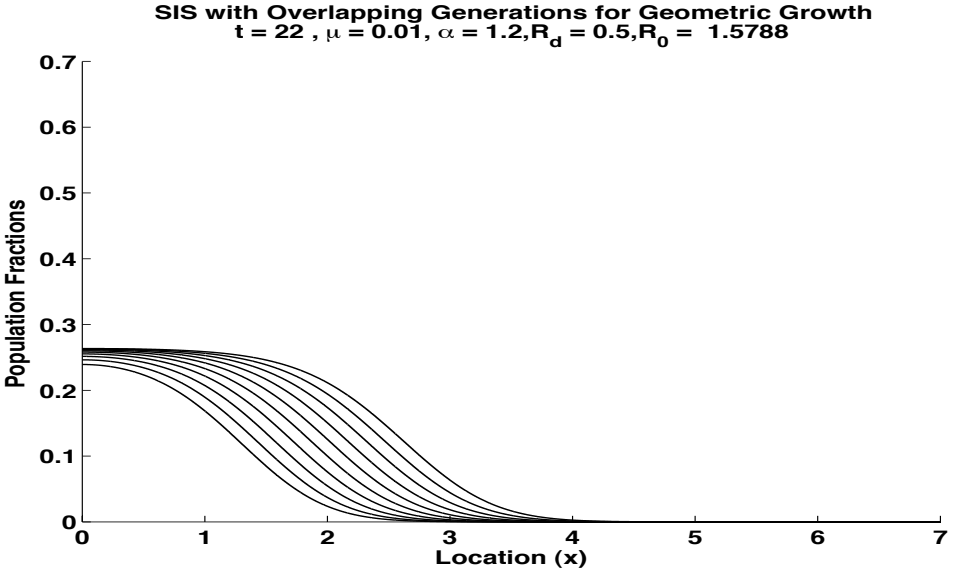

Figure 4.10: Travelling wave solutions for the SIS epidemic model with dispersal and geometric growth using the normal redistribution kernel where $\sigma_n = 0.2$, $\mu = 0.15$, $\alpha = 1.2$ and $R_d, R_0 > 1$. The graph show the last 10 solutions from 22 iterations.

wave solution for the SIS epidemic model with geometric growth and with damped oscillations around the fixed point are shown in Figure 4.12.

Theorem 3.2.1 guarantees that the positive fixed point I_2^* is globally stable when $R_0 > 1$. The epidemic model do not support non-trivial 2-cycles. Thus "travelling two cycles", like the ones on Figures 4.3 and 4.4 for the integrodifference logistic equation, are not supported for the SIS epidemic model with overlapping generations. Therefore, numerically it is shown that the SIS epidemic model with overlapping generations will support travelling wave solutions for all parameters of growth functions as long as $R_0 > 1$. The results of Li et al. (2008) can be applied to generate formal results. In summary, as it has been repeatedly seen (Anderson and May 1991, Brauer and Castillo-Chavez 2001, Castillo-Chavez et al. 2002a, 2002b, Gumel et al. 2006, Hethcote 2000 and the most recent book by Brauer

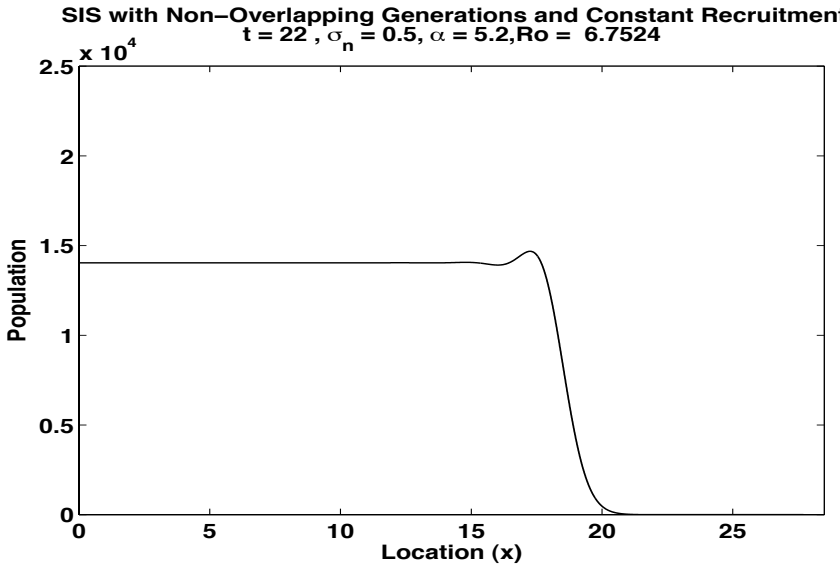

Figure 4.11: Travelling wave solutions with damped oscillations for epidemic model with dispersal and constant recruitment using the normal redistribution kernel, here $\sigma_n = 0.5$, $\alpha = 5.2$ and $c^* = 14040$, the fixed point is $I^* = 0.5534$. The graph shows the last of 22 iterations.

et al. 2008) epidemic models are unlikely to support complex dynamics. Here, we have studied the dynamics of discrete-time epidemic models with overlapping generations and found that the disease dynamics (non-monotone or oscillatory) approach an endemic state which carries its behavior to the qualitative behavior of the travelling wave solutions that it supports when $R_0 > 1$. The results of Li et al. (2008) only guarantee the existence of travelling wave solutions. These numerical results strengthen the possibility that there is in fact a unique (stable) travelling wave solution for functions g which are not monotone but can support two equilibria one stable (endemic) and another unstable (infection-free state).

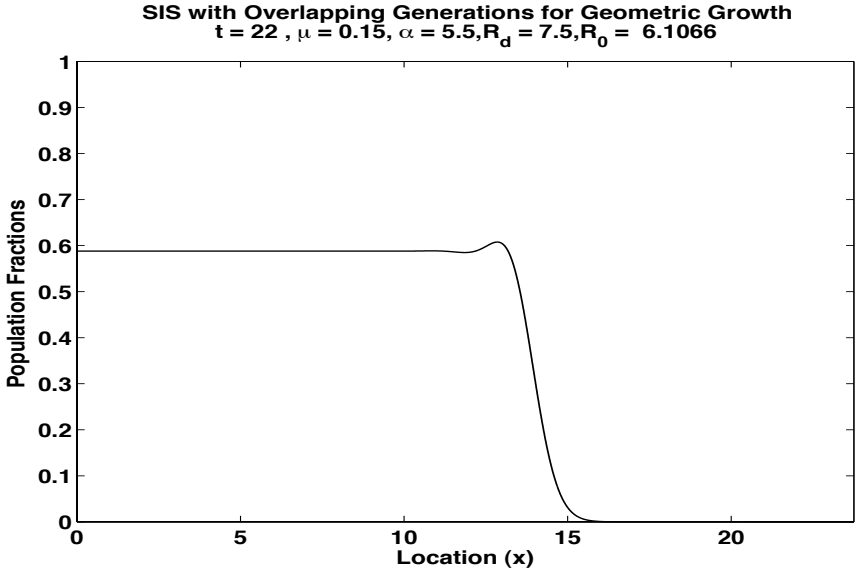

Figure 4.12: Travelling wave solutions with damped oscillations for SIS epidemic model with dispersal and geometric growth using the normal redistribution kernel, here $\sigma_n = 0.4$, $\mu = 0.15$, $\alpha = 5.5$ and $R_d, R_0 > 1$. The graph shows the last of 22 iterations.

4.5 Adding Spatial Dimensions

The main mathematical theory for integrodifference equation has been studied numerically precisely in one dimensional dispersal biological systems (Lewis et al. 2006). This is quite appropriate as dispersal can happen through coastlines or rivers like in the case of the spread of the California sea otter along the central California coast (Lubina and Levin 1988). However, dispersal in two spatial dimensions is relevant. Skellam (1951) was the first to use the diffusion equation to study movement of individuals in ecological contexts in two dimensions. Examples of two dimensional dispersal that have been modeled using reaction-diffusion equations include the muskrats populations of Skellam (1951), the spread of red deer in South Island New Zeland (Clarke 1971), and the spread of the house finch in

eastern North America (Mundiger and Hope, 1982), among others (Shigesada and Kawasaki 2001). Lewis et al. (2006) show that the application of one dimensional model to the study two dimensional system produces systematic bias in spread rates (analyses based on data). This observation was also made in the context of one dimensional reaction-diffusion equations (Shigesada and Kawasaki 2001).

There are studies of one dimensional integrodifference equations with dispersal data. In 1996, Kot et al. study the dispersal of the fruit fly insect following Dobzhansky and Wright (1943) dispersal data. Kot et al. use the Beverton-Holt recruitment curve,

$$N_{t+1} = \frac{rN_t}{1 + [(r-1)N_t/K]}, \tag{4.17}$$

(r is the growth rate and K the carrying capacity of the population) as the population growth model and compare the spread rates using five distinct redistribution kernels to fit the data. The fruit fly dispersion takes place in two dimensions but the authors approximated the problem as a one dimensional dispersal problem. Wallace (1966) and Taylor (1978) found that Dobzhansky and Wright spatial data fit a leptokurtic model in which the log of the number of recaptured flies decreases linearly with the square root of distance from the point of release, $ln(N) = a - b\sqrt{x}$. By normalizing the five fitting curves to get the five redistribution kernels, they found the best fit to be of the form $ln(N) = a - b\sqrt{x}$. Kot el at. also observe that the speed of invasion of a spreading population is extremely sensitive to the precise shape of the kernel and, in particular, to the tail of the distribution. Applications to data have shown the importance of studying epidemics in two spatial dimensions explicitly.

To decide on the appropriateness of one or two dimensional population dispersal models, it is extremely important to analyze the dispersal data. The relationship

between time and range expansion is of critical importance. It helps decide on the dispersal dimension and model structure. As described in the book by Shigesada and Kawasaki (2001), there are three phases of range expansion: the establishment phase, during which little or no expansion takes place; the expansion phase and the saturation phase if there are geographical limits. The expansion phase can be further subdivided into three types: type 1 shows linear expansion as in the case of the California sea otter, type 2 biphasic expansion with initial slope followed by steep linear slope, and type 3 which is continuously increasing with time, this is the case for all the epidemic dispersal from Chapter 3.

In their work, Li et. al (2008) only treat the integrodifference equation in the form of one dimensional dispersal, although the results hold for higher spatial dimensions. Li et al. argued that under the same conditions the existence of the travelling wave solution $N_t(\xi x - c)$ with speed c in two or more dimensions is guaranteed when the redistribution kernel depends on c and ξ. In other words, travelling wave solutions exist in two or more space dimensions if and only if $c \geq c^*(\xi)$, where $c^*(\xi)$ is the spreading speed defined by Eq. (3.59) in Chapter 3 (with the appropriate moment generating function) with the non-monotone fuction g replaced by g^+ (Eq. (4.10)). Naturally, the dispersal kernel has great impact on the asymptotic spread rate.

Simulations of the integrodifference equations in two spatial dimension are carried out using the bivariate normal distribution kernel

$$k(x_1, x_2) = \frac{1}{2\pi\sigma_1\sigma_2\sqrt{1-\rho^2}} \exp\left[\frac{1}{2(1-\rho^2)}\left(\frac{x_1^2}{\sigma_1} + \frac{x_2^2}{\sigma_2} - \frac{2\rho x_1 x_2}{\sigma_1\sigma_2}\right)\right] \qquad (4.18)$$

with mean $(0, 0)$. Here, ρ is the correlation coefficient between x_1 and x_2. That is,

$\rho = cor(x_1, x_2) = \frac{\sigma_{12}}{\sigma_1 \sigma_2}$ with covariance matrix

$$\Sigma = \begin{bmatrix} \sigma_1^2 & \rho\sigma_1\sigma_2 \\ \rho\sigma_1\sigma_2 & \sigma_2^2 \end{bmatrix}. \tag{4.19}$$

Figure 4.13 illustrates the results of simulations of two dimensional travelling wave solutions generated from the integrodifference equation for the SIS epidemic model with overlapping generations and constant recruitment, $\Lambda = 250$ and hence $P_t = \Lambda^* \equiv 12500$. The wave profile is monotone when $\alpha = 1.5$. The simulation is performed using the bivariate normal distribution as the dispersal redistribution kernel with standard deviation of 0.3 and correlation coefficients of 0.2. The integrodifference equation was iterated from times $t = 0$ to $t = 23$ on the domain $-15 \leq x_1, x_2 \leq 15$ with initial data $I_0(x_1, x_2) = 375$ on $-1 \leq x_1, x_2 \leq 1$ and $I_0(x_1, x_2) = 0$ elsewhere.

Figure 4.14 also provides travelling wave solutions for the SIS epidemic model with overlapping generations and constant recruitment using the bivariate normal redistribution kernel. However, in this case the transmission constant is $\alpha = 4.5$ and therefore damped oscillations around the fixed point are seen on the travelling waves. In this case the integrodifference equation was also iterated from times $t = 0$ to $t = 10$ on the domain $-15 \leq x_1, x_2 \leq 15$ with initial data again $I_0(x_1, x_2) = 375$ on $-1 \leq x_1, x_2 \leq 1$ and $I_0(x_1 x_2) = 0$ elsewhere.

4.6 The Role of the Redistribution Kernel

As mentioned throughout this work, it has been shown that the normal redistribution kernel can underestimate the rate of spread of invading populations, hence

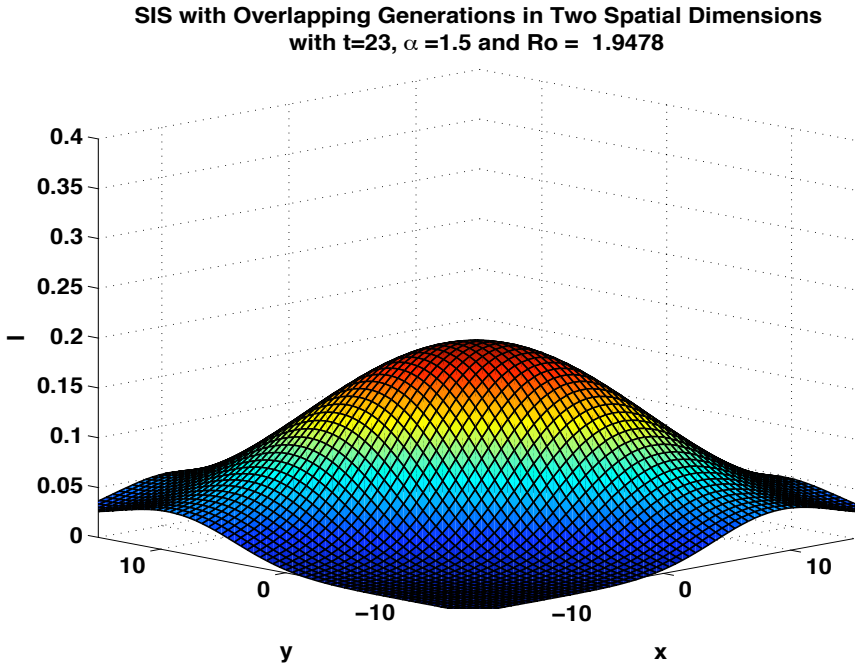

Figure 4.13: Monotone travelling wave solution for the integrodifference equation system with the SIS epidemic model with overlapping generations and constant recruitment in two spatial dimensions using the bivariate normal redistribution kernel. Here $\alpha = 1.5$ and $R_0 = 1.9478 > 1$ and the standard deviation is set to 0.3 and correlated coefficient to 0.2.

we decided to perform simulations using the bilaterial exponential (Laplace) redistribution kernel

$$k(x-y) = \frac{1}{2}\lambda e^{-\lambda|x-y|} \qquad \text{for } -\infty < x-y < \infty. \tag{4.20}$$

for comparisons. This redistributions kernel satisfies the conditions of been fat-tailed.

Figure 4.15 shows the travelling wave solution of the integrodifference equation for the SIS epidemic model with overlapping generations using the bilateral exponential redistribution kernel. The integrodifference equation was iterated for times t=0 to t=22 on the domain $-80 \leq x \leq 80$ with initial data $I(x) = 0.03$ on

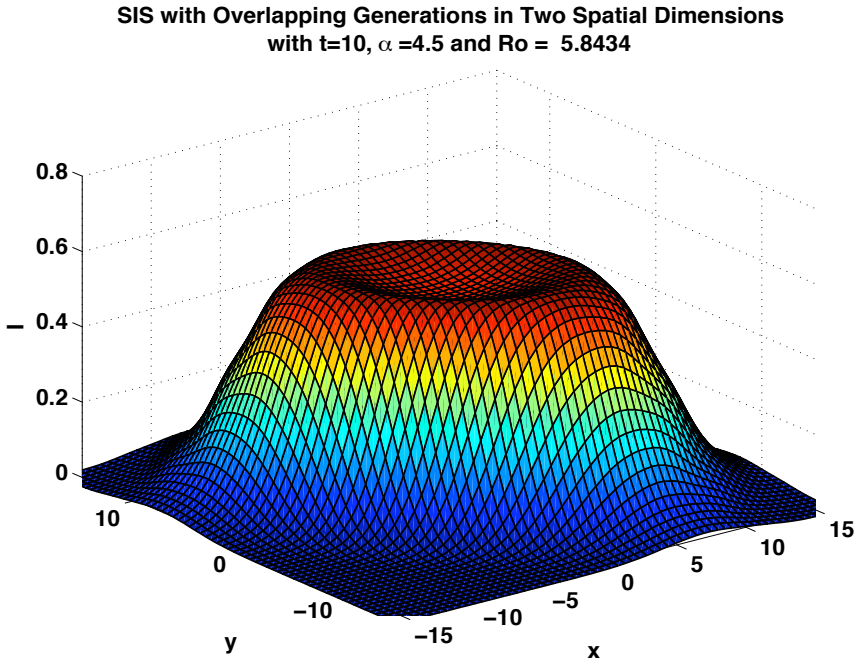

Figure 4.14: Travelling wave solution for the integrodifference equation with the SIS epidemic model with overlapping generations and constant recruitment in two spatial dimensions using the bivariate normal redistribution kernel. Here $\alpha = 4.5$, and $R_0 > 1$ hence damped oscillation are observed on the travelling waves.

$-1 \leq x \leq 1$ and $I_0(x) = 0$ elsewhere, this initial data is equivalent to an initial infective population of 750. Note the difference in the domain from previous figures. Through the simulations it was observed that there was not a significant difference between the shape of the travelling wave solutions with the normal redistribution kernel and the bilateral exponential kernel. However, for the bilateral exponential redistribution, dispersal will be on farther distances thus it will affect the minimum asymptotic speed of propagation given by Eq. (3.59), since it depends on the moment generating function of the kernel. In this case an algebraic expression of the speed cannot be computed explicitly.

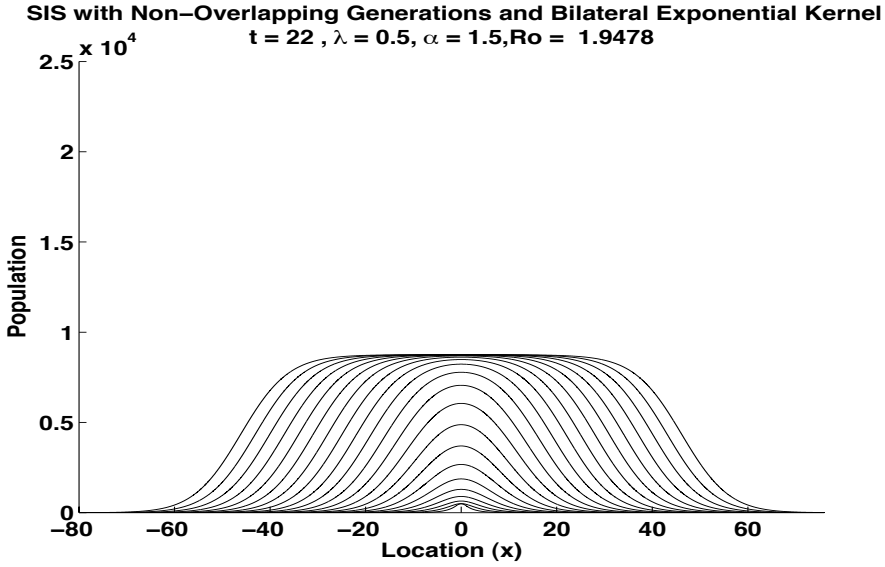

Figure 4.15: Monotone travelling wave solutions for the SIS epidemic model with dispersal using the bilateral exponential redistribution kernel with $\lambda = 0.5$.

4.7 Discussion

Travelling wave solutions of the integrodifference equation with non-monotone growth functions are studied. The potential dynamics are first highlighted using the logistic equation, commonly used in ecology, in order to provide a contrast to our numerical studies of epidemic models. It is corroborated (through numerical simulations) that travelling wave solutions for the epidemic integrodifference equation with both constant and geometric growth exist. The results of Li et al (2008) guarantee that our simulations are indeed representative. When the solution of the epidemic model approach monotonically the fixed point the travelling wave solution of the integrodifference equation will exhibit a monotone wave profile around the fixed point. However, when solutions of the epidemic model converges to the fixed point but via damped oscillations, the travelling wave solutions will also exhibit damped oscillations behavior around the fixed points. Our results

agree with the numerical results previously presented by Kot (1992) for ecological examples and our numerical study using the logistic growth function. Simulations with two spatial dimensions are carried out. We found travelling wave solutions with shapes similar ("monotone" and "oscillatory") to the one dimensional case.

CHAPTER 5

EPIDEMIC SPREAD OF AVIAN DISEASES: THE IMPACT OF MIGRATORY BIRDS ON LOCAL BIRD POPULATIONS

5.1 Introduction

The first chapters of this dissertation focuses on the study of disease dynamics in dispersing populations in one and two spatial dimensions. Our contribution is directly tied to the application of models for dispersal, base on integrodifference equations, to situations of disease dispersion through movement. The challenges of modeling the continuous dispersal in space of populations with discrete-generations were met via the identification of processes that involve non-overlappig and overlapping generations. Monotone growth functions and non-artificial non-monotone growth functions were explored in the context of epidemic spread. Unfortunately, we have not generated enough results for natural expansions that involve interacting populations. It is of critical importance to assess the role of animal reservoirs, particularly reservoirs involving highly mobile populations (like migratory birds), on disease dispersal and persistence.

As a first step, we have gone to the study of interacting populations with overlapping generations. Particularly, in situations that are of central importance to our overall effort to study the transmission dynamics and control of diseases in mobile populations. Hence, we devote this last chapter to the study of the role of transient populations on disease dispersal.

We introduced a general framework that models disease dispersal without the explicit inclusion of space variables. In fact, we use the metapopulation approach,

that has been extensively used to study ecological interactions (Hanski and Gilpin 1997). Naturally, the inclusion of multiple populations and realistic scenarios rapidly increases the complexity of the models and our ability to gain full understanding through mathematical analysis and simulations. Nevertheless, we believe that construction of two alternative frameworks (based on recent work) in the context of the interactions of migration and local bird populations has value. Finally, we carried out a preliminary mathematical and computational analysis of the case of one migratory and one local bird population under weak, strong and random mixing.

For decades the dynamics avian diseases have been a major concern worldwide. Wild birds are typically carriers of these diseases and often long range vectors for bacteria, viruses, parasites, or drug resistance organisms. They are known reservoirs for diseases like West Nile virus, influenza A virus, enteric bacterial pathogens and drug resistance bacteria. In addition, wild birds can be infested by arthropod vectors, that is, invertebrate animals with jointed legs, which can be drop from wild birds along migration routes, even if the avian host is not a competent reservoir of infection (Reed et al. 2003). Their movement increases the likelihood of establishing new endemic foci of disease along migration routes.

Generating an understanding of migratory bird movement into and within a region and the potential for their contact with domestic poultry is of vital importance (Food and Agricultural Organization of United Nations (FAO) 2005). Morrison (2005), in his review of the research presented at the conference of the International Waterbirds Society 2005, concluded that scientists agree that three issues need increased attention: information on migration patterns of birds flyways (which can be very complicated and varies between species), the evolution of the

impact of diseases events on migration, and studies on the impact of migration on disease distribution.

In this work a mathematical model is build to study, impact of migration on diseases, that is, the spread of avian diseases within migratory birds and local bird populations via contacts with migratory birds. The disease that motivates the models in this chapter is avian influenza. Our models are not tied in to a particular disease because in general the role of migratory birds is not easy to asses. For example, in the case of the avian flu, it is extremely difficult to know if migratory birds are sparkling new outbreaks in (domestic) poultry, or whether they pick up the virus from poultry infected by other routes (Butler 2006).

5.2 Migratory Routes and Diseases

Each autumn an estimated 5 billion of birds, representing 300 species, migrate from North America to Central and South America and similar numbers travel from Eastern Europe to Africa. Unfortunately, patterns of migration for wild birds tend to be highly complex. Furthermore, these patterns vary between species and can be radically different even within populations from the same species (Reed 2003). Migratory birds routes in the Atlantic, Mississippi, Central and Pacific flyways are oriented north to south because major wetlands in North America run in a similar direction. In contrast, migratory birds in some regions in Europe and Asia tend to move in a east to west fashion, corresponding to orientation of major coastlines and topography.

According to the 2006 Food and Agricultural Organization of the United Nations (FAO 2006) report, populations of ducks, geese and swans migrate between

wetlands in the northern breeding areas and southern non-breading areas and in doing so, regularly cross the borders of two or more countries. Southward migration for these northern breeding species starts in July and increases through the following months. The migration takes them north to reproduction areas at the end of winter, beginning of spring.

Several aspects linked to long distance migration contribute to the acquisition of zoonotic pathogens by migratory birds, that is, pathogens that are transmitted from vertebrate animals to humans. For some birds the stress of migration can lead to reactivation of otherwise latent infections (FAO 2006).

The movement of diseases via migration birds depend upon the ability of individual birds to migrate after becoming infected with a pathogen (Morrison 2005). Avian experts agree that sick and dying birds do not spread viruses very far (Normile 2005). It is unknown whether or not migratory birds survive infections to various diseases (Chen et al. 2006). Transmission of a disease is most common between individuals of the same species. Cross species transmission requires exposure and adaptation. Even adapted domestic poultry exhibits high degree of heterogeneity when it comes down to susceptibility and infectivity. Variation is related to these transmission factors, often high between subtypes and within each subtype (Morrison 2005).

5.3 Avian Influenza

Avian influenza is a non-clinical viral infection of wild birds caused by a group of viruses known as type A influenza. The viruses subtypes are identified and classified on the basis of two broad types of antigens, hemagglutinan (H) and

neuraminidase (N). Among all the type A influenza viruses 15H and 9N antigens have been identified (Friend and Franson 1999).

Infected birds shed influenza viruses in their saliva, nasal secretions and feces. Susceptible birds become infected when they have contact with contaminated secretions, excretions or with surfaces that are contaminated with secretions or excretions from infected birds (Center for Disease Control and Prevention (CDC) 2006a).

Wild birds, especially waterfowl and shorebirds, have long been the focus of concern by the poultry industry. These bird populations are seen as a source for influenza infections in poultry (Friend and Franson 1999). Avian influenza is very contagious among birds and can make some domesticated birds, including chickens, ducks and turkeys very sick. Disease-induced death can be high. Domesticated birds may become infected with avian influenza virus through direct contact with infected waterfowl or other infected poultry, or through contact with surfaces, such as dirt or cages, or materials, such as water or feed, that have been contaminated with the virus (CDC 2006a).

Viruses are classify as being low or high (they can change their status) depending on the effects they can generate on birds (Normile 2005). The avian influenza virus can evolve to a highly pathogenic form (HPAI) in domestic birds while it is almost always low pathogenic (LPAI) in wild birds (Morrison 2005). Low pathogenic avian influenza commonly causes mild symptoms, such as ruffled feathers and a drop in egg production. Most infections easily go undetected. Highly pathogenic types spread rapidly through poultry flocks, causing disease affecting multiple organs and has mortality that often approach 100%, been documented within 48 hours (World Health Organization 2005). Considerable circumstantial evidence

suggest that migratory birds can introduce low pathogenic H5 and H7 viruses to poultry flocks, forms that can and do mutate to highly pathogenic form (WHO 2005). Mutations from low to high pathogenicity, that resulted in bird flu epidemics among poultry, has been documented 19 times since 1959 (Normile 2005). It is very likely that some migratory birds are now directly spreading H5N1 virus in their highly pathogenic form (WHO 2005).

Wild waterfowls are considered the natural reservoir of all influenza A viruses. They have probably carried influenza viruses, with no apparent harm, for centuries (WHO 2005). Viruses have been recovered from infected waterfowl fecal material for 8 days, from fecal contaminated river water for 4 days, and from poultry houses more than 100 days after flock depopulation for markets (Friend and Franson 1999). It is believed that avian influenza in wild birds cannot be effectively controlled because of the large number of virus subtypes and the high frequency of virus genetic mixing resulting, key to the selection of new subtypes.

5.3.1 Avian Influenza and Migratory Birds

Wetland or lakes have been associated with the distribution of outbreaks of avian flu in Europe. As of 2006 the disease has emerged in Africa opening a new front that could vastly increase bird reservoir populations, a situation that could accelerate the timing of the next human pandemic (Butler 2006). The close proximity of people and animals, coupled with insufficient surveillance and limited disease control capacities in a rich wetland ecosystem of eastern African countries, are likely to create ideal breeding grounds for influenza. Around lakes and wetlands, poultry density is particularly high therefore, the enhancement and strengthening

of disease surveillance and emergency preparedness in these regions are essential (FAO 2005).

In Asia H5N1 spreads through the domestic poultry populations; through wild bird trade and by migratory birds (Morrison 2005). However, outbreaks do not match the migratory patterns of wild birds (Morrison 2005, Normile 2005). China is the most likely source of emergent and re-emergent of HPAI H5N1 influenza viruses (Chen et al. 2006). H5N1 viruses have been found in dead wild birds close to poultry farms (Chen et al 2005) and most recently in Qinghai Lake, one of the most important breeding location for migratory birds that over winter in Southeast Asia, Tibet and India (Liu 2005).

In April 2005 an outbreak in the Qinghai Lake killed 5000-6000 migratory water birds (Normile 2005), the first sustained transmission chain within migratory waterfowl in recent times. Overall 90% of the dead birds were bar-headed geese. In the past only two large die-offs in migratory birds, caused by highly pathogenic viruses have been documented. The first in South Africa in 1961 (H5N3) and the second in Hong Kong in the winter of 2002-2003 (H5N1) (WHO 2005). The virus was being transmitted by migratory birds in the lake, suggesting the possibility that H5N1 viruses can possibly be transmitted between migratory birds populations (FAO 2006).

In a recent published study Chen et al. (2006) founded that genetic relatedness of gene segments of H5N1 viruses isolated at Poyang and Qinghai Lakes strongly support the hypothesis that migratory birds can transfer the virus over long distances. Ongoing influenza surveillance data show that these viral strains were present in apparently healthy migratory birds just before the start of their migration trek. These viruses, isolated from apparently healthy migratory ducks,

are not invariably fatal. In fact, surviving ducks may shed the virus even 7 days after infection. Subsequent outbreaks of avian influenza in 13 countries, including Niger and regions in Europe and Asia, seem to have been ignited by strains related to the strain identified in Qinghai Lake (Normile 2006). These findings also strongly support the hypothesis that wild birds carry influenza viruses great distances.

According to Normile (2006) and Chen et al (2006), the best approach to avert a global threat of avian flue is to control H5N1 virus infections in domestic poultry. On the other hand, in China it is believed that circulation among poultry, not reintroduction from wild birds, is what is keeping the virus alive. There has been arguments that the cycle of transmission can be broken if the virus is eradicated from poultry flocks.

5.4 Modeling Approach 1: Mixing Weighted by Residence Times

Here, we introduce flexible modeling frameworks that can theoretically handle the interactions between multiple local (resident) and migratory bird populations. The resulting models are naturally complex but their potential usefulness is illustrated (later on) by the preliminary study of a rather simple case. The population of birds is divided in two groups: local birds such as domestic birds or poultry and migratory birds such as wild birds. The local and migratory birds are divided into $i = 1, .., s$ flocks and $j = 1, .., k$ flocks, respectively. The local birds as residents do not move from their current location, while the migratory birds do move. It is

assumed that local birds have contacts with local birds within their own habitat and with migratory birds in the same residence area. Migratory birds may have most of the contacts that lead to infections within their own flock, with migratory birds from other flocks at the temporary residence habitat (local bird residence area) and with local infected birds in their habitats (poultry markets).

Within each flock the birds are subdivided into different epidemiological classes. S_i^l and I_i^l denote the population of local birds in flock i who are susceptible and infectious, respectively; while S_j^m and I_j^m denote the corresponding classes for the population of migratory birds in flock j. The total population sizes of the two groups are given by $N_i^l = S_i^l + I_i^l$ and $N_j^m = S_j^m + I_j^m$. The constants a_i^l and b_j^m denote the per-capita contact rates of the local birds and migratory birds in flocks i and j, respectively. In addition, σ_{ij}^m is the rate at which migratory birds of flock j visit local birds of flock i and δ_{ij}^m is the rate at which migratory birds of flock j return to their own flock (j) from local bird flock i. For a given migratory bird

flock j the total events rate is given by $\sum_{i=1}^{s}(\sigma_{ij}^m + \delta_{ij}^m)$. Therefore,

$$\tau_{ij}^m = \frac{\delta_{ij}^m}{\sum_{i=1}^{s}(\sigma_{ij}^m + \delta_{ij}^m)}$$ is the proportion of time spend by migratory birds within their own flock j after leaving local bird flock i.

$$\omega_{ij}^m = \frac{\sigma_{ij}^m}{\sum_{i=1}^{s}(\sigma_{ij}^m + \delta_{ij}^m)}$$ is the proportion of time spend by migratory birds of flock j with local birds of flock i,

$$\omega_j^m = \sum_{i=1}^{s} \omega_{ij}^m = \frac{\sum_{i=1}^{s} \sigma_{ij}^m}{\sum_{i=1}^{s}(\sigma_{ij}^m + \delta_{ij}^m)}$$ is the proportion of time spend by migratory birds of flock j outside its residence area, while

$$\tau_j^m = \frac{\sum_{i=1}^{s} \delta_{ij}^m}{\sum_{i=1}^{s}(\sigma_{ij}^m + \delta_{ij}^m)}$$ is the proportion of time spend by migratory birds within their own flock j.

Figure 5.1 shows a caricature of the interactions between these populations.

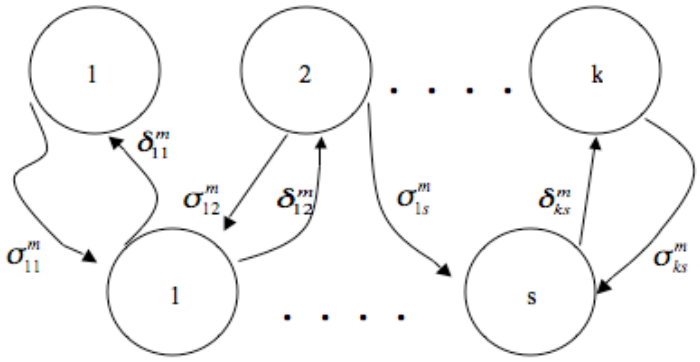

Figure 5.1: The migratory birds travel in flocks $j = 1, .., k$ while the local birds live in flocks/habitats $i = 1, ..., s$. Here, σ_{ij}^m is the rate at which migratory birds of type j visit local bird flock i and δ_{ij}^m is the rate at which migratory birds of flock j return to flock (j) from local bird flock i.

If birds mix according to proportional mixing (Castillo-Chavez et al. 1998 and

Castillo-Chavez et al. 2003) then the mixing probabilities can be define with the following formulae:

1. $P_{ii}^{ll} = \frac{a_i^l N_i^l}{a_i^l N_i^l + \sum_{j=1}^{k} b_j^m \omega_{ij}^m N_j^m}$, the mixing probability between local birds from the same flock i given there is contact in such habitat,
2. $P_{ij}^{lm} = \frac{b_j^m \omega_{ij}^m N_j^m}{a_i^l N_i^l + \sum_{j=1}^{k} b_j^m \omega_{ij}^m N_j^m}$, the mixing probability of local birds and migratory birds from flocks i and j, respectively given a contact by migratory bird of flock j,
3. $P_{ji}^{ml} = \frac{a_i^l N_i^l}{a_i^l N_i^l + \sum_{j=1}^{k} b_j^m \omega_{ij}^m N_j^m} \omega_{ij}^m$ the mixing probability of local birds and migratory birds from flocks i and j, respectively, given a contact by local bird of flock i,
4. $P_{jj}^{mm} = \frac{b_j^m \tau_j^m N_j^m}{b_j^m N_j^m} = \tau_j^m$ the mixing probability of migratory birds of flock j in their residence area given that there are contacts in such flock, and
5. $P_{ijf}^{mm} = \frac{b_f^m \omega_{if}^m N_f^m}{a_i^l N_i^l + \sum_{j=1}^{k} b_j^m \omega_{ij}^m N_j^m} \omega_{ij}^m$, the mixing probability of migratory birds of flock j with migratory birds from a different flock f at local birds habitat i given that there are contacts between migratory birds from such flocks.

Thus the following conditions most hold:

$$P_{ii}^{ll} + \sum_{j=1}^{k} P_{ij}^{lm} = 1, \qquad i = 1, 2, ..., s, \tag{5.1}$$

$$P_{jj}^{mm} + \sum_{i=1}^{s} \left[P_{ji}^{ml} + \sum_{f=1}^{k} P_{ijf}^{mm} \right] = \tau_j^m + \omega_j^m = 1, \quad \text{for} \quad j = 1, 2, ..., k. \tag{5.2}$$

The model equations for each of the populations, using the above mixing probabilities, are given below.

The equations for local birds (residents) are

$$\frac{dS_i^l}{dt} = \Lambda_i^l - B_i^l(t) - \mu_i^l S_i^l, \tag{5.3}$$

$$\frac{dI_i^l}{dt} = B_i^l(t) - (\mu_i^l + d_i^l) I_i^l, \tag{5.4}$$

where $i = 1, ..., s$. While for migratory birds

$$\frac{dS_j^m}{dt} = \Lambda_j^m - B_j^m(t) - \mu_j^m S_j^m, \tag{5.5}$$

$$\frac{dI_j^m}{dt} = B_j^m(t) - (\mu_j^m + d_j^m) I_j^m, \tag{5.6}$$

where $j = 1, ..., k$.

Table 5.1: Parameter definitions for modeling aproach 1: mixing weighted by residence times. Index Definition: $i = 1, ..., s$ represents the local birds flocks while $j = 1, ..., k$ represents the migratory birds flocks, $f = 1, ..., s$ is the location (habitat) relative to local birds.

Parameters	Definitions
Λ_i^l	recruitment/birth rate for the local birds
Λ_j^m	migratory birds recruitment/arrival rate
μ_i^l	natural/slaugtered mortality rate for local birds
μ_j^m	migratory birds departure rate
d_i^l, d_j^m	mortality rate due to disease
β_i^l, β_j^m	transmission rate per contact
a_i^l	average number of contacts of local birds per unit of time
b_j^m	average number of contacts of migratory birds per unit of time
δ_{ij}^m	rate at which migratory birds of flock j visit local birds of flock i
σ_{ij}^m	rate at which migratory birds of type j return to flock (j)

The (force of) infection rate for local birds is given by

$$B_i^l(t) = \beta_i^l a_i^l S_i^l \left[P_{ii}^{ll} \frac{I_i^l}{N_i^l + \sum_{j=1}^k \omega_j^m N_j^m} + \sum_{j=1}^k P_{ij}^{lm} \frac{\omega_j^m I_j^m}{N_i^l + \sum_{j=1}^k \omega_j^m N_j^m} \right] \tag{5.7}$$

while the (force of) infection rate for migratory birds is

$$\begin{aligned} B_j^m(t) &= \beta_j^m b_j^m S_j^m \left[\sum_{i=1}^{s} P_{ji}^{ml} \frac{I_i^l}{N_i^l + \sum_{j=1}^{k} \omega_j^m N_j^m} \right] \\ &\quad + \beta_j^m b_j^m S_j^m \left[\sum_{i=1}^{s} \sum_{f=1}^{k} P_{ijf}^{mm} \frac{\omega_f^m I_f^m}{N_i^l + \sum_{j=1}^{k} \omega_j^m N_j^m} + P_{jj}^{mm} \frac{I_j^m}{N_j^m} \right] \end{aligned} \quad (5.8)$$

In this model, birds actually do not move, instead their contacts are distributed via the mixing probabilities (weighted by average residence times in each habitat). The infection rates are generated by effectives contacts between local birds and by the contacts of those with migratory birds. The total population of local and migratory birds when there are no disease-induced deaths ($d_j^m = d_i^l = 0$) are given by $\sum_{j=1}^{k} \frac{\Lambda_j^m}{\mu_j^m}$ and $\sum_{i=1}^{s} \frac{\Lambda_i^l}{\mu_i^l}$, respectively. Hence, the disease free equilibrium is given by $(\Lambda_1^m/\mu_1^m, ..., \Lambda_k^m/\mu_k^m, 0, ..., 0, \Lambda_1^l/\mu_1^l, ..., \Lambda_s^l/\mu_s^l, 0, ..., 0)$.

Analysis of this model is very complicated. Hence, in the next section we introduced a simple model where we still consider mixing probabilities but with a different approaches.

5.5 Modeling Approach 2: Classical Mixing

Migratory birds that visit areas with large local populations for short periods of times may mix a lot or hardly mix with local populations. In order to look at these mixing regimes (strong versus weak mixing) we proceed to divide the bird population in two categories: local birds and migratory birds. Local birds are residents, while migratory birds only ones allow to move. We let $N_1, ..., N_s$ denote the total population of resident birds of flocks $l = 1, ..., s$ and $N_{s+1}, ..., N_{s+k}$ the total population of migratory birds of flocks $m = s + 1, ..., s + k$. The total

population of birds is

$$N = \sum_{r=1}^{s+k} N_r. \tag{5.9}$$

Within each flock, birds are subdivided into two epidemiological classes, susceptible birds, S_r, and infected birds, I_r, where $r = 1, ..., s + k$. The system of non-linear ordinary differential equations that models their interactions is given by

$$\frac{dS_r}{dt} = \Lambda_r - \beta_r S_r \sum_{z=1}^{s+k} P_{rz} \frac{I_z}{N_z} - \mu_r S_r, \tag{5.10}$$

$$\frac{dI_r}{dt} = \beta_r S_r \sum_{z=1}^{s+k} P_{rz} \frac{I_z}{N_z} - (\mu_r + d_r) I_r, \tag{5.11}$$

where $r = 1, ..., s + k$ and $\{P_{rz}\}$ are the mixing probabilities.

Table 5.2: Parameter definitions for model under classical mixing

Parameters	Definitions
Λ_r	birds birth/arrival rate
μ_r	birds slaughtered/departure mortality rate
d_r	mortality rate due to disease
β_r	transmission rate per contact
P_{rz}	mixing probability between birds from flock r and z

We focus on the use of two related types of mixing probabilities: proportionate and preferred mixing (Jacquez et al. 1988, Blythe et al. 1991, Blythe et al 1995) defined below. In order to illustrate the potential usefulness of this approach, we carried out a preliminary study of a two flock system. That is, a local and a

migratory bird population ($r = \{l, m\}$). Therefore, System (5.10) reduces to

$$\frac{dS_m}{dt} = \Lambda_m - \beta_m S_m \sum_{z=\{l,m\}} P_{mz} \frac{I_z}{N_z} - \mu_m S_m, \tag{5.12}$$

$$\frac{dI_m}{dt} = \beta_m S_m \sum_{z=\{l,m\}} P_{mz} \frac{I_z}{N_z} - (\mu_m + d_m) I_m \tag{5.13}$$

$$\frac{dS_l}{dt} = \Lambda_l - \beta_l S_l \sum_{z=\{l,m\}} P_{lz} \frac{I_z}{N_z} - \mu_l S_l, \tag{5.14}$$

$$\frac{dI_l}{dt} = \beta_l S_l \sum_{z=\{l,m\}} P_{lz} \frac{I_z}{N_z} - (\mu_l + d_l) I_l, \tag{5.15}$$

Furthermore, if migratory birds disperse quickly or unaffected by disease then we can take the disease induced mortality as negligible. That is, $d_m \equiv 0$ and the total population of migratory birds is constant, $N_m = \frac{\Lambda_m}{\mu_m}$. We further assume that both populations are equally susceptible to infection, that is, $\beta_m = \beta_l = \beta$. In addition, we assume that the rate of departure of migratory birds is much bigger than the slaughtered rate, that is, $\mu_m >> \mu_l$. These assumptions lead to the following three dimensional system

$$\frac{dI_m}{dt} = \beta(N_m - I_m)\left(P_{mm}\frac{I_m}{N_m} + P_{ml}\frac{I_l}{N_l}\right) - \mu_m I_m \tag{5.16}$$

$$\frac{dS_l}{dt} = \Lambda_l - \beta S_l \left(P_{ll}\frac{I_l}{N_l} + P_{lm}\frac{I_m}{N_m}\right) - \mu_l S_l, \tag{5.17}$$

$$\frac{dI_l}{dt} = \beta S_l \left(P_{ll}\frac{I_l}{N_l} + P_{lm}\frac{I_m}{N_m}\right) - (\mu_l + d_l) I_l. \tag{5.18}$$

5.5.1 Proportionate Mixing

If birds mix according to proportionate mixing (Blythe et al. 1991, Blythe et al 1995, Castillo-Chavez et al. 1998 and Castillo-Chavez et al. 2003) then the mixing

probabilities for System (5.10) are define as

$$P_{rz} = \frac{C_r N_r}{\sum_{z=1}^{s+k} C_z N_z}, \tag{5.19}$$

where C_r is the per-capita contact rate of birds of type $r \in \{l, m\}$ and

$$\sum_{r=1}^{s+k} P_{rz} = 1. \tag{5.20}$$

We now further assume that the contact rates are the same for local and migratory birds. That is, the mixing probabilities of the two groups, Model (5.16), are just frequently dependent. The explicit expressions are:

$$P_{ll} = \frac{N_l}{N_m + N_l} = P_{ml}, \tag{5.21}$$

$$P_{mm} = \frac{N_m}{N_m + N_l} = P_{lm}, \tag{5.22}$$

where $P_{ll} + P_{lm} = 1$ and $P_{mm} + P_{ml} = 1$.

Disease Free Equilibrium, Basic Reproductive Number and Endemic Equilibrium

The equilibrium for System (5.16) with proportionate mixing, Eqs. (5.21) are calculated. Thus, in this case the disease free equilibrium (DFE) is $(I_m, S_l, I_l) = \left(0, \frac{\Lambda_l}{\mu_l}, 0\right)$.

The basic reproductive number R_0, is defined as the average number of secondary infectious produced by a typical infected individual in a populations of susceptibles. It is computed using the next generator operator (Dieckmann et al. 1990, Castillo-Chavez et al. 2002 and van den Driessche and Watmough 2002) see Appendix C. R_0^{prop} for the SI epidemic model under proportionate mixing is given by

$$R_0^{prop} = \frac{\Lambda_l/\mu_l}{\Lambda_m/\mu_m + \Lambda_l/\mu_l}\left(\frac{\beta}{\mu_l + d_l}\right) + \frac{\Lambda_m/\mu_m}{\Lambda_m/\mu_m + \Lambda_l/\mu_l}\left(\frac{\beta}{\mu_m}\right). \tag{5.23}$$

Therefore, R_0^{prop} is given by the weighted average of the proportion of migratory and local birds in the population. The basic reproductive number of migratory birds is $R_0^m = \frac{\beta}{\mu_m}$ while the basic reproductive number of local birds is $R_0^l = \frac{\beta}{\mu_l + d_l}$. Here, $\frac{1}{\mu_m}$ is the average time spent by migratory birds of flock m in flock or habitat l and $\frac{1}{\mu_l + d_l}$ is the average infectious period of local birds of flock l. For the general proportionate mixing model, any number of groups (System (5.10)), R_0 is given by

$$R_0 = \sum_{l=1}^{s} \frac{\Lambda_m/\mu_m}{\sum_{r=1}^{s+k} \Lambda_r/\mu_r} \left(\frac{\beta}{\mu_l + d_l} \right) + \sum_{m=s+1}^{s+k} \frac{\Lambda_m/\mu_m}{\sum_{r=1}^{s+k} \Lambda_r/\mu_r} \left(\frac{\beta}{\mu_m} \right). \tag{5.24}$$

The stability of the DFE depends on the value of R_0. Typically, if $R_0 < 1$, the DFE is locally asymptotically stable while if $R_0 > 1$, the DFE is unstable. The following theorem establishes a slightly stronger result, that is, the global stability of the DFE.

Theorem 5.5.1. *Assume $\mu_m > \mu_l + d$. If $R_0^{prop} < 1$, then the disease free equilibrium $(N^0, 0, 0)$ is globally asymptotically stable where $N^0 = \Lambda/\mu_m + \Lambda/\mu_l$.*

Proof. Let $\Lambda_m = \Lambda_l = \Lambda$. Consider new variables $N = N_m + N_l$ and $I = I_m + I_l$ thus, the new system under study is:

$$\begin{aligned}
\frac{dN}{dt} &= (\Lambda + \mu_l N_m) - \mu_l N - d_l I_l, && (5.25)\\
\frac{dI}{dt} &= \beta I \left(1 - \frac{I}{N}\right) - \mu_m I + (\mu_m - \mu_l - d_l) I_l, && (5.26)\\
\frac{dI_l}{dt} &= \beta \left(1 - \frac{N_m}{N}\right) I - \beta I \frac{I_l}{N} - (\mu_l + d_l) I_l. && (5.27)
\end{aligned}$$

We need $N(t) \leq N^0 = N_m + N_l^0$ in our proof, where $N_l^0 = \Lambda/\mu_l$. This can be proved using

$$\frac{dN}{dt} = N' \leq (\Lambda + \mu_l N_m) - \mu_l N. \tag{5.28}$$

Consider the Liapunov function $L = (\mu_m - \mu_l - d_l)I_l + (\mu_l + d_l)I$ where $p = 1 - \frac{N_m}{N^0}$, then

$$\begin{aligned}
\frac{dL}{dt} &= (\mu_l + d_l)\left[\beta I\left(1 - \frac{I}{N}\right) - \mu_m I\right] \\
&\quad +(\mu_m - \mu_l - d_l)\left[\beta I\left(1 - \frac{N_m}{N}\right) - \beta I\frac{I_l}{N}\right] \\
&= (\mu_l + d_l)(\beta - \mu_m)I - (\mu_l + d_l)\beta\frac{I^2}{N} + (\mu_m - \mu_l - d_l)\beta\left(1 - \frac{N_m}{N_0}\right)I \\
&\quad +(\mu_m - \mu_l - d_l)\left[\beta\left(\frac{N_m}{N_0} - \frac{N_m}{N}\right)I - \beta I\frac{I_l}{N}\right] \\
&= I[(\mu_l + d_l)\beta - (\mu_m - \mu_l - d) + \beta\mu_m p - (\mu_l + d_l)\beta p] \\
&\quad -(\mu_l + d_l)\beta\frac{I^2}{N} - (\mu_m - \mu_l - d_l)\left[\beta\frac{N_m(N_0 - N)I}{N_0 N} + \beta I\frac{I_l}{N}\right] \\
&\leq I((1-p)\beta(\mu_l + d_l) + p\beta\mu_m - \mu_m(\mu_l + d_l)) \\
&= I(\mu_l + d_l)\mu_m\left(\frac{\beta}{\mu_m}(1-p) + \frac{\beta}{\mu_l + d_l}p - 1\right) \\
&= I(\mu_l + d_l)\mu_m(R_0^{prop} - 1) \\
&\leq 0.
\end{aligned}$$

Thus, the disease free equilibrium $(N^0, 0, 0)$ is globally asymptotically stable as $t \to \infty$. □

The following theorem establishes the existence of at least one endemic equilibrium if $R_0^{prop} > 1$.

Theorem 5.5.2. *If $R_0^{prop} > 1$, then there is at least one endemic equilibrium (I_m^*, S_l^*, I_l^*).*

Proof. The total population of local birds is governed by

$$\frac{dN_l}{dt} = \Lambda_l - \mu_l S_l - \mu_l I_l - d_l I_l, \tag{5.29}$$

therefore, we can write

$$\Lambda_l - \mu_l S_l - \mu_l I_l - d_l I_l = 0 \tag{5.30}$$

in two forms, that is,

$$S_l = \frac{(\mu_l + d_l)I_l - \Lambda_l}{\mu_l} = H_1(I_l), \quad \text{and} \tag{5.31}$$

$$N_l = \frac{\Lambda_l - d_l I_l}{\mu_l} = H_2(I_l), \tag{5.32}$$

Let $H(I_l) = N_m + H_2(I_l)$. From $\frac{dI_l}{dt} = 0$ and $\frac{dI_m}{dt} = 0$, we get

$$\beta H_1(I_l)\frac{I_m + I_l}{H(I_l)} = (\mu_l + d_l)I_l, \tag{5.33}$$

$$\beta[N_m - I_m]\frac{I_m + I_l}{H(I_l)} = \mu_m I_m. \tag{5.34}$$

Dividing Eq. (5.33) by Eq. (5.34), we obtain I_m in terms of I_l, that is,

$$I_m = \frac{N_m(\mu_l + d_l)I_l}{\mu_m H_2(I_l) + (\mu_l + d_l)I_l} = G(I_l). \tag{5.35}$$

Therefore, plugin in Eq. (5.35) into Eq. (5.33) and after canceling I_l (since $I_l = 0$ correspond to the DFE), we have $I_l = 0$ where

$$F(I_l) = \beta\frac{H_1(I_l)}{H(I_l)}\left(1 + \frac{N_m(\mu_l + d_l)}{\mu_m H_2(I_l) + (\mu_l + d_l)I_l}\right) - (\mu_l + d_l). \tag{5.36}$$

The zeroes of $H_1(I_l) = 0$, $H(I_l) = 0$ and $H_3(I_l) = \mu_m H_2(I_l) + (\mu_l + d_l) = 0$ are

$$\bar{I}_{l1} = \frac{\Lambda_l}{\mu_l + d_l}, \tag{5.37}$$

$$\bar{I}_{l2} = \frac{\mu_l N_m + \Lambda_l}{d_l} \quad \text{and} \tag{5.38}$$

$$\bar{I}_{l3} = \frac{\mu_m \Lambda_l}{d_l - (\mu_l + d_l)\mu_l}, \tag{5.39}$$

respectively.

(a) If $\bar{I}_{l1} = \min\{\bar{I}_{l1}, \bar{I}_{l2}, \bar{I}_{l3}\}$ then since F is continuous on $\left[0, \frac{\Lambda_l}{\mu_l + d_l}\right]$,

$$F(0) = (\mu_l + d_l)(R_0^{prop} - 1) > 0 \tag{5.40}$$

$$\text{and} \qquad F\left(\frac{\Lambda_l}{\mu_l + d_l}\right) = -(\mu_l + d_l) < 0, \tag{5.41}$$

by the intermediate value theorem, there must be at least one positive root for $I_l \in (0, \infty)$.

(b) If $\bar{I}_{l1} > \bar{I}_{l2} > \bar{I}_{l3}$ then since F is continuous in $(\bar{I}_{l3}, \bar{I}_{l2})$,

$$\lim_{I_l \to \bar{I}_{l2}^-} F(I_l) = \infty \tag{5.42}$$

$$\text{and} \qquad \lim_{I_l \to \bar{I}_{l3}^+} F(I_l) = -\infty \tag{5.43}$$

the by the intermediate value theorem, there must be at least one positive root for $I_l \in (0, \infty)$

(c) If $\bar{I}_{l1} > \bar{I}_{l3} > \bar{I}_{l2}$, similarly proceed as in (b).

(d) If $\bar{I}_{l3} > \bar{I}_{l1} > \bar{I}_{l2}$ then since F is continuous in $(\bar{I}_{l2}, \bar{I}_{l3})$,

$$\lim_{I_l \to \bar{I}_{l2}^+} F(I_l) = -\infty \tag{5.44}$$

$$\text{and} \qquad \lim_{I_l \to \bar{I}_{l3}^-} F(I_l) = \infty \tag{5.45}$$

the by the intermediate value theorem, there must be at least one positive root for $I_l \in (0, \infty)$

(e) If $\bar{I}_{l2} > \bar{I}_{l1} > \bar{I}_{l3}$, similarly proceed as in (d).

Hence, the existence of at least one endemic equilibrium for System (5.16), has been established whenever $R_0^{prop} > 1$. If we can show $F(I_l)$ is monotone, then we can set the uniqueness of the endemic equilibrium. □

5.5.2 Preferred Mixing

If birds mix according to preferred mixing (Jacquez et al. 1988, Blythe et al. 1991, Blythe et al 1995) then the mixing probabilities are given by

$$P_{rz} = f_r\delta_{rz} + (1 - f_r)\frac{(1 - f_z)C_zN_z}{\sum_{j=1}^{k+s}(1 - f_j)C_jN_j}. \tag{5.46}$$

Here, P_{rz} represent the proportion of contacts between birds of flock r and birds of flock z where, $\sum_{z=1}^{s+k} P_{rz} = \sum_{z=1}^{k} P_{rz} + \sum_{z=s+1}^{s+k} P_{rz} = 1$ and r is fixed. δ_{rz} is the delta function, thus $f_r\delta_{rz}$ models preferred contacts, that is, "reserve" contacts with your own type while $(1 - f_r)\frac{(1-f_z)C_zN_z}{\sum_{j=1}^{k+s}(1-f_j)C_jN_j}$ models contacts via proportionate mixing. As in the case of proportionate mixing, we assume that the average contacts rates are the same, that is, $C_r = C_z$ for any r and z. Thus, under this assumption, P_{rz} takes the simpler form

$$P_{rz} = f_r\delta_{rz} + (1 - f_r)\frac{(1 - f_z)N_z}{\sum_{j=1}^{k+s}(1 - f_j)N_j}. \tag{5.47}$$

For the case of only two groups model, System (5.16), these mixing probabilities become

$$\begin{aligned}
P_{ll} &= f_l + (1 - f_l)\frac{(1 - f_l)N_l}{(1 - f_m)N_m + (1 - f_l)N_l}, && (5.48)\\
P_{lm} &= (1 - f_l)\frac{(1 - f_m)N_m}{(1 - f_m)N_m + (1 - f_l)N_l}, && (5.49)\\
P_{ml} &= (1 - f_m)\frac{(1 - f_l)N_l}{(1 - f_m)N_m + (1 - f_l)N_l}, && (5.50)\\
P_{mm} &= f_m + (1 - f_m)\frac{(1 - f_m)N_m}{(1 - f_m)N_m + (1 - f_l)N_l}, && (5.51)
\end{aligned}$$

therefore, $P_{ll} + P_{lm} = 1$ and $P_{mm} + P_{ml} = 1$.

Disease Free Equilibrium and Basic Reproductive Number

The equilibrium for System (5.16) with preferred mixing, Eqs. (5.48), are calculated. The DFE for the SI system is $(I_m, S_l, I_l) = \left(0, \frac{\Lambda_l}{\mu_l}, 0\right)$. However, the basic reproductive number R_0 for the SI model under preferred mixing is given by (see Appendix C for calculations)

$$\begin{aligned} R_0^{pref} &= \frac{1}{2}\left[(1-P_{ml}^0)\frac{\beta}{\mu_m} + (1-P_{lm}^0)\frac{\beta}{\mu_l+d}\right] \\ &\quad + \frac{1}{2}\sqrt{\left[(1-P_{ml}^0)\frac{\beta}{\mu_m} - (1-P_{lm}^0)\frac{\beta}{\mu_l+d}\right]^2 + 4\frac{\beta}{\mu_m}P_{ml}^0\frac{\beta}{\mu_l+d}P_{lm}^0}, \end{aligned} \tag{5.52}$$

where

$$P_{ml}^0 = (1-f_m)\frac{(1-f_l)\Lambda_l/\mu_l}{\Lambda_m/\mu_m + \Lambda_l/\mu_l} \quad \text{and} \tag{5.53}$$

$$P_{lm}^0 = (1-f_l)\frac{(1-f_m)\Lambda_m/\mu_m}{\Lambda_m/\mu_m + \Lambda_l/\mu_l}. \tag{5.54}$$

Therefore, in this case R_0 is given by a nonlinear function of the basic reproductive numbers of migratory and local birds, R_0^m and R_0^l. Specifically,

$$\begin{aligned} R_0^{pref} &= \frac{1}{2}\left[(1-P_{ml}^0)R_0^m + (1-P_{lm}^0)R_0^l\right] \\ &\quad + \frac{1}{2}\sqrt{\left[(1-P_{ml}^0)R_0^m - (1-P_{lm}^0)R_0^l\right]^2 + 4R_0^m P_{ml}^0 R_0^l P_{lm}^0}. \end{aligned} \tag{5.55}$$

Typically, we expect that if $R_0 < 1$ the DFE is locally asymptotically stable while if $R_0 > 1$ the DFE is unstable. We conduct some simulations that support the likelihood that these results indeed hold.

5.6 Numerical Results

In this section the results of numerical simulations are presented to illustrate and compare the outcomes associated with the two cases of mixing probability models.

Since the mortality rate due to HPAI in poultry (local birds) is very high we only vary d_l and f_m and f_l, the proportion of contacts within your own type. We only choose values of the parameters that lead to values of R_0^{prop} and R_0^{pref} both greater than 1. We only vary the proportion of preferred contacts (f's). Hence, the solutions for the SI epidemic model corresponding to proportionate mixing are fixed as well as the corresponding basic reproductive number, $R_0^{prop} = 5.4183$. In addition, we fixed the rest of the parameters as follows: $\beta_m = 0.3, \beta_l = 0.6, \mu_m = 0.1, \mu_l = 0.01, \Lambda_m = 7.5$ and $\Lambda_l = 50$. The initial conditions for the epidemiological classes are set to $I_{m0} = 20$, $S_{l0} = 5000$ and $I_{l0} = 0$ that is, a total population of migratory birds, $\Lambda_m/\mu_m = 75$ and a total population of local birds, $\Lambda_m/\mu_m = 5000$.

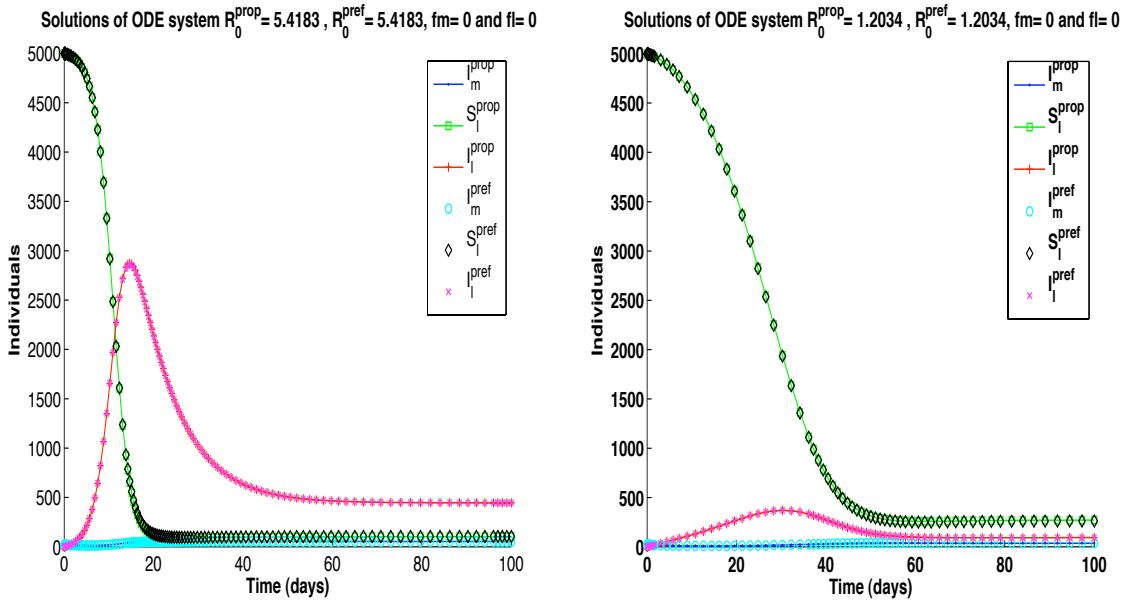

Figure 5.2: Solutions for the SI epidemic model for both proportionate mixing and preferred mixing. Since in this case $f_m = f_l = 0$ solutions are the same for both models. The difference is in the mortality rate due to disease, the figure on the left shows the solutions for $d_l = .1$ while the figure on the right shows solutions for $d_l = 0.5$.

Figure 5.2 shows solutions of the SI epidemic model for both proportionate and

preferred mixing. Hence, for both figures we set $f_m = f_l = 0$ and vary the local birds disease-induced mortality, d_l. The solutions for all the epidemiological classes overlap since the mixing probabilities are the same for both models ($P_{rz}^{prop} = P_{rz}^{pref}$ for $r, z = \{l, m\}$) and $R_0^{prop} = R_0^{pref}$ if $f_m = f_l = 0$ The figure on the left shows the case where $d = 0.1$ with $R_0^{prop} = R_0^{pref} = 5.4183$ while the figure on the right shows the case where $d = 0.5$ with $R_0^{prop} = R_0^{pref} = 1.2034$. If the disease-induced mortality is 0.5 then infected individuals die so fast that only a small window of time is available to infect others. Hence, when $d = 0.5$ we have a smaller (compare to the figure on the left) basic reproductive number and a lower number of infected cases. When $d = 0.1$ a larger number of infected cases are recorded and the epidemic takes over in less than 30 days (with a peak at 15 days). Since the average time that migratory birds spend with local birds is small $\left(\frac{1}{\mu_m} = 10 \text{ days}\right)$ their infected population basically remains constant.

Solutions of the SI epidemic model under true preferred mixing when $f_m = f_l = 0.5$ or when $f_m = f_l = 0.9$ with $d = 0.1$ are presented on Figure 5.3. The figure on the left shows the case $f_m = f_l = 0.5$, that is, when half of the contact are reserve for mixing within your own type and the other half reserve for random mixing with all other groups. In this case, there is not much qualitative changes between this plot and the left plot on Figure 5.2. We see a slightly shift on the solutions of local susceptible and infected birds as well as on the R_0's ($R_0^{prop} = 5.4183$ and $R_0^{prep} = 5.4295$). The figure on the right shows plots for the case $f_m = f_l = 0.9$. In this case, higher infected cases (higher peak) are seen under preferred mixing. Again, the population of migratory infected birds remains nearly constant.

Figure 5.4 on the left shows the solutions of the SI epidemic model for $f_m = f_l = 0.999$ with disease induced mortality $d = 0.1$. Even thought in this case must

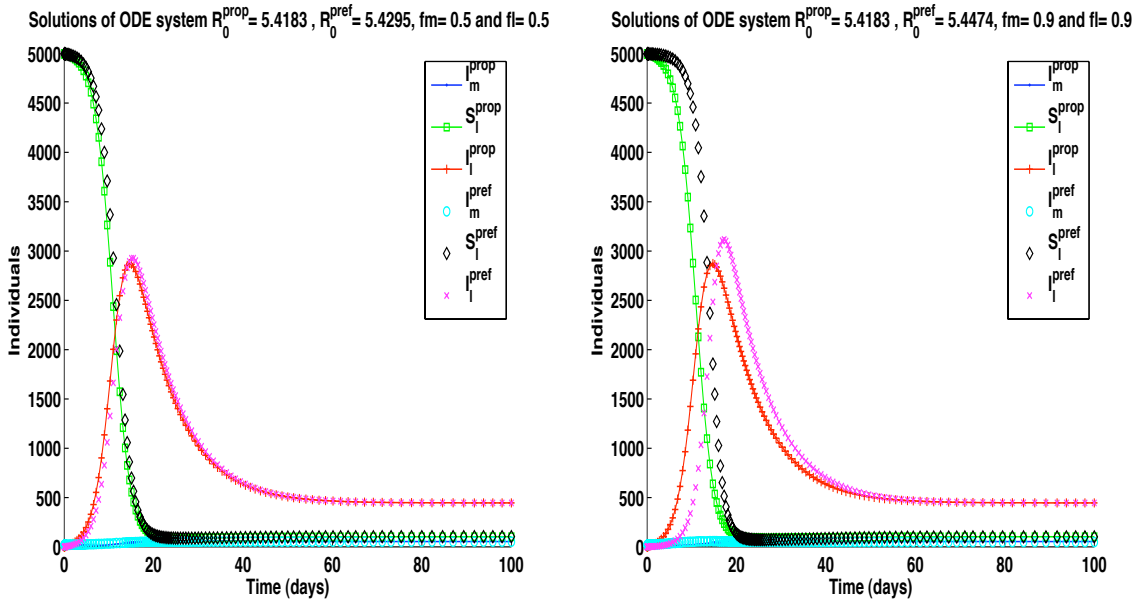

Figure 5.3: Solutions for the SI epidemic model for both proportionate and preferred mixing. The figure on the left shows solutions for $f_m = f_l = 0.5$ while the figure on the right show solutions for $f_m = f_l = 0.9$. As the proportion of contact with your own type increases the number of infected increases as well.

contacts are only within your own type, slight random mixing can still trigger an epidemic. The figure on the right show solutions where $f_m = f_l \approx 1$, that is under complete preferred mixing. In this case a higher number of local infected birds are reported, that is $I_l = 4288$. Therefore, contacts under preferred mixing give the worst case scenario as higher infections cases are seen in infected poultry. However, the epidemic takes longer (days) to be established in local birds populations. Therefore, timely control measures can be pursue to prevent further damage.

Figure 5.5 shows R_0^{prop} and R_0^{pref} as a function of the R_0's of migratory birds and local birds, that is, R_0^m and R_0^l respectively. All other parameters are fixed to $\beta_m = \beta_l = 0.4, \mu_l = 0.01, d_l = 0.1, \Lambda_m = 7.5, \Lambda_l = 50$ and $f_m = f_l = 0.999$. For preferred mixing (the figure on the right) we can observe that for small values of

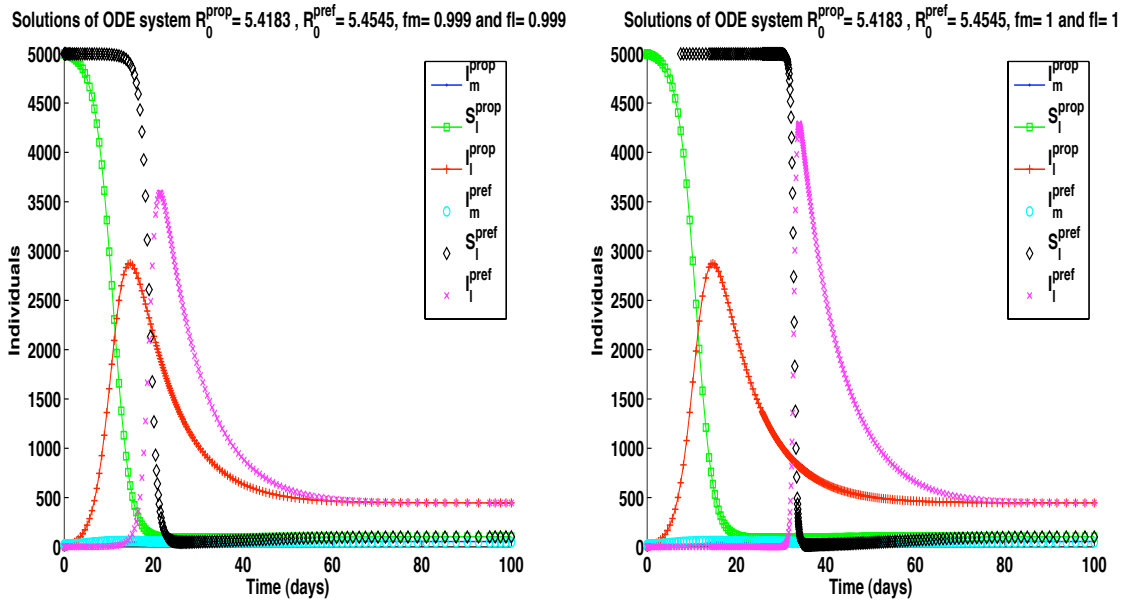

Figure 5.4: Solutions for the SI epidemic model for both proportionate and preferred mixing. The figure on the left shows solutions for $f_m = f_l = 0.99$. The figure on the right show solutions completely preferred mixing for $f_m = f_l \approx 1$. In this case higher reported cases are shown with 4288 local infected birds.

R_0^m, as R_0^l increases R_0^{pref} also increases. Therefore, R_0^{pref} can be larger when R_0^m and R_l varies, thus preferred mixing indeed can provide the worst case scenario.

5.7 Discussion

In this chapter a general metapopulation framework is introduced for the study of the dynamics of epidemics generated from weak or strong interactions between migratory birds and local birds. We reformulate two versions of this framework, the first base on resident times (see Castillo-Chavez et al. 1998 and Castillo-Chavez et al. 2003) and the second on classical mixing (Jacquez et al. 1988, Blythe et al. 1991, Blythe et al 1995). The overall analysis of models with complex mixing has turned out to be difficult but see Castillo-Chavez et al. (1989), Busenberg and

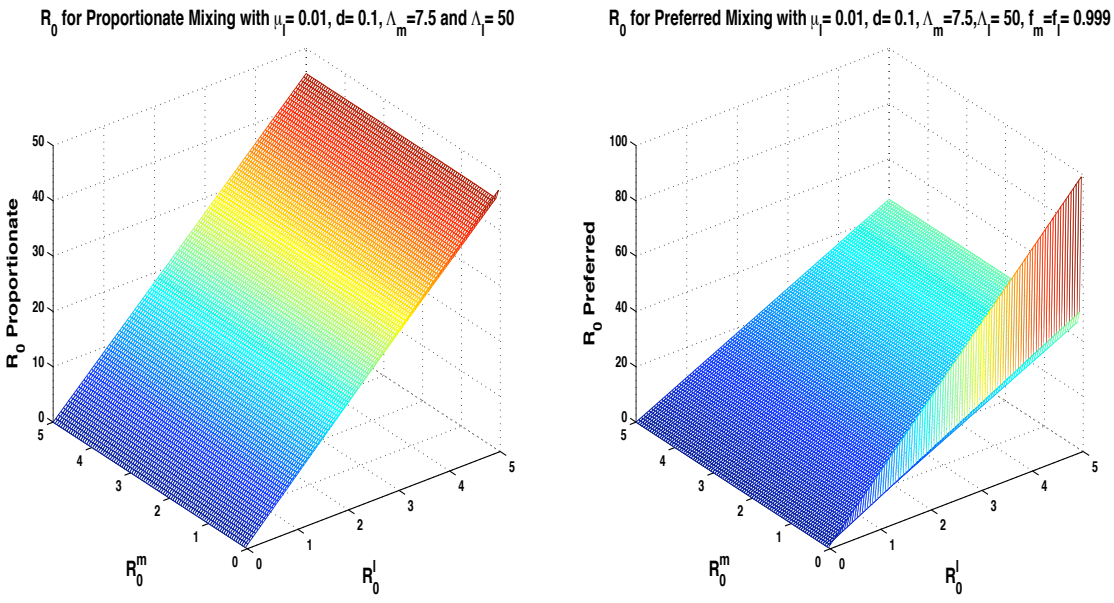

Figure 5.5: The graphs shows R_0^{prop} and R_0^{pref} as a function of R_0^m and R_0^l.

Castillo-Chavez (1991), Simon and Jacquez (1992), Huang et al. (1992), Castillo-Chavez et al. (2003), and Castillo-Chavez and Song (2004). Preliminary studies of the residence-time framework was carried out by Castillo-Chavez et al. 2003 in the context of mass transportation systems and smallpox outbreaks but there is not yet a clean analyses even of simple cases. Hence, here we focus on highlighting the potential use of classical mixing models through the preliminary analytical and computational analysis of a simple epidemic model that involves weak, strong or random interactions between two types of bird populations. We focus on epidemics driven by the interactions of one migratory (short residence-times) and one local populations of birds. We observe that the mixing not only impacts the value of the basic reproductive number but also the duration of an epidemic. Furthermore, we explore the case when disease (HPAI avian influenza) seriously impact the ability of local populations to survive. Hence, we study the impact of high-mortality

rates in local populations under weak, strong or random mixing. In this paper we observe that preferred mixing triggers a stronger epidemic (larger R_0) although in higher duration. Thus, control measures may be achievable in a timely manner under preferred mixing. The reduction of the avian flu epidemic may be achieved by effectively controlling the interactions between migratory and local bird populations along migration routes. The cycle of transmission between this populations should be broken if the virus is to be eradicated from poultry flocks.

CHAPTER 6

CONCLUSION

Tradiitionally, limited theoretical work on the spread of disease has been done that incorporates spatially explicit dynamics. In this dissertation, we deal with models that account for the explicit or implicit spatial spread of epidemics with the incorporation of space and time.

Chapter 2 is devoted to the study of diffusion models in biology, mainly reaction-diffusion equations. It introduces a modeling approach based on integrodifference equations. These models are known as discrete spatial contact models. Chapters 3 and 4 focuses on the study of epidemic dispersal model by nonlinear integrodifference equations. The models incorporate population growth (with discrete generations), disease dynamics and dispersal. We search for travelling wave solutions and minimum speed of propagation. We study epidemic models (SI, SIS) with non-overlapping and overlapping epidemiological generations, that is, models where the generation of secondary cases of infection are driven by carefully derived monotone and non-monotone growth functions. It is shown that when dispersal is added (via redistribution kernels) to epidemic models in populations with simple demographic patterns (constant and geometric growth) travelling wave solutions exist as long as the disease's basic reproductive number, R_0, is greater than one and the initial conditions have compact support. The minimal speed of propagation, c^*, is computed. Simulations that evaluate the role of the parameters of the model to the minimal speed are carried out. We find, for example, that c^* is positively correlated to changes in key epidemiological parameters. Furthermore, it is shown that controlling individuals' movement and reducing the infectious period

helps prevent the advancement of an epidemic. Numerical simulations are carried out that shows traveling wave solutions when $R_0 > 1$ in one and two spatial dimensions. In the case of non-monotone growth functions, it is shown numerically that when the solution of the epidemic model approaches monotonically a positive fixed point (local endemic state) the travelling wave solutions will have a monotone wave profile. On the other hand, when solutions approach the positive fixed point (local endemic) via damped oscillations, the traveling wave solution will experience damped oscillations around the fixed point. Simulations in two spatial dimensions are also carried out in this last scenario.

An alternative framework for the study of disease dispersal is introduced in Chapter 5. We focus on the role of transient populations on disease dynamics using a metapopulation model approach, that is, a model without explicit space variables. We consider two modeling schemes one base on mixing (contact between populations) weighted by residence-times in key environments and a second that uses a classical approach (classical mixing). In order, to explore the potential uses of these framework, we consider a rather simple case that involves only two groups: a local and a migratory bird population. It is observed that the mixing will not only impacts the value of R_0 but also the duration of the epidemic. It is shown that preferred (like-with-like) mixing triggers the stronger epidemic outbreaks.

Future work includes the exploration of the meta-population approach and the expansion of the integrodiffernce approach to the case of interacting populations. The application of these models to the study of specifics diseases and their connection to data are also part of a future research program.

APPENDIX A

HOMOCLINIC AND HETEROCLINIC ORBITS

Homoclinic orbits are trajectories that start and end at the same equilibrium points. More precisely, a homoclinic orbit lies in the intersection of the stable manifold and the unstable manifold of an equilibrium. They are common in conservative systems, but are rare otherwise. An homoclinic orbit does not correspond to a periodic orbit solution, because the trajectory takes "forever" to reach the equilibrium. These trajectories approach the fixed point as $t \to \pm\infty$.

Homoclinic orbits and homoclinic points are defined in the same way for iterated functions, as the intersection of the stable set and unstable set of some fixed point or periodic point of the system. Consider the continuous dynamical system described by the ordinary differential equation $\dot{x} = f(x)$. Suppose there is an equilibrium at $x = x_1$, then a solution $\vartheta(t)$ is a homoclinic orbit if $\vartheta(t) \to x_1$ as $t \to \pm\infty$.

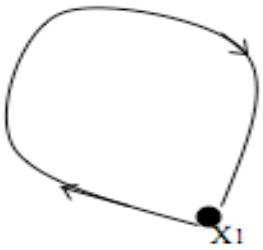

Figure A.1: Example of a homoclinic orbit.

As described in Guckenheimer and Holmes (2002) a heteroclinic orbit (sometimes called a heteroclinic connection) is a path in phase space which joins two different equilibrium points. Heteroclinic orbits are trajectories that connect two or more saddle points. Like homoclinic orbits, heteroclinic orbits are much more common in reversible or conservative systems than in orther types of systems.

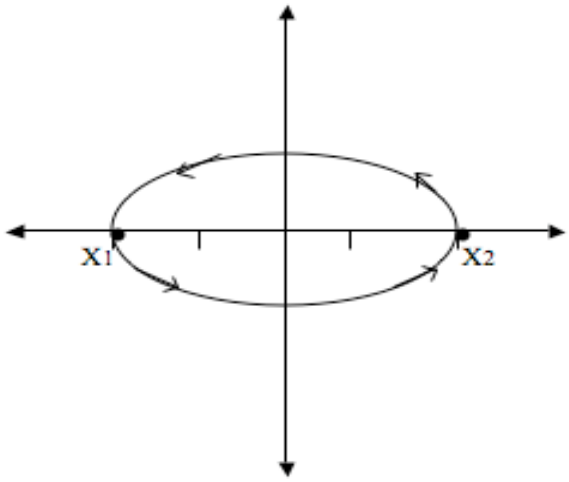

Figure A.2: Example of a heteroclinic orbit.

Consider the continuous dynamical system described by the ordinary differential equation $\dot{x} = f(x)$. Suppose there are equilibria at $x = x_1$ and $x = x_2$, then a solution $\vartheta(t)$ is a heteroclinic orbit from x_1 to x_2 if $\vartheta(t) \to x_1 \quad as \quad t \to -\infty$ and $\vartheta(t) \to x_2 \quad as \quad t \to +\infty$. This implies that the orbit is contained in the stable manifold of x_2 and the unstable manifold of x_1. For an example in the context of an epidemiological applications, see Faina et al. (2005).

APPENDIX B

R_0 FOR THE INTEGRODIFFERENCE EPIDEMIC MODEL

The R_0 for the integrodifference epidemic System (3.7) corresponds to the R_0 of the discrete time system (3.4). Linearizing Eq. (3.17) with

$$I_t(y) = \tilde{I}(y) + \bar{I}_t(y). \tag{B.1}$$

and substitution of Eq. $(B.1)$ into the integrodifference equation (3.17) gives

$$\begin{aligned} I_{t+1}(x) &\approx \int_{-\infty}^{\infty} g(I_t(y))\; k(x-y)\; dy \qquad \text{(B.2)} \\ \tilde{I}(x) + \bar{I}_{t+1}(x) &\approx \int_{-\infty}^{\infty} g(\tilde{I}(y) + \bar{I}_t(y))\; k(x-y)\; dy \\ &\approx \int_{-\infty}^{\infty} \left[1 - Q\left(\frac{\alpha(\tilde{I}(y) + \bar{I}_t(y))}{\Lambda + \Lambda^*}\right)\right] [\Lambda^* - \gamma(\tilde{I}(y) + \bar{I}_t(y))] + \\ &\quad \gamma\sigma(\tilde{I}(y) + \bar{I}_t(y))\; k(x-y)dy. \qquad \text{(B.3)} \end{aligned}$$

Thus, under a Taylor Series expansion:

$$\begin{aligned} \tilde{I}(x) + \bar{I}_{t+1}(x) &\approx \int_{-\infty}^{\infty} \left\{1 - Q\left(\frac{\alpha\tilde{I}(y)}{\Lambda + \Lambda^*}\right) - \frac{\alpha}{\Lambda + \Lambda^*} Q\left(\frac{\alpha\tilde{I}(y)}{\Lambda + \Lambda^*}\right) \bar{I}_t(y)\right\} \\ &\quad k(x-y)dy + \int_{-\infty}^{\infty} \{[\Lambda^* - \gamma\tilde{I}(y) - \gamma\bar{I}_t(y)] + \gamma\sigma\tilde{I}(y) \\ &\quad + \gamma\sigma\bar{I}_t(y)\} k(x-y)dy. \qquad \text{(B.4)} \end{aligned}$$

The steady state equation for the system of integrodifference equations is

$$\tilde{I}(x) = \int_{-\infty}^{\infty} \left\{\left[1 - Q\left(\frac{\alpha\tilde{I}(y)}{\Lambda + \Lambda^*}\right)\right] [\Lambda^* - \gamma\tilde{I}(y)] + \gamma\sigma\tilde{I}(y)\right\}\; k(x-y)dy. \tag{B.5}$$

Therefore, Eq. $(B.2)$ becomes

$$\begin{aligned} \bar{I}_{t+1}(x) &\approx \int_{-\infty}^{\infty} \left[1 - Q\left(\frac{\alpha\tilde{I}(y)}{\Lambda + \Lambda^*}\right)\right] [-\gamma\bar{I}_t(y)] + \left[\frac{-\alpha}{\Lambda + \Lambda^*} Q\left(\frac{\alpha\tilde{I}(y)}{\Lambda + \Lambda^*}\right) \bar{I}_t(y)\right] \\ &\quad [\Lambda^* - \gamma\tilde{I}(y)] + \gamma\sigma\bar{I}_t(y)\; k(x-y)dy. \qquad \text{(B.6)} \end{aligned}$$

If $\tilde{I}(y) = 0$, then

$$\bar{I}_{t+1}(x) = \int_{-\infty}^{\infty} \left[\frac{\alpha \Lambda^* Q(0)}{\Lambda + \Lambda^*} + \gamma\sigma \right] \bar{I}_t(y)\ k(x-y)dy \tag{B.7}$$

Thus we conclude that,

$$\bar{I}_{t+1}(x) = c \int_{-\infty}^{\infty} \bar{I}_t(y)\ k(x-y)dy \quad \text{where} \quad c = \frac{\alpha \Lambda^* Q(0)}{\Lambda + \Lambda^*} + \gamma\sigma. \tag{B.8}$$

The stability of $\tilde{I}(y) = 0$ under the perturbation $\bar{I}_t(x) = \lambda^t j(x)$ where $\lambda \neq 0$, $j(x) > 0$, $\int_{-\infty}^{\infty} j(x)dx < \infty$ is

$$\lambda^{t+1}\ j(x) = c \int_{-\infty}^{\infty} \lambda^t\ j(y)\ k(x-y)\ dy, \tag{B.9}$$

$$\lambda\ j(x) = c \int_{-\infty}^{\infty} j(y)\ k(x-y)\ dy, \tag{B.10}$$

$$\lambda \int_{-\infty}^{\infty} j(x)\ dx = c \int_{-\infty}^{\infty} \int_{-\infty}^{\infty} j(y)\ k(x-y)\ dy\ dx, \tag{B.11}$$

$$= c \left(\int_{-\infty}^{\infty} j(y)dy \right) \left(\int_{-\infty}^{\infty} k(x-y)dx \right) \tag{B.12}$$

Changing variables with $\beta = x - y$ then,

$\lambda = c \int_{-\infty}^{\infty} k(\beta)d\beta,$ and since the total mass of the kernel is one we conclude

$$\lambda = \frac{\alpha \Lambda^* Q(0)}{\Lambda + \Lambda^*} + \gamma\sigma > 0.$$

Therefore for $I_t(x) = \lambda^t i(x) > 0$ if $\lambda > 1$ then $\tilde{I}(x) \equiv 0$ is unstable while if $0 < \lambda < 1$ then $\tilde{I}(x)$ is locally asymptotically stable. Therefore, $\lambda > 1$ provides the equation for R_0 below. In conclusion this result is satisfied if and only if $R_0 > 1$ is unstable while $0 < R_0 < 1$ is locally asymptotically stable. Hence R_0 for the integrodifference equation model is provided by:

$$R_0 = \frac{\alpha}{1 - \gamma\sigma}[p + \gamma(1-p)]. \tag{B.13}$$

APPENDIX C

NEXT GENERATOR OPERATOR

In 1990 Dieckmann et al. define R_0 as the spectral radius of the next generator matrix. R_0 is typically found by calculating the eigenvalues of the Jacobian matrix at the DFE equilibrium, where the largest positive eigenvalue is R_0 (Castillo-Chavez et al. 2002). Here, the general idea of the next generator approach is explained following the work of van den Driessche and Watmough (2002).

The total population is divided in compartments according to their epidemiological status, that is, susceptible, exposed, infected, recovered and treated among others such that $x = (x_1, x_2, x_3, ...x_n)^t$ where $x_i \geq 0$ represent the number of individuals in each compartment. These compartments are further divided, $\mathcal{M}_i(x)$ corresponds to the rate of appearance of new infections into each compartment whereas $\mathcal{D}_i(x)^+$ is the transfer of individuals into each compartment by all other means and $\mathcal{D}_i(x)^-$ is the transfer of individuals out of each compartment. Therefore, disease transmission model correspond to the following system of equations:

$$\dot{x_i} = f(x_i) = \mathcal{M}_i(x) - \mathcal{D}_i(x), \qquad i = 1, ..., n \tag{C.1}$$

where $\mathcal{D}_i(x) = \mathcal{D}_i^+(x) - \mathcal{D}_i^-(x)$. Thus, if x_0 is the DFE of System (C.1) with Jacobian matrices

$$M = \left[\frac{\partial \mathcal{M}_i}{\partial x_j}(x_0)\right] \quad \text{and} \quad D = \left[\frac{\partial \mathcal{D}_i}{\partial x_j}(x_0)\right] \qquad \text{with} \qquad 1 \leq i, j \leq m \tag{C.2}$$

then

$$R_0 = \rho(MD^{-1}) \tag{C.3}$$

where $\rho(A)$ denotes the spectral radius of A, that is the largest eigenvalue λ of $A - \lambda I$.

C.0.1 R_0 for the Case of Proportionate Mixing

To obtain the R_0 of the SI epidemic model with proportionate mixing we let the vector of new infections be:

$$\mathcal{M} = \begin{pmatrix} \beta[N_m - I_m]\left[\frac{I_m+I_l}{N_m+N_l}\right] \\ 0 \\ \beta S_l\left[\frac{I_m+I_l}{N_m+N_l}\right] \end{pmatrix} \tag{C.4}$$

whereas

$$\mathcal{D} = \begin{pmatrix} \mu_m I_m \\ -\Lambda_l + \beta S_l[N_m - I_m]\left[\frac{I_m+I_l}{N_m+N_l}\right] + \mu_l S_l \\ (\mu_l + d)I_l \end{pmatrix}. \tag{C.5}$$

Thus, after computing the Jacobian matrices of $\mathcal{M}$ and $\mathcal{D}$, evaluating them at the DFE $x_0 = \left(0, \frac{\Lambda_l}{\mu_l}, 0\right)$, and doing some simplifications we obtain

$$M = \begin{bmatrix} \beta T_m & \beta T_m \\ \beta T_l & \beta T_l \end{bmatrix} \quad \text{and} \quad D = \begin{bmatrix} \mu_m & 0 \\ 0 & \mu_l + d \end{bmatrix}, \tag{C.6}$$

where $T_m = \frac{\Lambda_m/\mu_m}{\Lambda_m/\mu_m+\Lambda_l/\mu_l}$ and $T_l = \frac{\Lambda_l/\mu_l}{\Lambda_m/\mu_m+\Lambda_l/\mu_l}$. Therefore,

$$MD^{-1} = \begin{bmatrix} \frac{\beta T_m}{\mu_m} & \frac{\beta T_m}{\mu_l+d} \\ \frac{\beta T_l}{\mu_m} & \frac{\beta T_l}{\mu_l+d} \end{bmatrix} \tag{C.7}$$

and the basic reproductive number is

$$R_0^{prop} = \rho(MD^{-1}) = T_m\frac{\beta}{\mu_m} + T_l\frac{\beta}{\mu_l + d}. \tag{C.8}$$

C.0.2 R_0 for the Case of Preferred Mixing

For the case of preferred mixing, the vector of new infections is:

$$\mathcal{M} = \begin{pmatrix} \beta[N_m - I_m]\left[(1-P_{ml})\frac{I_l}{N_l} + P_{ml}\frac{I_m}{N_m}\right] \\ 0 \\ \beta S_l\left[(1-P_{lm})\frac{I_l}{N_l} + P_{lm}\frac{I_m}{N_m}\right] \end{pmatrix} \tag{C.9}$$

whereas

$$\mathcal{D} = \begin{pmatrix} \mu_m I_m \\ -\Lambda_l + \beta S_l\left[(1-P_{lm})\frac{I_l}{N_l} + P_{lm}\frac{I_m}{N_m}\right] + \mu_l S_l \\ (\mu_l + d)I_l \end{pmatrix}. \tag{C.10}$$

Thus, after obtain the Jacobian matrices of $\mathcal{M}$ and $\mathcal{D}$ evaluating them at the DFE $x_0 = \left(0, \frac{\Lambda_l}{\mu_l}, 0\right)$ and doing some simplifications we obtain

$$M = \begin{bmatrix} \beta(1-P^0_{ml}) & \beta P^0_{lm} \\ \beta P^0_{ml} & \beta(1-P^0_{lm}) \end{bmatrix} \quad \text{and} \quad D = \begin{bmatrix} \mu_m & 0 \\ 0 & \mu_l + d \end{bmatrix}, \tag{C.11}$$

where $P^0_{ml} = (1-f_m)\frac{(1-f_l)\Lambda_l/\mu_l}{\Lambda_m/\mu_m + \Lambda_l/\mu_l}$ and $P^0_{lm} = (1-f_l)\frac{(1-f_m)\Lambda_m/\mu_m}{\Lambda_m/\mu_m + \Lambda_l/\mu_l}$. Therefore,

$$MD^{-1} = \begin{bmatrix} \frac{\beta}{\mu_m}(1-P^0_{ml}) & \frac{\beta}{\mu_l+d}P^0_{lm} \\ \frac{\beta}{\mu_m}P^0_{ml} & \frac{\beta}{\mu_l+d}(1-P^0_{lm}) \end{bmatrix} \tag{C.12}$$

and the basic reproductive number is

$$\begin{aligned} R_0^{pref} &= \rho(MD^{-1}) = \frac{1}{2}\left[(1-P^0_{ml})\frac{\beta}{\mu_m} + (1-P^0_{lm})\frac{\beta}{\mu_l+d}\right] \\ &+\frac{1}{2}\sqrt{\left[(1-P^0_{ml})\frac{\beta}{\mu_m} - (1-P^0_{lm})\frac{\beta}{\mu_l+d}\right]^2 + 4\frac{\beta}{\mu_m}P^0_{ml}\frac{\beta}{\mu_l+d}P^0_{lm}}. \end{aligned} \tag{C.13}$$

BIBLIOGRAPHY

[1] Allen, E.J., Allen, L.J.S., and Gilliam, X. (1996). Dispersal and competition models for plants. *Journal of Mathematical Biology* **34**, 455-481.

[2] Allen, L.J.S. and Ernest, R.K. (2002). The impact of long-range dispersal on the rate of spread in population and epidemic models. In: *Mathematical Approaches for Emerging and Reemerging Diseases: an Introduction to Models, Methods and Theory.* IMA Volume 125. Castillo-Chavez, C., Blower, S., van den Driessche P., Kirschner, D. and Yakubu A.-A. (eds.). New York: Springer-Verlag, 183-197.

[3] Anderson, R.M. and May, R.M. (1991). Infectious Diseases of Humans. Oxford Science Publication.

[4] Aronson, D.G. and Weinberger, H.F. (1975). Nonlinear diffusion population genetics, combustion, and nerve pulse propagation. In: *Partial Differential Equations and Related Topics.* Lecture Notes in Mathematics 445. J. Goldstein (ed.). Springer-Verlag, Heidelberg, 5-49.

[5] Aronson, D.G. (1977). The asymptotic speed of propagation of a simple epidemic. In: *Nonlinear Diffusion.* Fitzgibbon, W.E. and Walker, H.F. (eds.). London: Pitman, 1-23.

[6] Berezovsky, F., Karev, G., Song, B. and Castillo-Chavez, C. (2005). A simple epidemic model with surprising dynamics. *Math. Biosci. Eng.* **2**, 133–152.

[7] Blythe, S., Castillo-Chavez, C. and Palmer, S. (1991). Toward a Unified Theory of Sexual Mixing and Pair Formation. *Math. Biosci.* **107** 379-405.

[8] Blythe, S., Busenberg, S. and Castillo-Chavez, C. (1995). Affinity in Paired Event Probability. *Math. Biosci.* **128**, 265-284.

[9] Brauer, F. and Castillo-Chavez, C. (2001). Mathematical Models in Population Biology and Epidemiology. Sringer-Verlag, New York.

[10] Brauer, F., van den Driessche P., Wu, J. (eds.) (2008). Mathematical Epidemiology. Lecture notes in Mathematics/Mathematical Biosciences Subseries. Springer-Verlag, Berlin Heidelberg.

[11] Britton, N.F. (1986). Reaction-Diffusion Equations and their Applications to Biology. Academic Press, New York.

[12] Busenberg, S., Castillo-Chavez, C. (1991). A general solution of the problem of mixing of subpopulations and its application to risk- and age-structured epidemic models for the spread of AIDS. *IMA J. Math. Appl. Med. Biol.* **8**, 1-29.

[13] Butler, D. (2006). Doubts hang over source of bird flu spread. *Nature* **439**, 772.

[14] Caley, M.J., Carr, M.H., Hixon, M.A., Hughes, T.P., Jones, G.P., and Menge, B.A. (1996). Recruitment and the local dynamics of open marine populations. *Annual Reviews of Ecology and Systematics* **27**, 477-500.

[15] Castillo-Chavez, C., Cooke, K., Huang, W.Z, Levin, S.A. (1989). The role of long periods of infectiousness in the dynamics of acquired immunodeficiency syndrome (AIDS). *Mathematical approaches to problems in resource management and epidemiology (Ithaca, NY, 1987)*, Lecture Notes in Biomath.. 8, Springer, Berlin,177-189.

[16] Castillo-Chavez, C., Capurro, A., Zellner, Z. and Velasco-Hernandez, J. X. (1998). El transporte publico y la dinamica de la tuberculosis a nivel poblacional. *Aportaciones Matematicas, Serie Comunicaciones* **22**, 209-225.

[17] Castillo-Chavez, C. and Yakubu, A.-A. (2001). Dispersal disease and life-history evolution. *Math. Biosc.* **173**, 35-53.

[18] Castillo-Chavez, C. and Yakubu, A.-A. (2002). Discrete-time SIS models with simple and complex population dynamics. In: *Mathematical Approaches for Emerging and Reemerging Diseases: an Introduction to Models, Methods and Theory.* IMA Volume 125. Castillo-Chavez, C., Blower, S., van den Driessche P., Kirschner, D. and Yakubu A.-A. (eds.). New York: Springer-Verlag, 153-163.

[19] Castillo-Chavez, C., Blower, S., van den Driessche P., Kirschner, D. and Yakubu A.-A. (eds.) (2002a). Mathematical Approaches for Emerging and Reemerging Diseases: an Introduction to Models, Methods and Theory. IMA Volume 125. New York: Springer-Verlag.

[20] Castillo-Chavez, C., Blower, S., van den Driessche P., Kirschner, D. and Yakubu A.-A. (eds.) (2002b). Mathematical Approaches for Emerging and Reemerging Diseases: an Introduction to Models, Methods and Theory. IMA Volume 126. New York: Springer-Verlag.

[21] Castillo-Chavez, C., Feng, Z., Huang, W. (2002). On the computation of R_0 and its role in global stability. In: *Mathematical Approaches for Emerging and Reemerging Infectious Diseases: An Introduciton.* Castillo-Chavez, C., with Blower, S., van den Driessche, P., Kirschner, D., and Yakubu, A.-A. (eds.). Springer, 229-250

[22] Castillo-Chavez, C., Song, B. and Zhang, J. (2003). An epidemic model with virtual mass transportation: the case of smallpox in a large city. In: *Bioterrorism: Mathematical Modeling Applications in Homeland Security.* Banks, H.T. and Castillo-Chavez, C. (eds.). SIAM Frontiers in Applied Mathematics, 173-197.

[23] Castillo-Chavez, C. and Song, B. (2004). Dynamical models of tuberculosis and their applications. *Math. Biosci. Eng. 1* 361-404.

[24] Caswell H. (2000). Matrix population models: construction, analysis, and interpretation. Sinauer Associates.

[25] Center for Disease Control and Prevention, (2006a). Key facts about avian influenza (bird flu) and avian influenza A (H5N1) virus. http://www.cdc.gov/flu/avian/gen-info/facts.htm

[26] Chen, H., Smith, G.J.D., Zhang, S.Y., Qin, K., Wang, J., Li, K.S., Webster, R.G., Peiris, J.S.M. and Guan, Y. (2005). H5N1 virus outbreak in migratory waterfowl. *Nature* **436**, 191-192.

[27] Chen, H. et al. (2006). Establishment of multiple sublineages of H5N1 influenza virus in Asia: implications for pandemic control. *PNAS* **103**, 2845-2850.

[28] Clarke, C.M.H. (1971). Liberations and dispersal of red deer in northern South Island districts. *New. Zeal. J. Sci.* **1**, 194-207.

[29] Cull, P. (1986). Local and global stability for populations models. *Biol. Cybernet.* **54**, 141-149.

[30] Dieckmann, O., Heesterbeek, J.A.P. and Metz, J.A.J. (1990). On the definition and the computation of the basic reproduction ratio R_0 in models for infectious diseases in heterogeneous population. *J. Math. Biol.* **28**, 365-382.

[31] Dobzhansky T. and Wright, S. (1943). Genetics of natural populations, X. dispersion rates in Drosophila pseudoobscura. *Genetics* **28**, 304-340.

[32] van den Driessche, P. and Watmough, J. (2002). Reproduction numbers and sub-threshold endemic equilibria for compartmental models of disease transmission. *Math. Biosc.* **180**, 29-48.

[33] Food and Agricultural Organization of the United Nations (2005). FAO AIDE News Special Issue. Update on Avian Influenza Situation. (As of 12/11/2005) - Issue no. 36, 1-7.

[34] Food and Agricultural Organization of the United Nations (Accessed 2006). Animal health special report, wild birds and avian influenza, 1-5. http://www.fao.org/ag/againfo/subjects/en/health/diseases-cards/avian_HPAIrisk.html

[35] Fisher, R.A. (1937). The wave of advance of advantageous genes. *Ann. Eugen. London* **7**, 355-369.

[36] Friend, M. and Franson C.J. (1999). Avian Influenza. In: *Field manual of wildlife diseases: general field procedures and diseases of birds.* U.S. Dept. of the Interior, U.S. Geological Survey, Washington D.C. 181-184.

[37] Guckenheimer, J. and Holmes, P. (2002). Nonlinear Oscillations, Dynamical Systems, and Bifurcations of Vector Fields. Applied Mathematical Sciences Vol. 42, Springer.

[38] Gumel, A.B., Castillo-Chavez, C., Mickens, R.E. and Clemence, D.P. (eds.) (2006). Mathematical Studies on Human Disease Dynamics Emerging Paradigms and Challenges. *CONM* **410**, American Mathematical Society, Rhode Island.

[39] Haberman, R. (2004). Applied Partial Differential Equations with Fourier Series and Boundary Value Problems, Pearson Prentice Hall, 4 ed.

[40] Hadeler, K.P. (1976). Nonlinear diffusion equations in biology. In: W. N. Everett and B. D. Sleeman (eds.), Ordinary and Partial Differential Equations. Lect. Notes in Mathematics 564, Springer-Verlag, Heidelberg.

[41] Hadeler, K.P. (2003). The role of migration and contact distributions in epidemic spread. In: *Bioterrorism: Mathematical Modeling Applications in Homeland Security.* Bank H.T. and Castillo-Chavez, C. (eds.). SIAM Frontier in Applied Mathematics, 199-210.

[42] Hanski, I. and Giplin, M.E. (1997). Metapopulation Biology: Ecology, Genetics and Evolution. Academic Press, California.

[43] Hastings, A. and Higgins, K. (1994). Persistence of transients in spatially structured ecological models. *Science* **263**, 1133-1136.

[44] Hethcote, Herbert, W. (2000). The mathematics of infectious diseases. *SIAM Rev.* **42** no. 4, 599-653.

[45] Huang, W.Z, Cooke, K.L., Castillo-Chavez, C. (1992). Stability and bifurcation for a multiple-group model for the dynamics of HIV/AIDS transmission. *SIAM J. Appl. Math.* **52**, 835-854.

[46] Jacquez, J.A., Simon, C.P., Koopman, J., Sattenspiel, L. and Perry, T. (1988). Modeling and analyzing HIV transmission: the effect of contact patters. *Math. Biosci.* **92**, 119-199.

[47] Kareiva P.M. (1983). Local movement in herbivorous insects: applying a passive diffusion model to markercapture field experiments. *Oecologia (Berlin)* **57**, 322-327.

[48] Kendall, M.G. (1948) A form of wave propagation associated with the equation of heat conduction. *Proc. Cambridge Phil. Soc.* **44**, 591-593.

[49] Kendall D.G. (1965). Mathematical models of spread of infection. *Conference on Mathematics and Computer Science in Biology and Medicine* Oxford 1964, 213-224.

[50] Kolmogorov, A., Petrovskij, I., and Piskunov, N. (1937). Etude de l'equation de la diffusion avec croissance de la quantite de la matiere et son application a

un probleme biologique. *Bull. Univ. Moscou Ser. Internation.,* Sec. A, **1 (6)**, 1-25.

[51] Kot, M. (1989). Diffusion-driven period-doubling bifurcations. *BioSystems.* **22**, 279-287.

[52] Kot, M. (1992). Discrete-time traveling waves: ecological examples. *J. Math. Biol.* **30**, 413-436.

[53] Kot, M., Lewis, M.A., and van den Driessche, P. (1996). Dispersal data and the spread of invading organisms. *Ecology* **77**, 2027-2042.

[54] Kot, M. and Schaffer, W.M. (1986). Discrete-time growth-dispersal models. *Math. Biosc.* **80**, 109-136.

[55] Latore, J., Gould, P., and Mortimer, A.M. (1998). Spatial dynamics and critical patch size of annual plant populations. *Journal of Theoretical Biology* **190**, 277-285.

[56] Levin, S.A. (1986). Random walk models of movement and their implications. In: *Mathematical Ecology*, Biomathematics Vol. 17. Springer-Verlag, 149-154.

[57] Lewis, M.A., Neubert, M.G., Caswell, H., Clark, J.S. and Shea, K. (2006). A guide to calculating discrete-time invasion rates from data. In: *Conceptual ecology and invasion biology: reciprocal approaches to nature.* Cadotte, M.W., McMahon S.M. and Fukami, T. (ed.). Invading Nature - Springer Series in Invasion Ecology **1**. Springer, 169-192.

[58] Li, B., Lewis, M.A., and Weinberger, H.F. (2008). Existence of traveling waves for integral recursions with nonmonotone growth functions. Submitted to *J. of Math. Biol.*.

[59] Liu, J. et al (2005). Highly pathogenic H5N1 influenza virus infection in migratory birds. *Science* **309**, 1206.

[60] Lubina, J.A. and Levin, S.A. (1988). The spread of a reinvading species: range expansion in the Califonia sea otter. *Am. Nat.* **131**, 526-543.

[61] Lui, R. (1983). Existence and stability of traveling wave solutions of a nonlinear operator. *J. Math. Biol.* **16**, 199-220.

[62] Lui, R. (1989). Biological growth and spread modeled by systems of recursions: I Mathematical theory. *Mathematical Biosciences* **93**, 269-295.

[63] McClusky, C.C. and Muldowney, J.C. (1998). Bendixson-Dulac criteria for difference equations. *J. Dyn. Diff. Eq.* **10**, 567-575.

[64] Medlock J. and Kot M. (2003). Spreading disease: integrodifferential equations old and new. *Math. Biosc.* **184**, 201-222.

[65] Mollison, D. (1972a). Possible velocities for a simple epidemic. *Adv. Appl. Probab.* **4**, 233-258.

[66] Mollison, D. (1972b). The rate of spatial propagation of simple epidemics. *Proc.* 6^{th} *Berkeley Symp. on Math. Statist. and Prob.* **3**, 579-614.

[67] Mollison, D. (1977) Spatial contact models for ecological and epidemic spread. *J. R. Stat. Soc. Ser. B* **39**, 283-326.

[68] Morrison, B. (2005) Report from Waterbirds 2005 Conference "Avian Diseases and Bird Migration". Avian Flu Information from the Nebraska Game and Parks Commission, 1-4. http://www.nebraskabirds.org/Library/Issues/Issues.htm

[69] Mundiger, P.C. and Hope, S. (1982). Expansion of the winter range of the House Finch: 1947-79. *Am. Birds* **36**, 347-353.

[70] Murray, J.D. (1989). Mathematical Biology. Springer-Verlag, Berlin Heidelberg.

[71] Murray, J.D. (2002). Mathematical Biology I: An Introduction, 3rd ed. Springer-Verlag, Berlin Heidelberg.

[72] Neubert, M.G., Kot, M. and Lewis, M.A. (1995). Dispersal and pattern formation in a discrete-time predator-prey model. *Theoretical Population Biology* **48**, 7-43.

[73] Neubert, M.G. and Caswell, H. (2000). Dispersal and demography: calculation and sensitivity analysis of invasion speed for structured populations. *Ecology* **81**, 1613-1628.

[74] Neubert, M.G., Caswell, H. and Murray, J.D. (2002). Transient dynamics and pattern formation: reactivity is necessary for turing instabilities. *Mathematical Biosciences* **175**, 1-11.

[75] Neubert, M.G. and Parker, I.M. (2004). Projecting rates of spread for invasive species. *Risk Analysis* **24**, 817-831.

[76] Normile, D. (2005). Are wild birds to blame? *Science* **310**. 426-428.

[77] Normile, D. (2006). Evidence points to migratory birds in H5N1 spread. *Science* **311**, 1225.

[78] Okubo, A. (1980). Diffusion and Ecological Problems: Mathematical Models. *Biomathematics, 10*. Sringer-Verlag, New York.

[79] Okubo, A. and Levin, S. (2001). Diffusion and Ecological Problems: A Modern perspective. *Interdisciplinary Applied Mathematics, 14*. Springer-Verlag, New York.

[80] Perez Velazquez, J. (1999). SIS nonlinear discrete-time models with two competing strains. *MTBI Cornell University Technical Report* (BU-1514-M).

[81] Redd, K.D., Meece, J.K., Henkel, J.S. and Shukla, S.K. (2003). Birds, migration and emerging zoonoses: West Nile virus, lyme diseases, influenza A and enteropathongens. *Clinical Medicine and Research* **1**, 5-12.

[82] Ríos-Soto, K.R., Castillo-Chavez, C.; Neubert, M.G.,Titi, E.S., Yakubu, A.-A. (2006). Epidemic spread in populations at demographic equilibrium. Mathematical studies on human disease dynamics, *Contemp. Math.* **410**, Amer. Math. Soc., Providence, RI, 297-309.

[83] Shigesada, N. and Kawasaki, K. (2001). Biological invasions: theory and practice. Oxford Series in Ecology and Evolution, Oxford University Press, New York.

[84] Skellam, J.G. (1951). Random dispersal in theoretical populations. *Biometrika*, **38**, 196-218.

[85] Skellam, J.G. (1973). The formulation and interpretation of mathematical models of diffusional processes in population biology. *In: he Mathematical Theory of Dynamics of Biological Populations*. M.S. Bartlett and R.W. Hiorns, (eds.). Academic Press, New York, 63-85.

[86] Simon, C.P. and Jacquez, J.A. (1992). Reproduction numbers and the stability of equilibria of SI models for heterogeneous populations. *SIAM J. Appl. Math.* **52**, 541-576.

[87] Strogatz, S.H. (2000) Nonlinear Dynamics and Chaos with Applications to Physics, Biology, Chemistry, and Engineering, Westview press.

[88] Taylor, R.A.J. (1978). The relationship between density and distance of dispersing insects. *Ecol. Entomol.* **3**, 63-70.

[89] Thieme, H.R. (1992). Convergence results and a Poincaré-Bendixson trichotomy for asymptotically autonomous differential equations. *J. Math. Biol.* **30**, 755.

[90] Thieme, H. and Castillo-Chavez, C. (1995). Asymptotically autonomous epidemic models. In: *Mathematical Population Dynamics: Analysis of Heterogeneity Vol. One: Theory of Epidemics* O. Arino, D. Axelrod, M. Kimmel and M. Langlais (eds.), 33-50.

[91] Ulbrich, K. (1930). Die Bisamratte. Dresden: Heinrich.

[92] Van Kirk, R. W., and Lewis, M.A. (1997). Integrodifference models for persistence in fragmented habitats. *Bulletin of Mathematical Biology* **59**, 107-137.

[93] Wallace, B. (1966). On the dispersal of Drosophila. *Am. Nat.* **100**, 551-563.

[94] Weinberger, H.F. (1978). Asymptotic behavior of a model of populations genetics, in *Nonlinear Partial Differential Equations and Applications* (J. Chadam, ed.), Lecture Notes in Mathematics 648, Springer, 47-98.

[95] Weinberger, H.F. (1982). Long-time behavior of a class of biological models. *SIAM J. Math. Anal.* **13**, 353-396.

[96] Weinberger, H.F., Lewis, M.A. and Li, B. (2002). Analysis of linear determinacy for spread in cooperative models. *J. Math. Biol.* **45**, 183-218.

[97] World Health Organization (2005). Avian Influenza frequently asked questions. http://www.who.int/csr/disease/avian_influeza/avian_faqs/en/index.html

[98] Yakubu, A.-A. and Castillo-Chavez, C. (2002). Interplay between local dynamics and dispersal in discrete-time metapopulation models. *J. Theor. Biol.* **218**, 273-288.

[99] Yakubu, A-A. (2007). Allee effects in a discrete-time SIS epidemic model with infected newborns. *J. Difference Equ. Appl.* **13**, 341-356.

[100] Zachmanoglou E.C. and Thoe D.W. (1986). Introduction to Partial Differential Equations with Applications, Dover.

[101] Zhao, X.-Q. (1996). Asymptotic behavior for asymptotically periodic semiflows with applications, *Commun. Appl. Nonlinear Anal.* **3** 43-66.